



VIBRATIONAL POWER METHODS IN CONTROL OF SOUND AND VIBRATION

Pertti Hynnä

Customer: Tekes / VÄRE technology programme



	A	Work report	
	B	Public research report	X
		Research report, confidential to	
Title Vibrational power methods in control of sound and vibration			
Customer or financing body and order date/No. Tekes VÄRE technology programme		Research report No. BVAL37-021229	
Project LIIKKUTEHO (Power methods in control of sound and vibration)		Project No. V9SU00184	
Author(s) Pertti Hynnä		No. of pages/appendices 106 /	
Keywords Structure-borne sound, source characterization, vibrational power methods			
Summary <p>Design of quiet machines and vehicles requires quantitative data of source strengths of sound and vibration sources. In addition mechanical mobility of structures and sources is needed for the estimation of vibrational power transmission from sources to receiving structures. These data are important if energy based methods are used in the estimation of sound and vibration characteristics of machines or vehicles.</p> <p>In this state-of-the-art literature review basic concepts of mechanical impedance and mobility of elements is discussed. Also impedance, mobility and four-pole parameters are included. Thereafter the important issue of characterization of structure-borne sound sources is considered. Methods for the determination of the structure-borne sound power transmission from machines and applications are presented. Special emphasis is given to applications in the ship context. In practise important power transmission through vibration isolators and measurement techniques are reviewed. Finally research and test facilities of vibration isolators in some countries are presented.</p>			
Date		Espoo, 5 November 2002	
Pekka Koskinen Deputy Research Manager		Pertti Hynnä Research Scientist	
		Checked	
Distribution (customers and VTT): VTT 2 copies			
<i>The use of the name of VTT in advertising, or publication of this report in part is allowed only by written permission from VTT.</i>			

VTT TECHNICAL RESEARCH CENTRE OF FINLAND

 VTT INDUSTRIAL SYSTEMS
 Tekniikantie 12, Espoo
 P.O. Box 1705, FIN-02044 VTT
 Finland

 Tel. +358 9 4561
 Fax +358 9 455 0619

name.surname@vtt.fi
www.vtt.fi/tuo
 Business ID 0244679-4

Foreword

VÄRE - Control of Vibration and Sound - Technology Programme 1999-2002 is a national technology programme launched by the National Technology Agency (Tekes). It raises the readiness of companies to meet the stricter demands set by market for the vibration and sound properties of products.

As to structure-borne sound power and the characterization of machines as a source of structure-borne sound there are not yet generally accepted international standards or methods. The research work on these topics is going on both in theoretical and practical aspects. Instead the properties of machines as a source of air borne sound are well established and standardised internationally.

This literature review belongs to the VÄRE subproject Control of vibration and noise of vehicles. The research is aimed to find in the literature methods for the characterisation of diesel engines of a ship as structure-borne sound sources and to find design methods to minimise the sound transmission from machines via foundation to the ship structure.

This project is financed by Tekes (that is the main financing organization for applied and industrial research and development in Finland), VTT Manufacturing Technology (nowadays VTT Industrial Systems) and Finnish companies: diesel engine manufacturer Wärtsilä NSD Finland Oy (nowadays Wärtsilä Finland Oy), ship yards Kvaerner Masa-Yards Inc., and Aker Finnyards Oy.

Licentiate in Technology Tapio Hulkkonen from Kvaerner Helsinki yard led the supervising group from the beginning to 10th of November 2000. Thereafter Master of Science in Technology Peter Sundström from Wärtsilä Finland Oy took the leadership. The other members of the supervising group have been: Masters of Science in Technology Jouko Virtanen, Berndt Lönnberg and Engineer Juhani Siren from Kvaerner; Masters of Science in Technology Jukka Vasama, Kari Kyyrö and Jari Lausmaa from Aker Finnyards Oy; and Master of Science in Technology Petri Aaltonen from Wärtsilä Finland Oy; project manager of "Vibration and noise control of transport equipment and mobile work machines" (LiikkuVÄRE) Master of Science in Technology Teijo Salmi and project director Doctor of Technology Matti K. Hakala from VTT Industrial Systems.

This study was financially supported by Tekes and Finnish companies, which made this project possible. This project was also supported financially by the Tekes VÄRE-project EMISSIO (Control of noise emission in machinery) through its subproject EMIPOWER (Diesel motor as a source of structure-borne sound). The project manager Master of Science in Technology Kari P. Saarinen made co-operation with this project possible, which is greatly appreciated.

The author wants to express his warm thanks to the supervising group for the support and encouragement during the work.

Espoo, 5 November 2002

Pertti Hynnä

Table of contents

1	Introduction	6
2	Definitions.....	7
2.1	Acoustics and sound	7
2.2	Airborne sound.....	8
2.3	Structure-borne sound.....	8
2.4	Sinusoidal disturbance	8
2.5	Time average of a product	10
2.6	Time average of power.....	10
3	Mechanical impedance and mobility of elements	11
3.1	Force and velocity phasors	11
3.2	Mechanical impedance of lumped elements	12
3.2.1	Mechanical impedance of resistance.....	12
3.2.2	Mechanical impedance of spring	13
3.2.3	Mechanical impedance of mass	15
3.3	Mechanical mobility of lumped elements.....	17
3.4	Impedance and mobility of connected elements	17
3.4.1	Impedance and mobility of parallel connected elements	17
3.4.2	Impedance and mobility of series-connected elements	19
4	Impedance and mobility concepts.....	20
4.1	Generalized mechanical mobility.....	20
4.2	Mechanical mobility.....	20
4.3	Driving-point and transfer mobility	21
4.4	Impedance	21
4.5	Mechanical impedance.....	21
4.6	Moment impedance.....	21
4.7	Driving-point and transfer impedance.....	22
4.7.1	Driving-point impedances of infinite plates and beams.....	22
4.8	Driving-point mobility	23
4.8.1	Driving-point mobility of infinite plates and beams.....	24
4.9	Mechanical free impedance and complex impedance.....	27
4.10	Blocked mechanical impedance	28
4.11	Frequency response functions related to mobility.....	28
4.12	Boundary conditions of experimentation.....	29
4.13	Mechanical mobility and impedance matrices	29
4.13.1	Definitions.....	29
4.13.2	Mechanical mobility matrix.....	30
4.13.3	Impedance matrix	31
5	Effective mobility.....	32
5.1	Definitions	32

5.1.1	Effective point mobility	34
5.1.2	Effective total mobility	36
5.1.3	Measurement of effective mobility	37
5.2	Applications of mechanical mobility measurements	41
6	Analysis of mechanical systems	42
6.1	Impedance and mobility of a system of elements.....	42
6.2	Kirchhoff's Laws.....	43
6.3	Superposition theorem	43
6.4	Reciprocity theorem	43
6.5	Thévenin's equivalent circuit.....	43
6.6	Norton's equivalent circuit.....	45
6.7	Analysis methods	46
6.8	Example of analysis	46
7	Impedance and mobility parameters	50
7.1	Impedance parameters	50
7.2	Mobility parameters	51
8	Four-pole parameters of mechanical systems	53
8.1	Theory	53
8.2	Four-pole parameters of a series connected system	55
8.3	Four-pole parameters of a parallel connected system.....	56
8.4	Four-pole parameters of lumped systems	56
8.4.1	Mass.....	56
8.4.2	Spring	57
8.4.3	Resistance.....	57
8.4.4	Parallel spring and resistance.....	58
8.4.5	Dynamic absorber	58
8.4.6	Dynamic absorber in a mechanical system	59
9	Characterization of structure-borne sound source.....	60
9.1	Introduction	60
9.2	Complex power transmission	60
9.2.1	Constant velocity and constant force source	62
9.2.2	Transmission loss of elastic elements	62
9.2.3	Source descriptor and coupling function.....	63
9.2.3.1	One-point-connected systems	63
9.2.3.2	Multi-point-connected systems	65
9.2.4	Characteristic power.....	67
10	Mobility functions and free velocities	69
10.1.1	Machine mobilities	69
10.1.1.1	Mobility in mass controlled region.....	70
10.1.1.2	Mobility in stiffness controlled region	71
10.1.1.3	Mobility in resonance controlled region.....	71
10.1.2	Floor mobilities	72
10.1.3	Free velocities of machine	72

11	Measurement techniques	73
11.1	Mobility measurement	73
12	Structure-borne sound power transmission from machines	74
12.1	Power calibration of receiving structure	74
12.1.1	Introduction.....	74
12.1.2	Power transmission from source machine to receiving structure.....	74
12.1.2.1	Power transmission estimate over contact zone	75
12.1.3	Power calibration of receiving structure	75
12.1.3.1	Calibration of receiving structure	75
12.1.3.2	Reference power estimate	77
12.1.3.3	Calibration with source machine installed.....	77
12.1.4	Application examples.....	79
12.1.4.1	Box receiver and engine foundation of ship.....	79
12.1.4.2	Helicopter fuselage	82
12.1.5	Applicability of in-situ estimation method	83
12.2	Surface power or equivalent source power.....	83
12.2.1	Excitation and response points.....	84
12.2.2	Machinery mounting conditions	85
13	Power transmission through vibration isolator.....	86
13.1	Dynamic stiffness matrix and general concepts.....	86
13.2	Determination of power transmitted via vibration isolator	90
13.2.1	Direct method	90
13.2.2	Indirect method.....	90
13.2.3	Generalization of the indirect method	92
14	Research and test facilities of vibration isolators.....	93
14.1.1	Research and facilities at KTH, Sweden	93
14.1.2	Research and facilities at AMRL, Australia.....	96
14.1.3	Research and facilities at TNO TPD, The Netherlands	97
14.1.4	Research and facilities at HUT and VTT, Finland.....	100
15	Conclusions.....	101
	References	102

1 Introduction

Today acoustics of vehicles or any kind of machines is important for the community and the industry. This interest in sound and vibration quality has been seen as numerous international and national regulations given for sound and vibration control to reduce the impact on man.

Low noise design ([1], [2], and [3]) and design of quiet structures [4] are getting more emphasis at the design stage and it has an important impact on the marketability and competitiveness of many products. At the design stage it is often asked to predict the resulted sound levels of a machine or component. To do this, one needs to analyze all the excitation sources and their interactions with the structures and transmission paths. For air-borne sound well-established design and measurement methods are nowadays available. Instead for structure-borne sound the methods for characterization of machines or components as sources of structure-borne sound are still in phase of intensive research and development.

Sound is propagated over long distances in built-up structures mainly as structure-borne sound because of low material damping. Instead air-borne sound has only meaning near the sound source or in spaces contiguous to the source space. Audible sound to a normal human ear covers roughly the frequency range from 20 Hz to 20 kHz [5, p. 25]. Usually at the design stage the frequency range is restricted to the frequencies including the octave bands from 31,5 Hz to 8 kHz. This means that in built-up systems composed typically of beams, plates and shells one or two dimensions are small compared with the structural wavelength. This requires very much from the analysis methods and engineers when typically only scarce input data is available to meet the requirements specified on a new product.

Analysis methods of structure-borne sound transmission must be able to handle with different parts of the structure and with the whole structure as well. Substructuring technique allows the properties of the assembled structure to be calculated using the properties of its parts. In the modelling using substructuring one important requirement is to be able to utilize also measured input data because the properties of mechanical parts vary and sometimes the only way is to use measured input data. The so-called impedance or mobility method allows both substructuring and use of measured input data [6]. The roles of experiments with computational experimentation are thoroughly discussed by Frank Fahy in [7].

Structural parts may be modelled and analyzed using several methods including theoretical and experimental modal methods, discrete Finite Element Methods (FEM) or using the mean value methods like Statistical Energy Analysis (SEA) [8]. Depending on the modelling work at hand, sometimes even empirical and semiempirical methods have to be used.

Characterization of machines as sources of structure-borne sound is the major problem when estimating the structure-borne sound emission [9]. Vibrational power transmission from a machine source to flexible machinery supporting structures has been under intensive research (see e.g., references [10], [11], [12], [13], [14], [15], [16], [17], [18] and [19]). Power transmission from a source structure to the receiving structure depends on the mobilities of the source and the receiving structure, respectively.

This literature review is concentrated to the structure-borne sound power and source characterization of diesel engines in the ship context (see Figure 1) and in an agricultural tractor (see Figure 2). The mobility technique is discussed as well, because it is well known that the transmitted power from source to the receiving structure is dependent on the mobilities of the source and the receiver. Also the determination of vibrational power transmission through vibration isolators is reviewed.

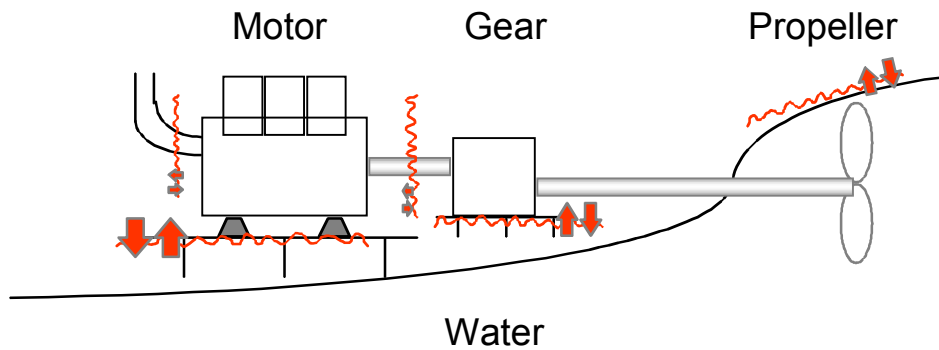


Figure 1. In the ship and small craft context interaction phenomena interconnect sources of sound and vibration with structures and the surrounding air and water.

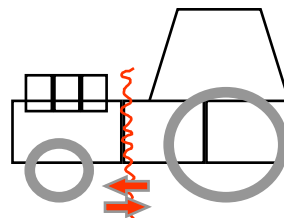


Figure 2. Diesel engine as a source of structure-borne sound in an agricultural tractor.

2 Definitions

2.1 Acoustics and sound

Acoustics is the science of sound (see [5]). It includes generation, transmission, and effects of sound. The term *sound* means not only the phenomena in air which cause the sensation of hearing but also those phenomena that are governed by analogous physical principles. Thus we use the terms infrasound and ultrasound even the frequency is either too low or too high to be heard by a person with normal hearing. In addition the terms underwater sound, sound in solids, and structure-borne sound are in common usage. The frequency range of audible sounds is roughly between 20 Hz and 20 000 Hz. Compared to optics sound is a mechanical wave motion whereas light is an electromagnetic wave motion.

2.2 Airborne sound

Sound that is transmitted from the sound source to its environment through air is called *airborne sound*. It propagates as longitudinal compressional waves. The speed of sound in air is about 340 m/s. A wave is a process where a disturbance from equilibrium in a material medium is transported through the medium without net transport of mass [20].

2.3 Structure-borne sound

Many sounds, which we sense to come from different activities, are either produced or conducted by vibrating solid bodies. These include for instance the sound of many musical instruments, engines, machines and the impact sound coming from the adjoining room. The field of physics which deals with the generation and propagation of motions and forces varying as a function of time in solid bodies and the associated sound radiation is called "structure-borne sound" [23]. Or alternatively structure-borne sound covers all forms of audio-frequency vibration of solid structures, because these vibrations are inevitably accompanied by the generation of sound in contiguous fluids [20]. In this context sound refers to the frequency range of interest that is the frequency range audible to a normal human ear roughly between 20 Hz and 20 kHz. However, the frequency limits are not to be considered as absolute limits [23]. The phenomena associated with structure-borne sound are complicated because sound is propagated in many waveforms, which couple with each other at structural junctions. In addition the speed of wave propagation may depend on frequency, as is the case with bending (flexural) waves. The range of amplitudes of structure-borne sound varies from less than 10^{-8} mm at high frequencies to several millimeters at low frequencies.

2.4 Sinusoidal disturbance

Small amplitude perturbations compared to an ambient state are called acoustic disturbances. The ambient state $(p_0, \rho_0, \mathbf{v}_0)$ for a fluid is characterized by the values of the pressure p_0 , density ρ_0 and fluid velocity \mathbf{v}_0 which prevail when there is no perturbation. Thus for instance the acoustic pressure is the perturbation equivalent to the deviation from the static pressure (total pressure) [5]. The hearing threshold for a person with acute hearing corresponds to the acoustic pressure of 20 μ Pa equivalent to 0 dB (re 20 μ Pa) and the pressure 63 Pa equivalent to 130 dB corresponds the threshold of pain. These pressures can be compared with the ambient static air pressure of 0,1 MPa to get an idea of the relative magnitudes of pressures. Also that is why the decibel scale is used to get numbers to a practical scale between 0 - 130 when expressing the magnitude of usually encountered acoustic pressures.

A field is a constant frequency if the field variables are varying sinusoidally with time, such that for instance for the acoustic pressure p [5]

$$p = p_{\text{pk}} \cos(\omega t - \phi) = p_{\text{pk}} \sin(\omega t - \phi') = \text{Re}[\hat{p} e^{-i\omega t}], \quad (1)$$

where the amplitude or peak pressure p_{pk} , the angular frequency ω , the complex pressure amplitude \hat{p} , and the phase constants ϕ and ϕ' are independent of time t . $\text{Re}[\]$ denotes real part. The relations in Eq. (1) are equivalent, if [5]

$$\phi' = \phi - \frac{\pi}{2}, \quad \hat{p} = p_{\text{pk}} e^{i\phi}, \quad (2)$$

since trigonometry and Euler's formula give the following equations, respectively,

$$\sin\left(\alpha + \frac{\pi}{2}\right) = \cos \alpha, \quad e^{i\alpha} = \cos \alpha + i \sin \alpha. \quad (3)$$

The pressure in Eq. (1) oscillates between positive and negative values and repeats itself when the arguments $\omega t - \phi$ or $\omega t - \phi'$ change by 2π when the sine or cosine function changes sign. Thus the period, the time per cycle, is $2\pi / \omega$ and the number of cycles per unit time, frequency, is

$$f = \frac{\omega}{2\pi}, \quad (4)$$

and the SI unit of frequency is hertz [Hz], where $1 \text{ Hz} = 1 \text{ s}^{-1}$ (or one cycle per second). The SI unit of angular frequency is [rad/s] (radians per second) often written in the form of only [1/s].

A plane travelling wave of constant frequency repeats itself also with distance of propagation and the repetition length is called wavelength $\lambda = 2\pi / k$, where k is the wave number. The relationships between wave number, angular frequency, frequency, speed of sound propagation c and wave length are obtained from

$$k = \frac{\omega}{c} = \frac{2\pi f}{c} = \frac{2\pi}{\lambda}. \quad (5)$$

The complex number representation introduced in Eq. (1) is frequently used in theoretical studies because it enables the expression of the amplitude and phase with only one complex number. The time dependence $e^{-i\omega t}$ is traditional in wave-propagation studies [5]. Some writers use instead the time dependence $e^{+i\omega t}$.

For sinusoidally varying pressure (see Eq. (1)) the mean squared pressure $(p^2)_{\text{av}}$ (many times denoted as $\overline{(p^2)}$ where the over-bar means time-averaging) and root-mean-squared (rms) pressure p_{rms} are defined as [5]

$$(p^2)_{\text{av}} = \overline{(p^2)} = \frac{1}{T} \int_{t_0}^{t_0+T} p^2(t) dt = p_{\text{rms}}^2, \quad (6)$$

where T is either an integral number of half-wave periods or an interminably long time. With the aid of Eqs. (1) and (6) one gets relationships [5]

$$(p^2)_{\text{av}} = \overline{(p^2)} = p_{\text{rms}}^2 = \frac{1}{2} p_{\text{pk}}^2 = \frac{1}{2} |\hat{p}|^2. \quad (7)$$

The spatial averaging over a surface or a volume is denoted often in the literature by angle brackets, e.g., $\langle \overline{p^2} \rangle$.

2.5 Time average of a product

If one considers with same frequency oscillating two signals X and Y denoted by

$$X = \text{Re}[\hat{X} e^{-i\omega t}] \quad \text{and} \quad Y = \text{Re}[\hat{Y} e^{-i\omega t}], \quad (8)$$

then the time average of their product is obtained from [5]

$$(XY)_{\text{av}} = \frac{1}{2} \text{Re}[\hat{X}\hat{Y}^*], \quad (9)$$

where \hat{Y}^* is the complex conjugate of \hat{Y} . This can be derived for example as follows: using the notation of Eq. (8) for X and Y one obtains

$$(XY)_{\text{av}} = \left[\text{Re}(\hat{X} e^{i\phi_X} e^{-i\omega t}) \text{Re}(\hat{Y} e^{i\phi_Y} e^{-i\omega t}) \right]_{\text{av}} = |\hat{X}| \cdot |\hat{Y}| \left[\text{Re}(e^{-i\alpha}) \text{Re}(e^{-i\beta}) \right]_{\text{av}},$$

where $\alpha = \omega t - \phi_X$ and $\beta = \omega t - \phi_Y$. The trigonometric identity [5]

$$\cos \alpha \cos \beta = \frac{1}{2} \cos(\alpha - \beta) + \frac{1}{2} \cos(\alpha + \beta) \quad (10)$$

gives

$$(XY)_{\text{av}} = |\hat{X}| \cdot |\hat{Y}| \left[\cos \alpha \cos \beta \right]_{\text{av}} = |\hat{X}| \cdot |\hat{Y}| \left[\frac{1}{2} \cos(\phi_Y - \phi_X) + \frac{1}{2} \cos(2\omega t - \phi_Y - \phi_X) \right]_{\text{av}}$$

where the second term averages out to zero when the time averaging is performed, and one obtains the relation presented in Eq. (9)

$$(XY)_{\text{av}} = \frac{1}{2} |\hat{X}| \cdot |\hat{Y}| \cos(\phi_Y - \phi_X) = \frac{1}{2} \text{Re}(|\hat{X}| \cdot |\hat{Y}| e^{\pm i(\phi_Y - \phi_X)}) = \frac{1}{2} \text{Re}[\hat{X}^* \hat{Y}] = \frac{1}{2} \text{Re}[\hat{X}\hat{Y}^*].$$

2.6 Time average of power

A time-harmonic force being a real quantity can be considered to be of the form $F(t) = \text{Re}[\hat{F} e^{-i\omega t}]$. This force excites the structure at the contact point to vibrate with velocity $v(t) = \text{Re}[\hat{v} e^{-i\omega t}]$. The time average of the power \bar{P} transmitted to the structure by this excitation can be evaluated using Eq. (9) as ([23], [26], [31])

$$\bar{P} = \frac{1}{T} \int_0^T P(t) dt = \frac{1}{T} \int_0^T \text{Re}[\hat{F} e^{-i\omega t}] \text{Re}[\hat{v} e^{-i\omega t}] dt = \frac{1}{2} \text{Re}[\hat{F} \hat{v}^*], \quad (11)$$

where $P(t)$ is the instantaneous power at time t , \hat{F} is the complex amplitude of force, \hat{v} is the complex amplitude of velocity, and $\omega = 2\pi f$ is the angular frequency at frequency f . This power is only due to the product of force and velocity not including the contribution of the product of moment and angular velocity.

3 Mechanical impedance and mobility of elements

3.1 Force and velocity phasors

The motion of a linear mechanical system can be expressed with differential equations in terms of the driving force and the acceleration, velocity, or displacement of the elements of the system. When the driving force is sinusoidal, the steady-state response is also sinusoidal at the driving frequency with a fixed phase difference to the driving force. Because any time-varying signal may be expressed as a superposition of sinusoids, one may consider one sinusoid at a time and then superpose the results, without losing generality of analysis [36].

Using the rotating phasor notation the sinusoidally varying force can be presented on the complex plane, as shown in Figure 3. The force phasor has a length or magnitude F_0 and it rotates counterclockwise with angular velocity ω making the angle ωt with the positive real axis at time t . The real instantaneous force $F_0 \cos \omega t$ is the projection

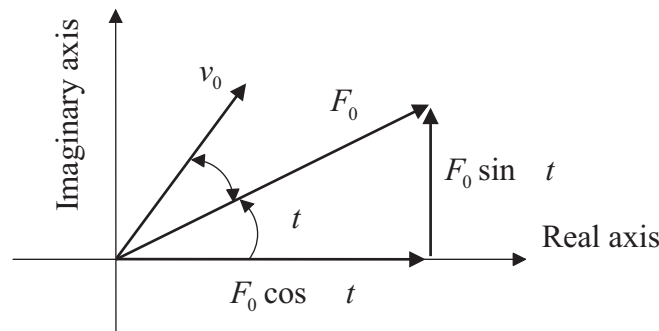


Figure 3. A sinusoidal force and velocity in the complex plane.

of the force phasor on the real axis. The force F can be expressed with its real and imaginary components as

$$F = F_0 \cos \omega t + iF_0 \sin \omega t . \tag{12}$$

It is convenient for the analysis purposes to represent the force in terms of its magnitude F_0 and its phase angle ωt as

$$F = F_0 e^{i\omega t} . \tag{13}$$

A sinusoidally varying velocity can also be represented as a phasor (see Figure 3). If the velocity phasor, magnitude v_0 , is rotating at the same angular velocity ω as the force phasor, magnitude F_0 , the velocity v can be represented as

$$v = v_0 [\cos(\omega t + \phi) + i \sin(\omega t + \phi)] = v_0 e^{i(\omega t + \phi)} , \tag{14}$$

where ϕ is the phase angle between the force F and velocity v , and the velocity is leading the force with angle ϕ . If the phase reference is force F instead of the positive real axis, then the velocity may be given as

$$v = v_0 e^{i\phi}. \quad (15)$$

The displacement x of a sinusoidal vibration is obtained by integrating the velocity expressed as $v = v_0 e^{i\omega t}$, and noticing that $x = \int v dt$ as

$$x = \frac{v}{i\omega}. \quad (16)$$

The acceleration a of a sinusoidal vibration is obtained from velocity using the relation $a = \ddot{x} = dv/dt$ as

$$a = \dot{v} = i\omega v. \quad (17)$$

3.2 Mechanical impedance of lumped elements

3.2.1 Mechanical impedance of resistance

Real physical systems can be modelled using idealized mechanical system elements with lumped constants: resistance, spring, and mass [36]. A mechanical resistance is defined as a device in which the relative velocity between its end points is proportional to the force applied to its end points (Figure 4).

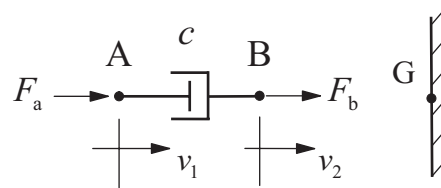


Figure 4. Ideal mechanical resistance element [36].

In an ideal resistance element the force resisting the extension or compression of the element is viscous friction force. In (Figure 4) the relative velocity of point A relative to point B is

$$v = (v_1 - v_2) = \frac{F_a}{c}, \quad (18)$$

where the proportionality constant c is mechanical resistance (or damping constant), and F_a is the viscous friction force acting at point A. If there is a relative velocity at point A as a result

of force F_a acting on it, there must be a reaction force at point B of equal strength. The velocities v_1 and v_2 are measured relative to a common stationary reference point G.

When the sinusoidal force $F_0 e^{i\omega t}$ (Eq. (13)) is acting on the ideal resistance element at the point A and the point B is attached to a fixed point, then the velocity of point A is obtained from Eq. (18) as

$$v_1 = \frac{F_0 e^{i\omega t}}{c} = v_0 e^{i\omega t}. \quad (19)$$

From Eq. (19) it is seen that the force and the resulted velocity phasors are rotating at the same angular velocity ω and that they are in the same phase (see Figure 5).

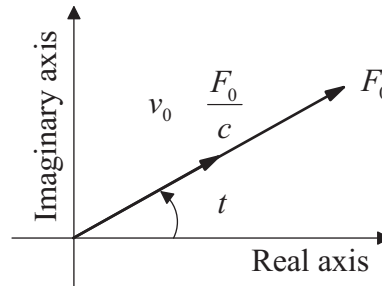


Figure 5. Force (magnitude F_0) acting upon an ideal resistance results in a velocity (magnitude v_0) in the same phase, adapted from [36].

Using Eq. (13) and (19) one gets for the mechanical impedance of a resistance element as

$$Z_c = \frac{F}{v} = \frac{F_0 e^{i\omega t}}{\frac{F_0}{c} e^{i\omega t}} = c. \quad (20)$$

From Eq. (20) it is seen that the impedance of a resistance is equal to its damping constant c .

3.2.2 Mechanical impedance of spring

A linear spring is defined as a device for which the relative displacement between its end points is proportional to the force acting on the spring in its main direction. The displacement of the end points of a spring is mathematically represented as (Figure 6)

$$\delta x = x_1 - x_2 = \frac{F_a}{k}, \quad (21)$$

where k is the spring stiffness and x_1 and x_2 are the displacements of the end points A and B relative to the stationary point G.

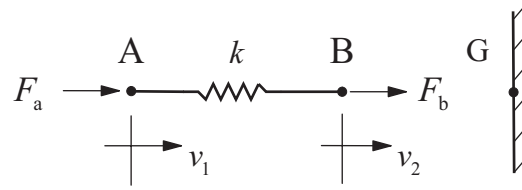


Figure 6. An ideal spring. The force F_a is acting on the end point A causing the reaction force $F_b = F_a$ at point B. The spring stiffness is k , v_1 and v_2 are the velocities of the end points relative to a stationary point G, adapted from [36].

If the point B is fixed, and one applies the force of Eq. (13), then the displacement of point B is obtained from Eq. (21) as

$$x_1 = \frac{F_0 e^{i\omega t}}{k} = x_0 e^{i\omega t}. \quad (22)$$

It is seen from Eq. (22) that the displacement varies sinusoidally at the same angular frequency as the applied force and that it is in the same phase with the force. The velocity v_1 of the end point A is obtained by differentiating the displacement with respect to time t , so

$$v_1 = \dot{x}_1 = \frac{i\omega F_0 e^{i\omega t}}{k} = i v_0 e^{i\omega t}. \quad (23)$$

From Eq. (13) and (23) one obtains the mechanical impedance of an ideal spring as

$$Z_k = \frac{F}{v} = \frac{F_0 e^{i\omega t}}{i\omega F_0 e^{i\omega t} / k} = \frac{k}{i\omega} = \frac{-ik}{\omega}. \quad (24)$$

It is seen from Eq. (24) that the impedance of an ideal spring is imaginary and depends on the spring stiffness k and the angular frequency ω . The velocity in Eq. (23) may be written in the form of Eq. (12) as

$$v_1 = \frac{F_0}{k} (-\omega \sin \omega t + i\omega \cos \omega t) = \frac{\omega}{k} F_0 e^{i(\omega t + \pi/2)}. \quad (25)$$

From Eq. (25) it is seen that the velocity phasor of an ideal spring leads the force phasor by the angle $\pi/2 = 90^\circ$ (see Figure 7). The same thing is indicated by the imaginary unit i in the Eq. (23), because $i = e^{i\pi/2} = \cos \frac{\pi}{2} + i \sin \frac{\pi}{2} = 0 + i = i$.

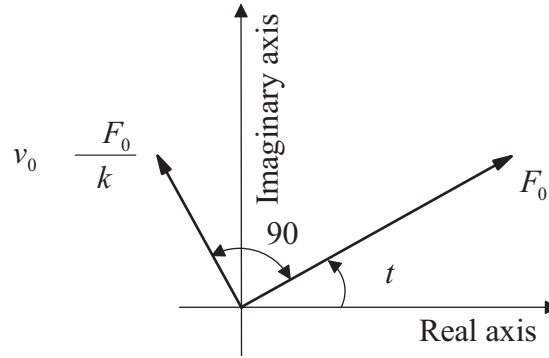


Figure 7. Force (magnitude F_0) and velocity (magnitude v_0) phasors at the end point of an ideal spring, adapted from [36].

3.2.3 Mechanical impedance of mass

The mass of a rigid body can be assumed to be constant when speaking of conventional velocities. The ideal mass is illustrated in Figure 8. Noticing that the acceleration \ddot{x} of the rigid body is proportional to the accelerating force F , one obtains at point A

$$\ddot{x}_1 = \dot{v}_1 = \frac{F_a}{m}, \quad (26)$$

where m is the mass of the body and $\ddot{x}_1 = \ddot{x}_2$ since the body is rigid. The force F_a in Eq. (26) is required to give the mass m the acceleration \ddot{x}_1 and therefore the transmitted force F_b is zero [36]. If the force is sinusoidal $F_a = F_0 e^{i\omega t}$, then the acceleration

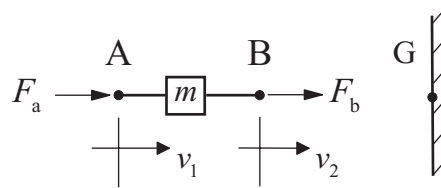


Figure 8. An ideal mass, adapted from [36].

$$\ddot{x}_1 = \frac{F_0 e^{i\omega t}}{m}, \quad (27)$$

is also sinusoidal and in phase with the accelerating force. The velocity \dot{x}_1 of the mass is obtained by integrating Eq. (27) as

$$\dot{x}_1 = v = \frac{F_0 e^{i\omega t}}{i\omega m} = -iv_0 e^{i\omega t}. \quad (28)$$

Dividing the force $F_a = F_0 e^{i\omega t}$ by the velocity given in Eq. (28) one obtains the mechanical impedance of the mass as

$$Z_m = \frac{F}{v} = \frac{F_0 e^{i\omega t}}{F_0 e^{i\omega t} / i\omega m} = i\omega m. \quad (29)$$

From the Eq. (29) one sees that the mechanical impedance of the mass is imaginary and depends on the magnitude of mass and on the angular frequency. The velocity in the Eq. (28) can be written in the form

$$v = \frac{F_0}{\omega m} (\sin \omega t - i \cos \omega t) = \frac{F_0}{\omega m} e^{i(\omega t - \pi/2)}. \quad (30)$$

From Eq. (30) it is seen that the phasor of the velocity is $\pi/2 = 90^\circ$ behind the force phasor (see Figure 9), this is indicated also by $-i$ in Eq. (28).

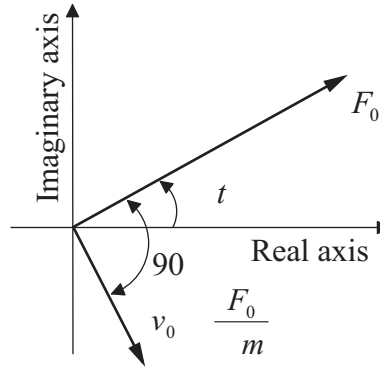


Figure 9. Force and velocity phasor of ideal mass in the complex plane, adapted from [36].

The magnitude of the mechanical impedance of ideal mass, resistance and spring as a function of frequency is presented schematically in Figure 10.

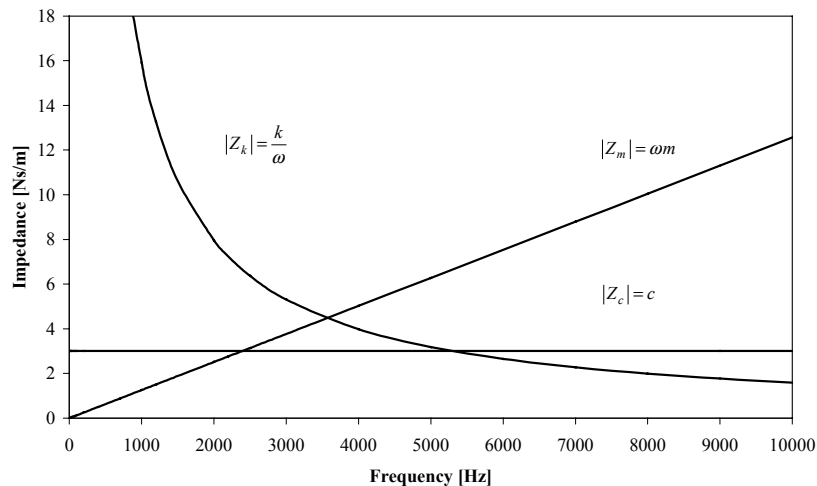


Figure 10. The magnitude of the mechanical impedance of ideal resistance, spring and mass, adapted from [36].

3.3 Mechanical mobility of lumped elements

Real structures or physical systems can be modelled using idealized mechanical elements with lumped constants. Such elements are mechanical resistance (or damping), spring, and mass. For these elements the mobilities are [36]:

resistance:
$$Y_c = \frac{1}{c}, \tag{31}$$

where c is mechanical resistance with SI unit $[(N \cdot s)/m]$;

spring:
$$Y_k = \frac{i\omega}{k}, \tag{32}$$

where k is spring stiffness with SI unit $[N/m]$; and

mass:
$$Y_m = \frac{1}{i\omega m} = \frac{-i}{\omega m}, \tag{33}$$

where m is element mass with SI unit $[kg]$. The mobility magnitude as a function of frequency of these idealized mechanical elements is presented in Figure 11.

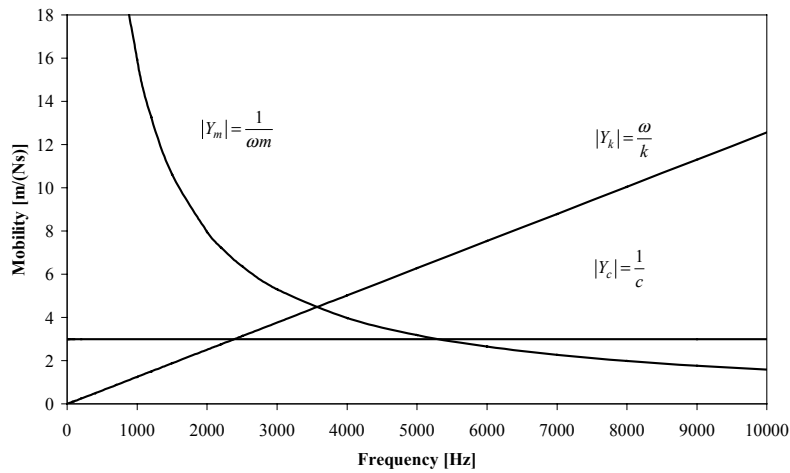


Figure 11. The mobility magnitudes of an ideal mechanical resistance $|Y_c|$, spring $|Y_k|$ and mass $|Y_m|$ as a function of frequency.

3.4 Impedance and mobility of connected elements

3.4.1 Impedance and mobility of parallel connected elements

The properties of mechanical systems can be analyzed using mechanical impedance or mobility concepts. In the analysis impedance and mobility are determined at the points of force excitation or paths for transmitting forces, or at points of common velocities [36]. In

Figure 12 the exciting force F causes the common velocity at the connection point A, which is common for the parallel connected spring and resistance.

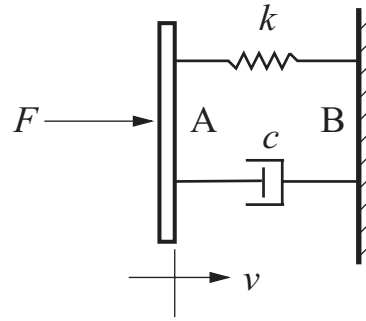


Figure 12. Schematic presentation of a mechanical system consisting of a spring (spring stiffness k) and a mechanical resistance (resistance c) connected parallel at points A and B. The exciting force F gives a common velocity v for both elements at point A referred to the stiff point B.

The force required to give the resistance the velocity v is obtained from Eqs. (39) and (31)

$$F_c = \frac{v}{Y_c} = \frac{v}{1/c}.$$

The force required to give this same velocity for the spring is obtained from Eqs. (39) and (32)

$$F_k = \frac{v}{Y_k} = \frac{v}{i\omega/k}.$$

The total force F is the sum of parallel forces

$$F = F_c + F_k = v \left(\frac{1}{1/c} + \frac{1}{i\omega/k} \right) = \frac{v}{Y_p}.$$

From this it is seen that the inverse of the total mobility Y_p of the parallel-connected elements is

$$\frac{1}{Y_p} = \sum_{i=1}^n \frac{1}{Y_i}, \quad (34)$$

where n is the number of parallel-connected elements. The total impedance Z_p of parallel-connected elements can be obtained from [36]

$$Z_p = \sum_{i=1}^n Z_i, \quad (35)$$

where n is the number of parallel-connected elements with mechanical impedances Z_i .

3.4.2 Impedance and mobility of series-connected elements

Another basic way of connecting elements is series connection, which is presented in Figure 13.

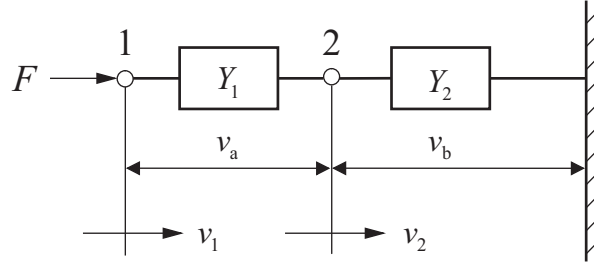


Figure 13. A system consisting of two series-connected mechanical elements with mobilities Y_1 and Y_2 . The exciting force F gives relative velocities v_a and v_b between the end connections of each element. The velocities of the connection points 1 and 2 relative to the stationary reference are v_1 and v_2 .

The velocities of the connection points 1 and 2 are:

$$v_2 = v_b \text{ and } v_1 = v_2 + (v_1 - v_2) = v_b + v_a .$$

The total mobility at point number 1 is $Y = v_1 / F$, and the same force F is acting on both elements. The relative velocities expressed with mobilities are:

$$v_a = FY_1 \text{ and } v_b = FY_2 .$$

So the total mobility is

$$Y = \frac{v_1}{F} = \frac{v_a + v_b}{F} = \frac{FY_1 + FY_2}{F} = Y_1 + Y_2 .$$

The total mobility Y_s of n series connected elements is thus

$$Y_s = \sum_{i=1}^n Y_i , \tag{36}$$

where Y_i is the mobility of element i .

The total impedance Z_s of ideal series connected elements is obtained from

$$\frac{1}{Z_s} = \sum_{i=1}^n \frac{1}{Z_i} , \tag{37}$$

where n is the number of series-connected elements with mechanical impedances Z_i .

4 Impedance and mobility concepts

4.1 Generalized mechanical mobility

Consider a linear and time invariant system, which is excited by a force field $\hat{f} \cdot \exp(i\omega t)$ expressed as complex force amplitude \hat{f} times a harmonically varying function of time $\exp(i\omega t)$. Owing to the system linearity the corresponding velocity field is also harmonic, $\hat{v} \cdot \exp(i\omega t)$, and the ratio \hat{v}/\hat{f} is independent of the amplitude of the exciting force [6]. When the excitation is harmonic at angular frequency ω , the generalized mechanical mobility can be defined as the ratio between the complex amplitudes of the velocity field and the force field as [6]

$$y(\omega) = \frac{\hat{v}(\omega)}{\hat{f}(\omega)}. \quad (38)$$

4.2 Mechanical mobility

ISO 7626-1 [21] defines mechanical mobility Y_{ij} as: "The frequency-response function formed by the ratio of the velocity-response phasor at point i to the excitation force phasor at point j , with all other measurement points on the structure allowed to respond freely without any constraints other than those constraints which represent the normal support of the structure in its intended application." The definition is given mathematically in Eq. (39)

$$Y_{ij} = v_i / F_j, \quad (39)$$

where v_i is the velocity-response phasor at point i and F_j the force phasor at point j .

The velocity response can be either translational or rotational, and the excitation can be either a rectilinear force or a moment. Frequency response function is defined as the frequency dependent ratio of the motion-response phasor to the phasor of the excitation force [21].

Mechanical mobility is sometimes called mechanical admittance. Likewise the complex mobility Y can be written as

$$Y = G + iB, \quad (40)$$

where the real part G is called the conductance and the imaginary part B the susceptance. The SI unit of mechanical mobility is $[m/(N \cdot s)]$.

4.3 Driving-point and transfer mobility

Direct (mechanical) mobility or driving-point (mechanical) mobility Y_{ii} is the complex ratio of velocity and force taken at the same point in a mechanical system during simple harmonic motion [22]. Here point means both a location and a direction. Sometimes the term coordinate is used instead of point. Transfer mechanical mobility Y_{ij} is the complex ratio of the velocity v_i measured at the point i in the mechanical system to the force excitation F_j at the point j in the same system during simple harmonic motion [22].

4.4 Impedance

Impedance is defined as the complex ratio of a harmonic excitation of a linear system to its response during simple harmonic vibration. Both the excitation and the response are complex and their magnitudes increase linearly with time at the same rate [22].

4.5 Mechanical impedance

The mechanical impedance is defined in a mechanical system as the complex ratio of force to velocity as [23], [24]

$$Z = \frac{\hat{F}}{\hat{v}}, \quad (41)$$

where \hat{F} is the phasor of the exciting force, and \hat{v} is the phasor of the velocity as a response at the excitation region. The mechanical impedance is generally a complex function of frequency, because the force and resulting velocity vary with frequency. This general definition is not unique, because the excitation region can be a finite area, and the velocity can vary within this area.

4.6 Moment impedance

In practical situations the force impedance does not cover all the possibilities. Especially this is true in the case of flexural vibrations when moments and angular velocities are of equal importance as forces and translational velocities. The moment impedance W is defined with the exciting moment M and the resulting angular velocity w as [23]

$$W = \frac{M}{w}. \quad (42)$$

The force and moment impedances are not enough to describe completely the response for a point excitation; in general a coupling term is needed [23]. So one must consider carefully if there is only a force or moment excitation and if any coupling terms are needed.

4.7 Driving-point and transfer impedance

Driving-point impedance of a linear mechanical system undergoing sinusoidal vibration is defined as the complex ratio of the exciting force to the velocity response when both are taken at the same point [22]. Here point means both a location and a direction.

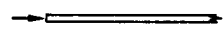
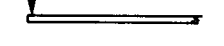
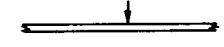

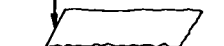


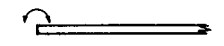
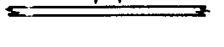

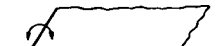
When measuring the point impedance of beam or plate structures, the diameter of the contact area should be less than one-tenth of a flexural wavelength, and not much less than the thickness of the structure under measurement [23].

Transfer impedance of a linear mechanical system undergoing sinusoidal vibration is defined as the complex ratio of the exciting force to the velocity response at another point [22]. Here point means both a location and a direction.

4.7.1 Driving-point impedances of infinite plates and beams

In Table 1 is given some impedance formulas of practical interest in noise control work. In many practical problems these impedance formulas can be applied for finite built-up structures when the frequency is high enough as often is when consideration is given to structure-borne sound.

Table 1. Driving-point impedances of infinite beams and plates [23].

Beam, longitudinal		$Z = S\sqrt{E\rho} = \rho S c_L = \omega \rho S \frac{\lambda_L}{2\pi}$
Thin beam ¹		$Z = \frac{1}{2} \rho S c_B (1 + j)$ $\approx 0.67 \rho S \sqrt{c_L h f} (1 + j)$ $\approx \omega \rho S \frac{\lambda_B (1 + j)}{4\pi}$
		$Z = 2 \rho S c_B (1 + j)$ $\approx 2.67 \rho S \sqrt{c_L h f} (1 + j)$ $\approx \omega \rho S \frac{\lambda_B (1 + j)}{\pi}$
Thin Iso-tropic plate		$Z = 8\sqrt{B'\rho h} \approx 2.3 c_L \rho h^2 \approx \omega \rho h \frac{\lambda_B^2}{5}$
		$Z = 3.5\sqrt{B'\rho h} \approx c_L \rho h^2 \approx \omega \rho h \frac{\lambda_B^2}{11.5}$
Thick Beam		see Eq.(78b) for $\frac{1}{Z}$
Thick Plate		see Eq.(78a) for $\frac{1}{Z}$
Thin beam ¹		$W = \frac{1}{2} \rho S c_B \frac{(1 - j)}{k_B^2}$ $\approx 0.03 \rho S \sqrt{c_L^3 h^3} \frac{(1 - j)}{\sqrt{f}}$
		$W = 2 \rho S c_B \frac{(1 - j)}{k_B^2}$ $\approx 0.12 \rho S \sqrt{c_L^3 h^3} \frac{(1 - j)}{\sqrt{f}}$
Thin Iso-tropic plate ¹		$\frac{1}{W} = \left(1 - \frac{4j}{\pi} \ln 0.9ka\right) \frac{\omega}{16B'}$ $\approx \left(1 - \frac{4j}{\pi} \ln 0.9ka\right) \frac{4.8f}{c_L^2 \rho h^3}$
		$\frac{1}{W} = (1 - 1.46j \ln 0.9ka) \frac{\omega}{5.3B'}$

¹ Flexure, or predominantly flexure.

4.8 Driving-point mobility

Mechanical driving-point mobility is defined as the frequency response function formed by the ratio of the velocity response phasor at point i to the excitation force phasor at the same point i . The velocity response can be either translational (velocity v) or rotational (angular velocity $\omega = \dot{\theta}$, where θ is angular displacement), and the excitation force can be either a rectilinear force F or torque T .

4.8.1 Driving-point mobility of infinite plates and beams

The driving-point mobilities given in Table 2 apply to infinite structures in which no resonances can occur. In real finite structures there are always reflections from discontinuities e.g. from junctions and these usually give a resonant response. The damping in the structure controls the magnitude of the vibration amplitudes in the resonance. Usually the largest amplitude will occur at the first resonance frequency. So the largest error in the response will occur at the resonance frequency if the finite structure is replaced by an equivalent infinite structure. The driving-point mobility of a finite structure (for $e^{-i\omega t}$ notation) can be written as [27]

$$\frac{v}{F} = -i\omega \sum_N \frac{[\psi_n]^2}{\omega_n^2(1-i\eta) - \omega^2}, \quad (43)$$

where ω_n is the real resonance angular frequency, η the hysteretic loss factor, n the mode number, and ψ_n is the amplitude of the mode shape. If the damping is small then the effect of the off-resonance terms is small on the amplitude. For a finite structure an approximate driving-point mobility can be written as

$$\frac{v}{F} = \frac{[\psi_n]^2}{\omega_n \eta}, \quad (44)$$

if the spacing between resonances is large [27].

If the largest peak mobility values are used when a finite structure is modelled using mobilities of an infinite structure, then the worst case and the largest errors are obtained [27]. The ratio of the point mobility of a finite structure to the point mobility of an infinite structure is also represented in Table 2. From this table it is seen that in practical cases a good approximate mobility is obtained if the properties of an infinite structure is used when estimating the properties of a finite structure.

Table 2. Properties of infinite system (notes: *, torque applied about axis parallel to I_2 ; time dependence of form $e^{i\omega t}$ assumed) [27].

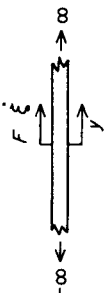


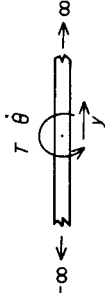


System	Driving point mobility	Power flow into system (P_s) force or torque source	Power flow into system; velocity or angular velocity source
Beam longitudinal wave motion; force excitation	 $\frac{\xi}{F} = \frac{1}{2A\sqrt{E\rho}}$	$P_s = \frac{ F ^2}{4A\sqrt{E\rho}}$	$P_s = 4 \xi ^2 A\sqrt{E\rho}$
Beam torsional wave motion; torque excitation	 $\frac{\theta}{T} = \frac{1}{2\sqrt{GQJ}}$	$P_s = \frac{ T ^2}{4\sqrt{GQJ}}$	$P_s = 4 \theta ^2 \sqrt{GQJ}$
Beam flexural wave motion; force excitation	 $\frac{\xi}{F} = \frac{(1-i)}{4A\rho\sqrt{\omega}} \left(\frac{A\rho}{EI}\right)^{1/4}$	$P_s = \frac{ F ^2}{8A\rho\sqrt{\omega}} \left(\frac{A\rho}{EI}\right)^{1/4}$	$P_s = \xi ^2 A\rho\sqrt{\omega} \left(\frac{EI}{\rho A}\right)^{1/4}$
Beam flexural wave motion; torque excitation	 $\frac{\theta}{T} = \frac{(1+i)\sqrt{\omega}}{4EI} \left(\frac{EI}{\rho A}\right)^{1/4}$	$P_s = \frac{ T ^2\sqrt{\omega}}{8EI} \left(\frac{EI}{\rho A}\right)^{1/4}$	$P_s = \frac{ \theta EI}{\sqrt{\omega}} \left(\frac{\rho A}{EI}\right)^{1/4}$
Plate flexural wave motion; force excitation	 $\frac{\xi}{F} = \frac{1}{8\sqrt{B_p\rho h}}$	$P_s = \frac{ F ^2}{16\sqrt{B_p\rho h}}$	$P_s = 4 \xi ^2 \sqrt{B_p\rho h}$
Plate flexural wave motion; torque excitation	 $\frac{\theta}{T} = \frac{\omega}{8B_p(1+L)} \times \left[1 - \frac{i4}{\pi} \ln ka + \frac{i8L}{\pi(1-\nu)} \left(\frac{h}{\pi a}\right)^2 \right]$	$P_s = \frac{\omega T ^2}{16B_p(1+L)}$	$P_s = \frac{4 \theta ^2 B_p(1+L)}{\omega \left\{ 1 + \left[\frac{4}{\pi} \ln ka - \frac{8L}{\pi(1-\nu)} \left(\frac{h}{\pi a}\right)^2 \right]^2 \right\}}$

Table 2. Continued

System	Onset of infinite behaviour	Largest point mobility of finite system	Ratio of finite system maximum to infinite system	Wavenumber (k)	Displacement of structure
Beam longitudinal wave motion; force excitation	$\omega > \frac{\pi}{\eta l} \sqrt{\left(\frac{E}{\rho}\right)}$	$\beta_1 = \frac{2}{\pi A \eta \sqrt{E \rho}}$	$\frac{ \beta_1 }{ \beta_\infty } = \frac{4}{\pi \eta}$	$k = \omega \sqrt{\left(\frac{\rho}{E}\right)}$	$\xi(y) = \frac{-iF e^{-iky}}{2\omega A \sqrt{E \rho}}$
Beam torsional wave motion; torque excitation	$\omega > \frac{\pi}{\eta l} \sqrt{\left(\frac{GQ}{J}\right)}$	$\beta_1 = \frac{2}{\pi \eta \sqrt{GQJ}}$	$\frac{ \beta_1 }{ \beta_\infty } = \frac{4}{\pi \eta}$	$k = \omega \sqrt{\left(\frac{J}{GQ}\right)}$	$\theta(y) = \frac{-iT e^{-iky}}{2\omega \sqrt{GQJ}}$
Beam flexural wave motion; force excitation	$\sqrt{\omega} > \frac{4\pi}{\eta l} \left(\frac{EI}{\rho A}\right)^{1/4}$	$\beta_1 = \frac{2l}{\pi^2 \eta \sqrt{\rho A EI}}$	$\frac{ \beta_1 }{ \beta_\infty } = \frac{4\sqrt{2}}{\pi \eta}$	$k = \sqrt{\omega} \left(\frac{\rho A}{EI}\right)^{1/4}$	$\xi(y) = \frac{-iF}{4EI k^3} [e^{-iky} - i e^{-ky}]$
Beam flexural wave motion; torque excitation	$\sqrt{\omega} > \frac{4\pi}{\eta l} \left(\frac{EI}{\rho A}\right)^{1/4}$	$\beta_1 = \frac{2}{\eta \eta \sqrt{\rho A EI}}$	$\frac{ \beta_1 }{ \beta_\infty } = \frac{2\sqrt{2}}{\pi \eta}$	$k = \sqrt{\omega} \left(\frac{\rho A}{EI}\right)^{1/4}$	$\xi(y) = \frac{T}{4EI k^2} [e^{-iky} - e^{-ky}]$
Plate flexural wave motion; force excitation	$\omega > \frac{8}{\eta l_1 l_2} \sqrt{\left(\frac{B_p}{\rho h}\right)}$	$\beta_1 = \frac{4l_1 l_2}{\pi^2 \eta \sqrt{\rho h B_p (l_1^2 + l_2^2)}}$	$\frac{ \beta_1 }{ \beta_\infty } = \frac{32l_1 l_2}{\pi^2 \eta (l_1^2 + l_2^2)}$	$k = \sqrt{\omega} \left(\frac{\rho h}{B_p}\right)^{1/4}$	Valid in far field only $\xi(r, \phi) = \frac{-iF}{8B_p k^2} \sqrt{\left(\frac{2}{rk\pi}\right)} e^{-i(ck - \eta/4)}$
Plate flexural wave motion; torque excitation	$\omega > \frac{8}{\eta l_1 l_2} \sqrt{\left(\frac{B_p}{\rho h}\right)}$	$\beta_1 = \frac{16l_2}{\eta \sqrt{\rho h B_p l_1 (2l_2^2 + l_1^2)}}$	*	$k = \sqrt{\omega} \left(\frac{\rho h}{B_p}\right)^{1/4}$	Valid in far field only $(r, \phi) = \frac{T}{8B_p k} \sqrt{\left(\frac{2}{rk\pi}\right)} e^{-i(ck - \pi/4)} \sin \phi$

Table 2. Continued. List of symbols [27].

A	cross-sectional area of beam	l	length of beam or plate; subscript, longitudinal waves
B_p	bending stiffness of plate [$= Eh^3/12(1-\nu)$]	m	bending moment
E	Young's modulus	r, ϕ	polar co-ordinates
F	force or pressure	t	time; subscript, torsional waves
GQ	torsional stiffness	u	shear force
I	second moment of area of beam	v	velocity
J	polar moment of inertia per unit length	x, y, z	Cartesian co-ordinates
L	parameter, from reference [9], which tends to unity for large a/h	β	mobility
P_a	power flow at station a	δ	dirac delta function
P_m	power flow associated with bending	η	loss factor
P_s	power supplied by source	θ	angular displacement
P_u	power flow associated with shear	ν	Poisson's ratio
T	torque	ξ	displacement
a	radius of disc over which torque applied to plate acts	ζ	imaginary component of flexural wavenumber ($1+i\zeta$)
e	2.718 ...	π	3.1415 ...
h	plate thickness	ρ	density
i	imaginary operator ($\sqrt{-1}$)	λ	wavelength
i	subscript, instantaneous value	ψ	mode shape
k	wavenumber	ω	radian frequency

4.9 Mechanical free impedance and complex impedance

The mechanical free impedance Z_{ij} is defined as the ratio of the excitation force phasor F_j at point j to the resulting velocity response-phasor v_i at point i , with all other connection points (Here point means both a location and a direction.) of the system having zero restraining forces

$$Z_{ij} = \frac{F_j}{v_i} = \frac{1}{Y_{ij}}. \quad (45)$$

Free impedance is the arithmetic reciprocal of a single element of the mobility matrix.

ISO 7626-1 [21] gives two important notes when utilizing measured or analytical impedance data: "1) Historically, no distinction has often been made between blocked impedance and free impedance. Caution should, therefore, be exercised in interpreting published data. 2) While experimentally determined free impedances could be assembled into a matrix, this matrix would be quite different from the blocked impedance matrix resulting from mathematical modelling of the structure and, therefore, would not conform to the requirements discussed in annex A for using mechanical impedance in an overall theoretical analysis system."

The complex impedance Z can be written as

$$Z = R + iX, \quad (46)$$

where the real part R is called the resistance and the imaginary part X the reactance. The SI unit of the mechanical impedance is $[(N \cdot s)/m]$.

4.10 Blocked mechanical impedance

ISO 7626-1 [21] defines blocked impedance Z_{ij} as follows: "The frequency-response function formed by the ratio of the phasor of the blocking or driving-point force response at point i to the phasor of the applied excitation velocity at point j , with all other measurement points on the structure "blocked" (i.e. constrained to have zero velocity). All forces and moments required to constrain fully all points of interest on the structure shall be measured in order to obtain a valid blocked impedance matrix. Blocked impedance measurements (see Cansdale, R. & al. A technique for measuring impedances of a spinning model rotor. Technical report TR 71092, Royal Aircraft Establishment, Farnborough, United Kingdom, May 1971) are, therefore, seldom made and are not dealt with in the various parts of ISO 7626. Notes: 1) Any changes in the number of measurement points or their location will change the blocked impedances at all measurement points. 2) The primary usefulness of blocked impedance is in the mathematical modelling of a structure using lumped mass, stiffness and damping elements or finite element techniques. When combining or comparing such mathematical models with experimental mobility data, it is necessary to convert the analytical blocked impedance matrix into a mobility matrix, or vice versa, as discussed in annex A."

4.11 Frequency response functions related to mobility

Other frequency-response functions, structural response ratios, which are used instead of mobility, are shown in Table 3.

Table 3. Equivalent definitions to be used for various kinds of measured frequency response functions related to mechanical mobility [21].

	Motion expressed as velocity	Motion expressed as acceleration	Motion expressed as displacement
Term	Mobility	Accelerance	Dynamic compliance
Symbol	$Y_{ij} = v_i / F_j$	a_i / F_j	x_i / F_j
Unit	m/(N·s)	m/(N·s ²) = kg ⁻¹	m/N
Boundary conditions	$F_k = 0; k \neq j$	$F_k = 0; k \neq j$	$F_k = 0; k \neq j$
Comment	Boundary conditions are easy to achieve experimentally		
Term	Blocked impedance	Blocked effective mass	Dynamic stiffness
Symbol	$Z_{ij} = F_i / v_j$	F_i / a_j	F_i / x_j
Unit	(N·s)/m	(N·s ²)/m = kg	N/m
Boundary conditions	$v_k = 0; k \neq j$	$a_k = 0; k \neq j$	$x_k = 0; k \neq j$
Comment	Boundary conditions are very difficult or impossible to achieve experimentally		
Term	Free impedance	Effective mass (free effective mass)	Free dynamic stiffness
Symbol	$F_j / v_i = 1 / Y_{ij}$	F_j / a_i	F_j / x_i
Unit	(N·s)/m	(N·s ²)/m = kg	N/m
Boundary conditions	$F_k = 0; k \neq j$	$F_k = 0; k \neq j$	$F_k = 0; k \neq j$
Comment	Boundary conditions are easy to achieve, but results shall be used with great caution in system modelling		

4.12 Boundary conditions of experimentation

In experimental determination of mechanical mobility, a dynamic exciting force is applied to the structure at one point at a time. Thus the force boundary conditions are [21]

$$F_k = 0; k \neq j, \quad (47)$$

where j is the point of excitation and k denotes all other points of interest. When the same force boundary conditions are valid, measurement of the velocity response at point i and the exciting force at j yields the ij th element of the mobility matrix [21]:

$$Y_{ij} = (v_i / F_j)_{F_k = 0; k \neq j}. \quad (48)$$

These force boundary conditions can easily be achieved in practise.

Instead the elements of the impedance matrix Z are [21]:

$$Z_{ij} = F_i / v_j, \quad (49)$$

where the boundary conditions

$$v_k = 0; k \neq j \quad (50)$$

are very difficult or impossible to fulfil in practice. Eqs. (49) and (50) describe mathematically the definition of blocked impedance. These boundary conditions imply that it is not generally possible to determine experimentally the impedance matrix. The difference between force and velocity boundary conditions (Eqs. (47) and (50)) must be kept in mind when using mobility and impedance data.

4.13 Mechanical mobility and impedance matrices

4.13.1 Definitions

It is assumed that linear, elastic structures are being considered, so that superposition and normal calculation rules are valid. The set of mobility elements y_{ij} is defined as follow [30]:

$$v_i = \sum_j y_{ij} f_j. \quad (51)$$

The set of impedance elements is defined as follow [30]:

$$f_i = \sum_j z_{ij} v_j. \quad (52)$$

4.13.2 Mechanical mobility matrix

Mechanical mobility is a tensor (or tensor component) which describes the effects upon the resultant velocity of the application of a force or forces on a structure [30]. It can be presented in the frequency domain by a matrix Eq. [30]:

$$\mathbf{V}(\omega) = \mathbf{Y}(\omega)\mathbf{F}(\omega), \quad (53)$$

where $\omega = 2\pi f$ is the angular frequency, f is frequency, $\mathbf{F}(\omega)$ is the column vector of exciting forces at various points, $\mathbf{V}(\omega)$ is the column vector of velocity responses at the points of interest, and $\mathbf{Y}(\omega)$ is symmetric tensor of mobilities y_{ij} . This matrix Eq. (53) in the expanded form looks like

$$\begin{aligned} v_1 &= y_{11}f_1 + y_{12}f_2 + y_{13}f_3 + \dots, \\ v_2 &= y_{21}f_1 + y_{22}f_2 + y_{23}f_3 + \dots, \\ v_3 &= y_{31}f_1 + y_{32}f_2 + y_{33}f_3 + \dots, \\ v_4 &= y_{41}f_1 + y_{42}f_2 + y_{43}f_3 + \dots, \text{ etc.} \end{aligned} \quad (54)$$

The term $y_{ij}f_j$ defines a velocity at point i caused by a force acting at a point j . If this velocity is noted by \bar{v}_{ij} , then [30]

$$v_i = \sum_j \bar{v}_{ij}. \quad (55)$$

It is seen from this equation that the mobility is a concept that sums velocity response [30].

The elements of the matrix \mathbf{Y} can be measured by applying the forces one at a time to each point of interest allowing the structure to respond as it chooses, and the individual elements are obtained as the complex ratio of the particular velocity response to the single exciting force. If for example only the force f_2 is applied, then Eq. (54) would reduce to the set [30]

$$\begin{aligned} \bar{v}_{12} &= y_{12}f_2, \\ \bar{v}_{22} &= y_{22}f_2, \\ \bar{v}_{32} &= y_{32}f_2, \end{aligned} \quad (56)$$

and so on, since $f_k = 0, k \neq 2$. Then the element y_{12} is obtained as the complex ratio

$$y_{12} = \bar{v}_{12} / f_2, \text{ etc.} \quad (57)$$

The reciprocity theorems of vibrations hold, and thus $y_{ij} = y_{ji}$ [30].

4.13.3 Impedance matrix

Impedance is a tensor (or tensor component) which describes the effects upon the resultant force (or several forces) of the application of a velocity or velocities on the structure. [30]. This can be represented by the matrix equation

$$\mathbf{F}(\omega) = \mathbf{Z}(\omega)\mathbf{V}(\omega), \quad (58)$$

where $\omega = 2\pi f$ is the angular frequency, f is frequency, $\mathbf{F}(\omega)$ is the column vector of resultant forces f_i , $\mathbf{V}(\omega)$ is the column vector of applied velocities v_j , and $\mathbf{Z}(\omega)$ is symmetric tensor of impedances z_{ij} . This matrix equation can be expanded as follow [30]

$$\begin{aligned} f_1 &= z_{11}v_1 + z_{12}v_2 + z_{13}v_3 + \dots, \\ f_2 &= z_{21}v_1 + z_{22}v_2 + z_{23}v_3 + \dots, \\ f_3 &= z_{31}v_1 + z_{32}v_2 + z_{33}v_3 + \dots, \\ f_4 &= z_{41}v_1 + z_{42}v_2 + z_{43}v_3 + \dots, \text{ etc.} \end{aligned} \quad (59)$$

The term $z_{ij}v_j$ defines a force at the point i caused by an applied velocity at the point j . If this force is called \bar{f}_{ij} , then

$$f_i = \sum_j \bar{f}_{ij}. \quad (60)$$

From Eq. (60) it is seen, that impedance is a concept that sums force response [30].

When determining the elements of impedance matrix \mathbf{Z} the velocities are applied one at a time to each point of interest, the structure is not allowed to response freely, instead it is constrained to have zero velocity at the points where other velocities will be applied, and the individual elements are obtained as the complex ratio of the particular force response to the single exiting velocity [30]. Consider an example were only the velocity v_2 is applied on the structure at the point 2 then the Eq. (59) will reduce to the set

$$\begin{aligned} \bar{f}_{12} &= z_{12}v_2, \\ \bar{f}_{22} &= z_{22}v_2, \\ \bar{f}_{32} &= z_{32}v_2, \end{aligned} \quad (61)$$

and so on, since $v_k = 0$, $k \neq 2$. In this case \bar{f}_{j2} ($j \neq 2$) is the blocking (constraining) force at the point j , when the structure is excited by a velocity at the point 2, which is necessary to constrain the velocity at the point j to zero, and \bar{f}_{22} is the force which results from the excitation motion at the point 2 [30]. The element of the impedance matrix is obtained from

$$z_{j2} = \bar{f}_{j2} / v_2. \quad (62)$$

According to reciprocity $z_{ij} = z_{ji}$ [30]. From Eqs. (53) and (58) it is easily seen that $\mathbf{Z} = \mathbf{Y}^{-1}$. According to matrix calculation the individual elements of impedance matrix are

not the arithmetic reciprocals of the elements of the mobility matrix, and vice versa, that is $z_{ik} \neq y_{ik}^{-1}$ except in the trivial case of only one point [30].

Notice that the point means the location and the corresponding direction. If in a system the number of points is N , then the order of vectors is N and the order of matrices is $N \times N$. The concept of immittance (impedance or admittance) and transmission matrices in the context of the vibration of mechanical systems is discussed in [33]. The mobilities on the contrary to the impedances of a given structure do not interdepend upon both the location and number of points of interest [30]. Mobilities describe invariant characteristics of the whole structure; instead impedances describe only substructures. During the mobility measurements the observations made anywhere on the system do not affect each other. Thus the mobility element y_{ij} remains the same although measurements are made at other points. Instead the impedance elements depend upon the number of observation points and the set of blocking forces used. So the impedance elements cannot be considered as invariant characteristics of the structure [30].

In some applications a complete mobility matrix has to be measured for the description of the dynamic characteristics of a structure. So translational forces and motions along three mutually perpendicular axes as well as moments and rotational motions may be required to be measured depending on the applications. These measurements result in a 6×6 mobility matrix for each measurement location. For N measurement locations this means a full $6N \times 6N$ mobility matrix.

However, in practice only seldom the full mobility matrix needs to be measured. Usually it suffices to measure only the driving-point mobility in the excitation location and a few transfer mobilities in locations of interest on the structure. Sometimes the dynamics of the system needs to be determined only in one co-ordinate direction, e.g., in vertical direction. Also in many practical engineering applications the influence of rotational motions and moments is negligible.

5 Effective mobility

5.1 Definitions

The elements of the mobility matrix are independent of the number of contact points. This is advantageous in practical analysis of the dynamical behaviour of structures. The mobility can be defined generally as [30], [37]

$$Y_{ij}^{km} = \frac{v_i^k}{F_j^m}, \quad k, m = 1, 2, \dots, N; \quad i, j = 1, 2, \dots, 6, \quad (63)$$

where F_j^m is the complex force applied in the direction j on an area m which is assumed to be small compared with the wavelength, and v_i^k is the complex spatially averaged velocity of another point k in the direction i due to that force. If the system considered consists of passive and linear elements, the reciprocity principle is valid and the mobility matrix is symmetric. In this case the indices of the elements can be transposed, if sub- and superscripts are transposed

simultaneously [37]. If the subscripts are omitted, the general definition of the mobility for each direction is [37]

$$Y^{km} = \frac{v^k}{F^m}, \quad (64)$$

where, for $k = m$, the mobility is called the point mobility of point k and for $k \neq m$, the mobility is called the transfer mobility from point k to point m .

The magnitude of a typical ordinary point mobility peaks at resonance frequencies (see Figure 14). Minima instead are observed at frequencies where the response is formed by a destructive interference of a couple of vibration modes whose eigenfrequencies are near each other.

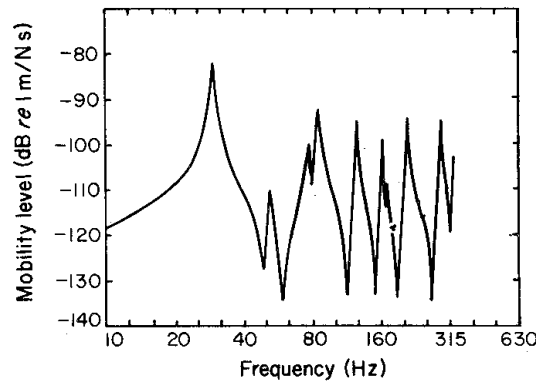


Figure 14. Plot of a typical, ordinary point mobility [37].

If the structure is excited by a force with complex amplitude \hat{F} in one point giving the structure in this same point a velocity in the same direction with complex amplitude \hat{v} , then the structure-borne input sound power P , which is a real quantity, is obtained from [23]

$$P = \frac{1}{2} \text{Re}[\hat{F} \hat{v}^*]. \quad (65)$$

Using the definition of point mobility and taking into account that $Y^* = \hat{v}^* / \hat{F}^*$, the power can be expressed as

$$P = \frac{1}{2} |\hat{F}|^2 \text{Re}[Y] = \frac{1}{2} \frac{|\hat{v}|^2}{|Y|^2} \text{Re}[Y]. \quad (66)$$

When the structure is excited simultaneously in N points, the power injected in each point n can be calculated separately, if the contributions from other points are taken into account properly. This can be done using the general mobility as

$$P^n = \frac{1}{2} \text{Re} \left[F^{n*} \sum_{k=1}^N Y^{nk} F^k \right] \quad (67)$$

and the total power from all points is

$$P^n = \frac{1}{2} \operatorname{Re} \sum_{n=1}^N \left[F^{n*} \sum_{k=1}^N Y^{nk} F^k \right]. \quad (68)$$

5.1.1 Effective point mobility

Let us consider a system with N contact points between the source of structure-borne sound and the receiving structure sketched in Figure 15. Then the transmitted power into the n th contact point can be calculated from [37]

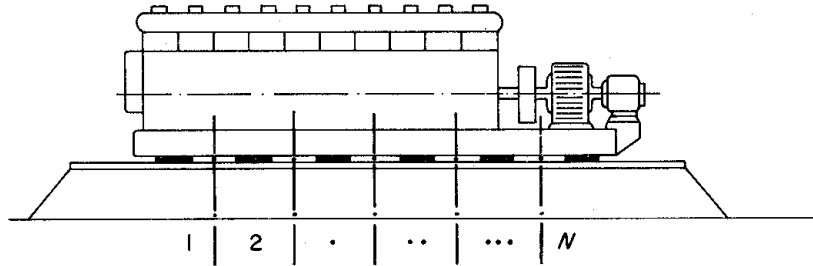


Figure 15. An example of a multi-point coupled structure-borne sound source and receiving structure [37].

$$P^n(\omega) = \frac{1}{2} \operatorname{Re} \left[F^n(\omega) v^{n*}(\omega) \right], \quad (69)$$

where F^n is the complex force and v^{n*} is the complex conjugate of the velocity at the same contact point n .

Considering at the k th contact point the velocity response, which is caused by the forces acting at all N contact points, the actual velocity v^k is obtained using the transfer mobilities Y^{kn} from point n to k as

$$v^k = Y^{k1} F^1 + Y^{k2} F^2 + \dots + Y^{kk} F^k + \dots + Y^{kN} F^N \quad (70)$$

the effective point mobility can be defined as [37], [40]

$$Y_{ii}^{nn\Sigma} = \left(\sum_{k=1}^N \sum_{j=1}^N Y_{ij}^{nk} F_j^k \right) / F_i^n = v_i^n / F_i^n, \quad (71)$$

where the superscript Σ means that contributions from all contact points are within the summation. Remember that the mobility is a concept, which sums (see Eq. (55)) velocity response [30]. In the Eq. (71) Y^{nk} is the general mobility element when F^k is the complex force acting at point k and velocity is measured at point n . So the effective mobility gives the ratio of the total velocity due to all applied forces to the force acting at the same point n .

The power transmitted through the n th connection point is [37]

$$P^n = \frac{1}{2} |F^n|^2 \operatorname{Re}[Y^{nn\Sigma}]. \quad (72)$$

The effective impedance is defined analogously as [37]

$$Z^{nn\Sigma} = \left(\sum_{k=1}^N Z^{kn} v^k \right) / v^n = F^n / v^n \quad (73)$$

and using the effective impedance the power is obtained from [37]

$$P^n = \frac{1}{2} |v^n|^2 \operatorname{Re}[Z^{nn\Sigma}]. \quad (74)$$

It should be noted that for effective mobility and impedance matrix elements [37]

$$Y^{nn\Sigma} = 1/Z^{nn\Sigma}, \quad (75)$$

whereas for ordinary mobility and impedance matrix elements this relationship does not hold. The negative real part of the effective mobility means that the energy is flowing from the receiver to the source at that contact point [37]. It can be shown [39] that the real part of the effective mobility can be calculated from

$$\operatorname{Re}[Y^{nn\Sigma}] = \operatorname{Re}[Y^{nn}] + \operatorname{Re} \left[\sum_{\substack{k=1 \\ k \neq n}}^N Y^{kn} e^{j\varphi^F_{kn}} \right] \approx \operatorname{Re}[Y^{nn}], \quad (76)$$

which means that the real part of the ordinary mobility can be used. So the structure-borne sound power through the n th contact point is obtained from [37]

$$P^n \approx \frac{1}{2} |F^n|^2 \operatorname{Re}[Y^{nn}] = \frac{1}{2} |v^n|^2 \operatorname{Re}[Y^{nn}] / |Y^{nn\Sigma}|^2. \quad (77)$$

The magnitude of the effective mobility $|Y^{nn\Sigma}|$ can be estimated in two important cases as [37]

(a) When the magnitudes $|Y^{nk}|$ are approximately alike and the phase angles of \underline{Y}^{nk} are randomly distributed and furthermore

$$|Y^{nk}| \approx |Y^{nn}| \text{ for all } n \neq k, \quad (78)$$

then

$$|Y^{nn\Sigma}| \approx \sqrt{N} \cdot |Y^{nn}|. \quad (79)$$

(b) When the following inequality holds

$$|Y^{nk}| \ll |Y^{nn}| \text{ for all } n \neq k, \quad (80)$$

then the magnitude is obtained from

$$|Y^{nn\Sigma}| \approx |Y^{nn}|. \quad (81)$$

5.1.2 Effective total mobility

The power transmitted through all the contact points can be treated formally like in a single contact point case. In doing so one needs the effective force defined as [37]

$$F^{EFF} = S / \sqrt{\langle \tilde{v}^2 \rangle}, \quad (82)$$

where S is the total, transmitted, complex power and $\langle \tilde{v}^2 \rangle$ is the spatially averaged mean square velocity. Analogously to the one contact point case the effective total mobility can be defined as [37]

$$Y^{EFF} = \sqrt{\langle \tilde{v}^2 \rangle} / F^{EFF} = \langle \tilde{v}^2 \rangle / S. \quad (83)$$

If the source and receiver are connected by N similar vibration isolators and the vibrations are approximately uncoupled between different directions of motion, then the effective mobility of the receiver can be obtained from [37]

$$Y_R^{EFF} = \langle \tilde{v}_R^2 \rangle / \sum_{k=1}^N \left[\left(Z_{21}^{kk} \frac{v_S^k}{v_R^k} + Z_{22}^{kk} \right) \right] (\tilde{v}_R^k)^2, \quad (84)$$

where $\langle \tilde{v}_R^2 \rangle$ is the average mean square velocity of the receiver, Z_{21}^{kk} is the transfer impedance of one single isolator, Z_{22}^{kk} is the input impedance of one isolator seen from the receiver side, v_S^k and v_R^k are the complex vibration velocities of the source and receiving structure at the contact point k , respectively. If the overall effective mobility is developed for the source then Z_{22} is replaced by Z_{11} for the isolators and $Z_{12} = Z_{21}$ due to reciprocity.

Using the effective total mobility the power transmitted to the receiver is obtained from [37]

$$P_R = \left\{ \text{Re} \left[Y_R^{EFF} \right] \langle \tilde{v}_R^2 \rangle \right\} / \left| Y_R^{EFF} \right|^2. \quad (85)$$

If the input impedance Z_{22}^{kk} is small compared to the other term ($Z_{21}^{kk} v_S^k / v_R^k$) in Eq. (84), the total power can be approximated by [37]

$$P_R \approx \sum_{k=1}^N \text{Re} \left[Z_{21}^{kk} v_S^k / v_R^k \right] (\tilde{v}_R^k)^2. \quad (86)$$

This approximation is valid when the transfer impedance of the isolator is much smaller than the effective point impedance of the receiving structure [37]. A similar result for the transmitted power is obtained using the effective point impedance, which is obtained from [37]

$$Z_R^{kk\Sigma} \approx Z_{21}^{kk} v_S^k / v_R^k. \quad (87)$$

Notice that the effective mobilities are not invariant quantities of the structure. The effective point mobility of any point depends on what other points are considered in the analysis and on the force distribution in that particular case [37].

5.1.3 Measurement of effective mobility

Petersson and Plunt [37], [38] examined theoretically and in the laboratory both the effective point mobility and effective overall mobility. The determination of the effective point mobility was made attaching an accelerometer at one position and exciting the structure with a hammer stroke at this point and the other points sequentially. The force in the stroke area of the hammer was measured using a force transducer. At least ten samples of each transfer function were averaged. This method was applied when the point and transfer mobilities were measured. Thereafter the effective point mobility was calculated from Eq. (71) assuming that the forces had equal magnitude at each point. During the measurements the structure was loaded neither by the equipment nor by the experimenter.

The measurement arrangement used during the determination of the effective mobility is sketched in Figure 16. In these test a number of vibration isolators was thoroughly tested and matched with respect their impedance characteristics. The cylindrical

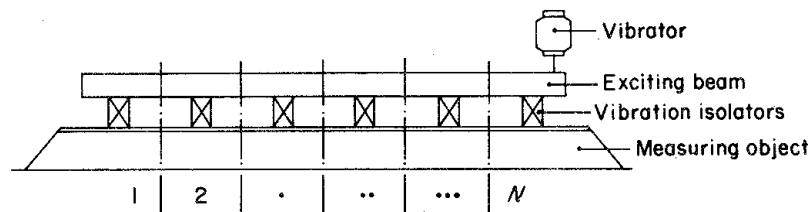


Figure 16. Principal sketch showing the experimental arrangements for the investigations of the effective overall mobility [37].

isolators were glued to the measuring object and screwed to the specially designed I-beam above them. The beam was excited using a vibrator via a steel rod that was attached nearly at the end of the beam. The velocities and their phase were measured above and below of each isolator representing a contact point. The overall effective mobility was calculated using Eq. (84). In this equation the impedance characteristics of the isolators are needed in addition to the measured velocities and their phase angle information.

Petersson and Plunt used a stiffened steel deck mock-up (see Figure 17) and a homogenous concrete plate as test objects.

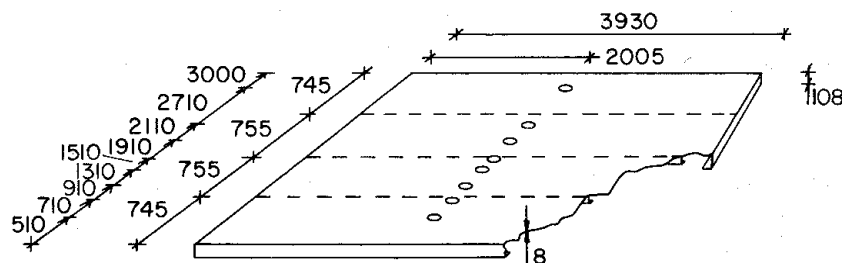


Figure 17. Sketch of the stiffened steel deck showing the dimensions (mm), the frame spacing and the measurement positions, \circ [37].

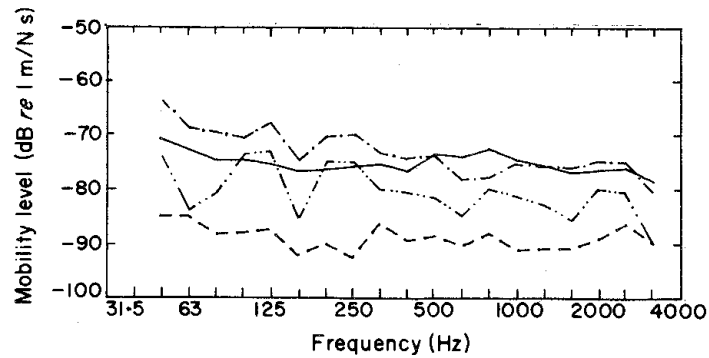


Figure 18. Comparison of point mobility and effective point mobilities for a frame-stiffened steel deck. — Point mobility, and - - - - - effective point mobility for a point on a subplate. Point mobility, and - · - · - effective point mobility for a point at a stiffener [37].

In Figure 18 are seen the ordinary point mobility and the effective point mobility of a point on one of the subpanels of the steel deck shown in Figure 17 compared with that at one point on a stiffener. The point mobility of the point on a stiffener is much lower than for a point on a subpanel. The difference between ordinary and effective mobility levels is rather small for a point on a subpanel. This means that the vibration levels are mainly affected by interactions between points on the same subpanel. In Figure 19 typical transfer mobilities and the ordinary point mobilities for a frame-stiffened steel deck are compared in some points on a subplate and on a stiffener. In Figure 20 Petersson and Plunt give an example of the magnitude of the effective overall mobility of the steel deck and of the concrete plate.

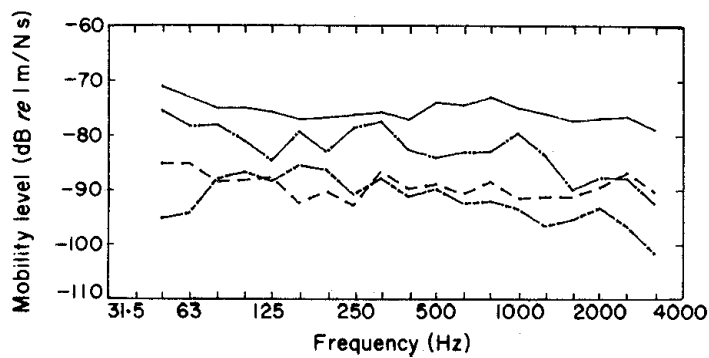


Figure 19. Comparison of typical point and transfer mobilities for a frame-stiffened steel deck. — Point mobility for a point on a subplate, - - - - - point mobility for a point at a stiffener, - · - · - transfer mobility between two points on the same subplate, transfer mobility between two points on either side of a stiffener [37].

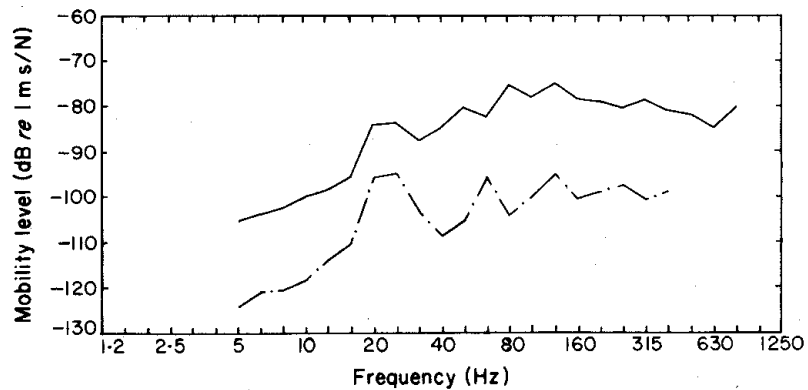


Figure 20. — Effective overall mobility level for a stiffened steel deck and --- a concrete plate [37].

Petersson and Plunt investigated typical relations between magnitudes of point and transfer mobilities making measurements of a large diesel generator (see Figure 21) and a ship structure (see Figure 22) [38]. The double-bottom structure under measurements was the foundation structure on board a ship for the same type of diesel generator set. The measurement method was described in [37], [39]. They observed from measurements on ship foundation models that the ordinary point mobility seems to be determined by the static stiffness of the excited substructure when the frequency is below the first resonance frequency of this structure. Above the first resonance frequency the effect of the characteristic mobility is seen. Then the ordinary point mobility is the mobility of the corresponding infinite system added with the effect of resonances.

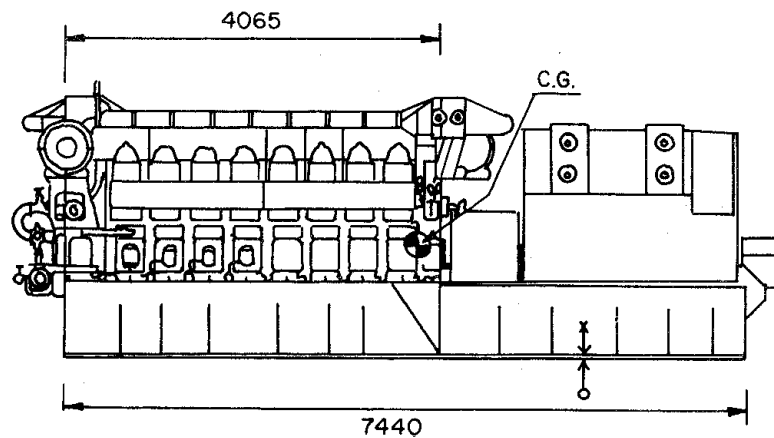


Figure 21. Sketch showing the diesel generator. Examples of measurement and excitation positions are marked by $\circ\uparrow$ and $\circ\downarrow$ respectively [38].

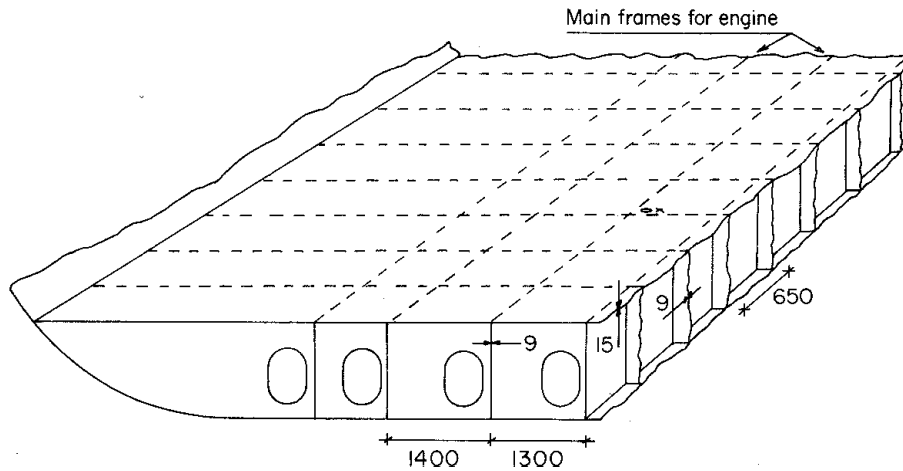


Figure 22. Sketch showing the double-bottom structure. Examples of measurements and excitation positions are marked by \circ and \times respectively [38].

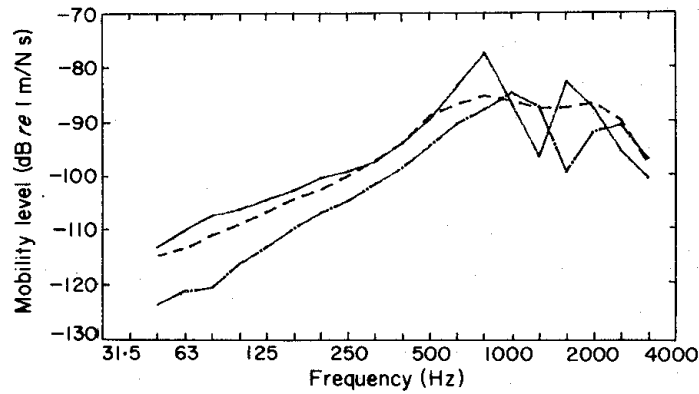


Figure 23. Examples of the ordinary point mobility for the diesel generator baseplate, measured in the vertical direction [38].

In Figure 23 are shown some measured point mobilities in the vertical direction for the diesel generator baseplate in one-third octave bands with centre frequencies from 50 Hz to 3 200 Hz. From this Figure it can be noticed that the curve resembles the behaviour of a stiffness-controlled system in the frequency range from 50 Hz to 500 Hz [38]. After the first natural frequency of the subplates between the vertical stiffeners and upwards the resonant subplate response is observed in the mobility curve [38].

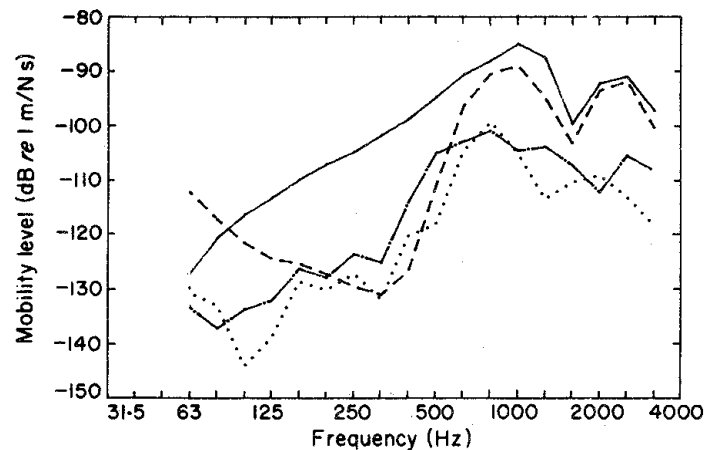


Figure 24. ---, ····, -·-· Comparison of transfer mobilities and — an ordinary point mobility, measured in the vertical direction on a diesel generator baseplate [38].

Above the frequency 50 Hz the typical transfer mobilities are lower than the ordinary point mobility, see Figure 24. The difference is large in the frequency range where the mobility curve is dominated by the stiffness of the subplate excited [38]. In the frequency region where the subplates resonate the transfer and ordinary mobilities are almost of the same magnitude.

For the double-bottom structure the comparison of typical transfer mobilities and point mobility is given in Figure 25. It is seen that the transfer mobilities are much smaller than the ordinary point mobility in magnitude. The measurement results that Petersson and Plunt obtained for a diesel generator baseplate and for the double-bottom show that the transfer mobilities between contact points are smaller than ordinary point mobilities if the contact points are separated at least by one stiffener between them [38].

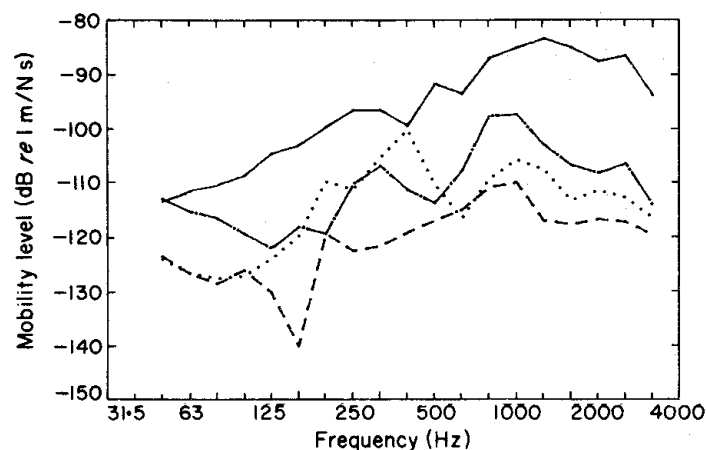


Figure 25. ---, ····, -·-· Comparison of transfer mobilities and — ordinary point mobility, measured in the vertical direction on the bedplate of a diesel engine foundation [38].

5.2 Applications of mechanical mobility measurements

Applications where mobility measurements are used include [21]: a) prediction of the dynamic response of structures to known or assumed input excitation; b) determination of the modal

properties of a structure, e.g., natural frequencies, mode shapes and damping ratios; c) prediction of the dynamic interaction of interconnected structures; d) checking of the validity and improvement of the accuracy of mathematical models; and e) determination of dynamic properties, e.g., the complex modulus of elasticity of materials.

6 Analysis of mechanical systems

6.1 Impedance and mobility of a system of elements

The mechanical impedance or mobility of a system of connected elements at a point of interest can be calculated using Eqs. (34) through (37) and the properties of ideal mechanical elements presented in Table 4. Generally this results in a complex impedance or mobility function which represents an equivalent system for the original system of connected elements. This equivalent system has same dynamic characteristics as the original system. According to Eq. (35) complex impedance represents parallel-connected elements from which the real part represents a purely resistive element and the imaginary part a purely reactive element. A complex mobility represents according to Eq. (36) series connected elements from which the real part represents a purely resistive element and the imaginary part a purely reactive element. These two elements of an equivalent system need not to be the ideal resistance, spring or mass. For instance the resistance may vary with frequency and the reactance may behave springlike, masslike or even be zero depending on frequency. The characteristics of real physical elements may be nonlinear and all elements have some mass, and at very high frequencies when the wavelength becomes comparable with the element dimensions the wave phenomena may arise [36].

Table 4. Impedance and mobility of ideal lumped elements, parallel and series connected elements.

Ideal mechanical element or system	Impedance [(N·s)/m]	Mobility [m/(N·s)]
mass	$i\omega m$	$\frac{1}{i\omega m} = \frac{-i}{\omega m}$
resistance	c	$1/c$
spring	$\frac{k}{i\omega} = \frac{-ik}{\omega}$	$\frac{i\omega}{k}$
parallel connected elements	$Z_p = \sum_{i=1}^n Z_i$	$\frac{1}{Y_p} = \sum_{i=1}^n \frac{1}{Y_i}$
series connected elements	$\frac{1}{Z_s} = \sum_{i=1}^n \frac{1}{Z_i}$	$Y_s = \sum_{i=1}^n Y_i$

6.2 Kirchhoff's Laws

Kirchhoff's Laws:

1) The sum of all the forces F_i which act at a connection point of elements is zero

$$\sum_i^n F_i = 0. \quad (88)$$

2) The sum of the relative velocities v_i around a closed loop of series-connected elements is zero

$$\sum_i^n v_i = 0. \quad (89)$$

6.3 Superposition theorem

Superposition theorem: The response at a point of a mechanical system formed by linear bilateral elements can be calculated summing the response to each vibration source at a time when the other sources are not supplying energy but they are taken into account by their internal impedances in the mechanical system.

The superposition method is applicable for instance when there are several vibration sources in a system to be analyzed.

6.4 Reciprocity theorem

Reciprocity theorem in acoustics may be stated as follows [23, p. 550]: "If a force F_1 that acts at a point P_1 produces a velocity v_{12} at point P_2 , then this same force ($F_1 = F_2$) acting at the point P_2 will produce at point P_1 the velocity $v_{21} = v_{12}$. Thus, the ratio of the exciting force to the observed velocity remains the same if the excitation and observation points are interchanged, provided also that the direction in which the force acts in each case is the same as that in which the velocity is measured in the other case." Reciprocal measurements can be used e.g. for the measurement of transfer functions in linear mechano-acoustical systems [25].

6.5 Thévenin's equivalent circuit

Thévenin's equivalent circuit: A mechanical circuit formed by linear bilateral elements, which contains vibrational force sources and which produces an output to a load impedance at some attachment point at any particular frequency, can be replaced at that frequency by a single constant frequency vibrational force source F_c in parallel with the internal impedance Z_i of the circuit connected to the load [36].

The force F_c , called clamped force, represents the transmitted force by the attachment point when it is connected to an infinitely rigid structure (see Figure 26) [36]. The internal impedance Z_i of the circuit can be determined from the circuit when the force source is

removed from it. When there is no load at the attachment point, then the free velocity v_f can be measured and $v_f = F_c / Z_i$.

When the point b is attached to a rigid structure, there is no motion at the impedance Z_3 , which is why it is omitted in the Figure 26 b). The impedances Z_1 and Z_2 are connected in parallel in the Figure 26 b) and their total impedance is obtained from Eq. (35). Using the Kirchhoff's first law which states that the sum of the node forces is zero one obtains at the point a that the force $F = v_a(Z_1 + Z_2)$. So the velocity $v_a = F / (Z_1 + Z_2)$ and the clamped force transmitted by point b is $F_c = v_a Z_2 = F Z_2 / (Z_1 + Z_2)$. The internal impedance of the circuit seen at the point b in Figure 26 c) is calculated using Eqs. (35) and (37) as $Z_i = Z_3 + \frac{1}{1/Z_1 + 1/Z_2}$. Thus the parameters needed for the Thévenin's equivalent circuit given in Figure 26 d) are determined using the known values of impedances and force.

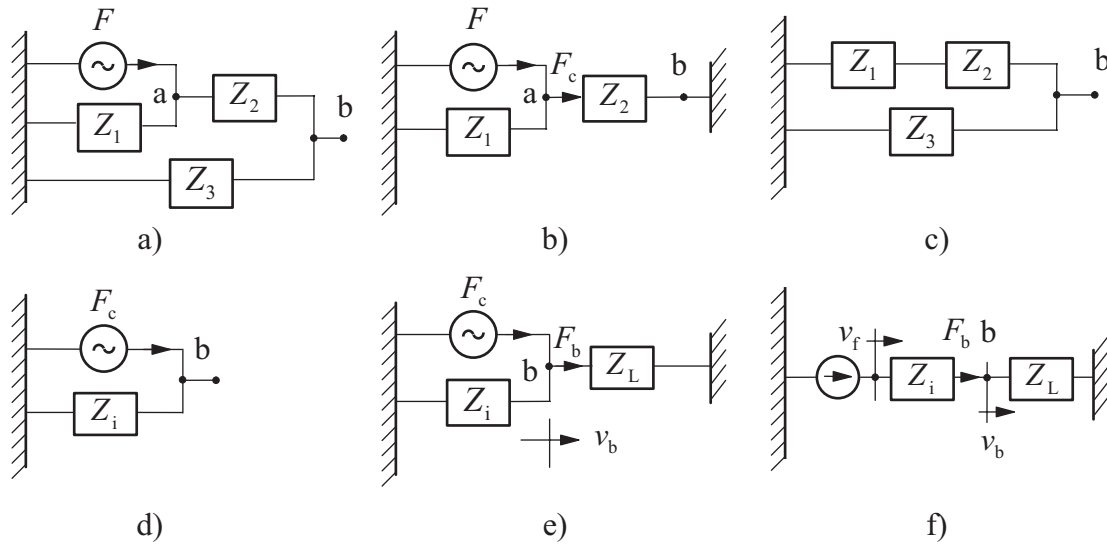


Figure 26. A circuit formed by mechanical elements: a) element impedances Z_1 , Z_2 , and Z_3 including vibrational force source F and the connection point b for a load impedance Z_L , b) F_c is the constant force transmitted to a rigid immovable structure when the point b is clamped to it, c) the circuit for the determination of the internal impedance Z_i of the Thévenin's equivalent circuit when the force source F is removed from the original circuit described in a), d) the Thévenin's equivalent circuit, e) the Thévenin's equivalent circuit exerting the force F_b and velocity v_b to a load impedance Z_L , and f) the Norton's equivalent circuit comprising of a velocity source v_f in series with an internal impedance Z_i is connected to a load impedance Z_L at the point b exerting the force F_b and generating the velocity v_b , adapted from [36].

When the load impedance Z_L is connected to the circuit at the point b (see Figure 26 e)) the velocity v_b and the force F_b exerted to the load impedance can be calculated as follows: using the Kirchhoff's first law which states that the sum of the node forces is zero one obtains at the point b $F_c = v_b(Z_i + Z_L)$. And solving for velocity one obtains

$$v_b = \frac{F_c}{Z_i + Z_L}. \quad (90)$$

The force at the point b is then $F_b = v_b Z_L$ or

$$F_b = \frac{F_c Z_L}{Z_i + Z_L} = F_c - Z_i v_b. \quad (91)$$

The force and velocity at point b can be calculated for any load impedance Z_L from Eqs. (90) and (91).

6.6 Norton's equivalent circuit

A mechanical system of linear and bilateral elements containing vibration sources and an output connection for load impedance can be analyzed using Norton's equivalent circuit. At any particular frequency this replaces the circuit of mechanical elements by a single constant-velocity vibration source v_f in series with internal impedance Z_i . Norton's equivalent circuit is the counterpart of the Thévenin's equivalent circuit. It depends on the system to be analyzed which of these is easier to apply, the series equivalent or the parallel equivalent representation of source and internal impedance. The clamped force used in the Thévenin's equivalent circuit is obtained easily from the free velocity and the internal impedance as $F_c = v_f Z_i$.

For the mechanical circuit presented in Figure 26 a) the Norton's equivalent circuit can be determined as follows: The free velocity v_f needed at the load connection point b can be determined with the aid of Figure 26 a) applying the Kirchhoff's first law at the points a and b and denoting $v_b = v_f$, then

$$F = (Z_1 + Z_2)v_a - Z_2 v_f,$$

$$0 = -Z_2 v_a + (Z_2 + Z_3)v_f.$$

These equations are solved for v_f

$$v_f = \frac{FZ_2}{Z_1 Z_2 + Z_1 Z_3 + Z_2 Z_3}.$$

The internal impedance of the circuit seen at the point b in Figure 26 c) is calculated using Eqs. (35) and (37) as $Z_i = Z_3 + \frac{1}{1/Z_1 + 1/Z_2}$. Figure 26 f) shows the Norton's equivalent circuit connected to the load impedance Z_L at the point b. The elements are connected in series and transmit the same force F_b which is obtained with the mobility or impedance of elements using Eq. (36) for the series connected mobilities as

$$F_b = \frac{v_f}{Y_i + Y_L} = \frac{v_f}{1/Z_i + 1/Z_L} = \frac{v_f Z_i Z_L}{Z_i + Z_L}. \quad (92)$$

The velocity at the point b is obtained from

$$v_b = \frac{F_b}{Z_L} = \frac{v_f Z_i}{Z_i + Z_L} = \frac{v_f Y_L}{Y_i + Y_L}. \quad (93)$$

So the force and velocity at the connection point b can be determined for any load mobility Y_L (load impedance Z_L) in terms of the constant free velocity v_f and the internal mobility Y_i (impedance Z_i) from the Norton's equivalent circuit as shown above.

6.7 Analysis methods

As a result of an analysis of a mechanical system using impedance methods one obtains the forces acting on the elements forming the system and the velocities of their connection points. Many other quantities can be derived from these quantities e.g. displacement and acceleration of a sinusoidal vibration [36].

Kirchhoff's force law at a point Eq. (88) allows one to write down simultaneous equations for the determination of all forces and velocities in a system of mechanical elements. Usually this is made for each connection point of elements (force node) in terms of impedances and velocities. At a connection point of elements there is a same velocity compared to a stationary reference point.

Instead the Kirchhoff's velocity law around a loop Eq. (89) allows one to write down velocity equations for each independent mechanical circuit loop in terms of forces and mobilities. This method can be applied in the analysis of series-connected elements.

6.8 Example of analysis

The general laws of circuit analysis are applied in a practical example to see how they work in practise. Determine the velocities of all the connection points and the forces, which act on the elements in the system of Figure 27. There are two velocity sources v_1 and v_6 of known strength operating at the same frequency but in opposite phase.

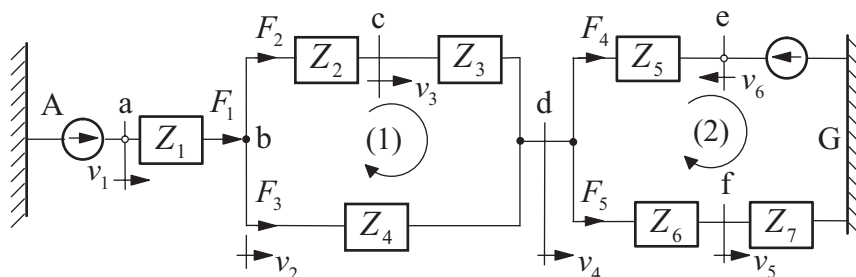


Figure 27. A mechanical system with two vibration sources v_1 and v_6 of known strength operating at the same frequency but in the opposite phase and seven impedances $Z_1 \dots Z_7$ [36].

Solutions (see [36]):

A: Using Kirchhoff's force law (Eq. (88)) let us first write down a force equilibrium equation at each connection point except at points a and e.

At the point b: $F_1 - F_2 - F_3 = 0$. This can be expressed with the aid of velocities and impedances remembering that relative velocity over the ends of an element times impedance is force ($v_{\text{rel}}Z = F$) as

$$(v_1 - v_2)Z_1 - (v_2 - v_3)Z_2 - (v_2 - v_4)Z_4 = 0. \quad (\text{a})$$

At the point c: at the connection point of two series elements the same force is acting on both elements, thus $F_2 - F_2 = 0$. With the aid of velocities and impedances one gets

$$(v_2 - v_3)Z_2 - (v_3 - v_4)Z_3 = 0. \quad (\text{b})$$

At the point d: $F_2 + F_3 - F_4 - F_5 = 0$. With the aid of velocities and impedances and noting that v_6 is (+) because there is a 180° phase difference compared to v_1 one gets

$$(v_3 - v_4)Z_3 + (v_2 - v_4)Z_4 - (v_4 + v_6)Z_5 - (v_4 - v_5)Z_6 = 0. \quad (\text{c})$$

At the point f: $F_5 - F_5 = 0$. With the aid of velocities and impedances one obtains

$$(v_4 - v_5)Z_6 - v_5Z_7 = 0. \quad (\text{d})$$

From the above four equations the four unknown velocities v_2 , v_3 , v_4 , and v_5 can be solved. With the obtained velocities the forces are calculated from

$$\begin{aligned} F_1 &= (v_1 - v_2)Z_1 & F_2 &= (v_2 - v_3)Z_2 = (v_3 - v_4)Z_3 \\ F_3 &= (v_2 - v_4)Z_4 & F_4 &= (v_4 + v_6)Z_5 \\ F_5 &= (v_4 - v_5)Z_6 = v_5Z_7 \end{aligned}$$

B: The method of *node forces*, rule: At each connection point with a common velocity (force node), equate the force generators to the sum of the impedances connected to that node multiplied by the velocity of that node minus the impedances multiplied by the velocities of their other connection points. Using this rule the equations of solution A can be rewritten in the form (see Figure 27)

$$v_1Z_1 = (Z_1 + Z_2 + Z_4)v_2 - Z_2v_3 - Z_4v_4. \quad (\text{a}')$$

$$0 = -Z_2v_2 + (Z_2 + Z_3)v_3 - Z_3v_4. \quad (\text{b}')$$

$$-v_6Z_5 = -Z_4v_2 - Z_3v_3 + (Z_3 + Z_4 + Z_5 + Z_6)v_4 - Z_6v_5. \quad (\text{c}')$$

$$0 = -Z_6v_4 + (Z_6 + Z_7)v_5. \quad (\text{d}')$$

C: Using Kirchhoff's law (89) for loop velocities to be zero one can write a velocity equation in terms of forces and velocities around a closed loop. One needs as many loops as there are unknowns to be solved. From Figure 27 one sees that

$$F_3 = F_1 - F_2 \quad \text{and} \quad F_5 = F_1 - F_4.$$

Loop (1) equation:

$$F_2(Y_2 + Y_3) - (F_1 - F_2)Y_4 = 0. \quad (\text{e})$$

The minus sign of the second term takes into account that the loop goes across element 4 in a direction opposing the direction of the force direction shown in the Figure 27.

Loop (2) equation:

$$F_4Y_5 - v_6 - (F_1 - F_4)(Y_6 + Y_7) = 0. \quad (\text{f})$$

Loop from A to B along the upper branch: Notice that the velocities are relative velocities ($v = FY$) across the elements, thus the first term is $(0 - v_1)$ and the last one $-(v_1 - 0)$ owing to the sign rule

$$(0 - v_1) + F_1Y_1 + F_2(Y_2 + Y_3) + F_4Y_5 - (v_1 - 0) = 0. \quad (\text{g})$$

Solving the Eqs. (e), (f), and (g) one obtains the unknown forces F_1 , F_2 , and F_4 . The other forces are obtained from $F_3 = F_1 - F_2$, and $F_5 = F_1 - F_4$. The velocities are obtained from

$$v_2 = v_1 - F_1Y_1, \quad v_3 = v_2 - F_2Y_2, \quad v_4 = v_2 - F_3Y_4, \quad \text{and} \quad v_5 = F_5Y_7.$$

A numerical example: calculate the velocities and forces in the previous example using the values without SI units: $v_1 = 1$, $v_6 = 2$; $Z_1 = 1$, $Z_2 = 2$, $Z_3 = 3$, $Z_4 = 4$, $Z_5 = 5$, $Z_6 = 6$, and $Z_7 = 7$.

Solution:

A: After inserting the values given into the Eqs. (a), (b), (c), and (d) one obtains four simultaneous equations

$$\begin{bmatrix} -7v_2 & 2v_3 & 4v_4 & 0 \\ 2v_2 & -5v_3 & 3v_4 & 0 \\ 4v_2 & 3v_3 & -18v_4 & 6v_5 \\ 0 & 0 & 6v_4 & -13v_5 \end{bmatrix} = \begin{bmatrix} -7 & 2 & 4 & 0 \\ 2 & -5 & 3 & 0 \\ 4 & 3 & -18 & 6 \\ 0 & 0 & 6 & -13 \end{bmatrix} \begin{Bmatrix} v_2 \\ v_3 \\ v_4 \\ v_5 \end{Bmatrix} = \begin{Bmatrix} -1 \\ 0 \\ 10 \\ 0 \end{Bmatrix}$$

$$\Rightarrow \begin{Bmatrix} v_2 \\ v_3 \\ v_4 \\ v_5 \end{Bmatrix} = \begin{Bmatrix} -0,686 \\ -0,88 \\ -1,01 \\ -0,466 \end{Bmatrix}.$$

Notice that the impedance matrix is symmetric about the main diagonal. As the impedance matrix is always symmetric, this serves as a useful check for the correctness of the equations.

B: Inserting the given values to Eqs. (a'), (b'), (c'), and (d') one obtains

$$\begin{bmatrix} 7v_2 & -2v_3 & -4v_4 & 0 \\ -2v_2 & 5v_3 & -3v_4 & 0 \\ -4v_2 & -3v_3 & 18v_4 & -6v_5 \\ 0 & 0 & -6v_4 & 13v_5 \end{bmatrix} = \begin{bmatrix} 7 & -2 & -4 & 0 \\ -2 & 5 & -3 & 0 \\ -4 & -3 & 18 & -6 \\ 0 & 0 & -6 & 13 \end{bmatrix} \begin{Bmatrix} v_2 \\ v_3 \\ v_4 \\ v_5 \end{Bmatrix} = \begin{Bmatrix} 1 \\ 0 \\ -10 \\ 0 \end{Bmatrix}$$

$$\Rightarrow \begin{Bmatrix} v_2 \\ v_3 \\ v_4 \\ v_5 \end{Bmatrix} = \begin{Bmatrix} -0,686 \\ -0,88 \\ -1,01 \\ -0,466 \end{Bmatrix}.$$

C:

$$\begin{bmatrix} -0,25F_1 & 1,0833F_2 & 0 \\ -0,3095F_1 & 0 & 0,5095F_4 \\ F_1 & 0,833F_2 & 0,2F_4 \end{bmatrix} = \begin{bmatrix} -0,25 & 1,0833 & 0 \\ -0,3095 & 0 & 0,5095 \\ 1 & 0,833 & 0,2 \end{bmatrix} \begin{Bmatrix} F_1 \\ F_2 \\ F_4 \end{Bmatrix} = \begin{Bmatrix} 0 \\ 2 \\ 3 \end{Bmatrix}$$

$$\Rightarrow \begin{Bmatrix} F_1 \\ F_2 \\ F_4 \end{Bmatrix} = \begin{Bmatrix} 1,686 \\ 0,389 \\ 4,949 \end{Bmatrix}.$$

and the other forces are obtained from:

$$F_3 = F_1 - F_2 = 1,686 - 0,389 = 1,297$$

$$F_5 = F_1 - F_4 = 1,686 - 4,949 = -3,263.$$

The velocities can be calculated with the solved forces and known mobilities (1/Z):

$v_1 = 1$ was known

$$v_2 = v_1 - F_1 Y_1 = 1 - 1,686 \cdot (1/1) = -0,686$$

$$v_3 = v_2 - F_2 Y_2 = -0,686 - 0,389 \cdot (1/2) = -0,881$$

$$v_4 = v_2 - F_3 Y_4 = v_2 - (F_1 - F_2) Y_4 = -0,686 - (1,686 - 0,389)(1/4) = -1,01$$

$$v_5 = F_5 Y_7 = -3,263 \cdot (1/7) = -0,466$$

$$v_6 = 2 \text{ was known.}$$

7 Impedance and mobility parameters

7.1 Impedance parameters

In a generalized two-connection system shown in Figure 28 a force F_1 is applied to excite the input and as a result a velocity v_1 is obtained. The ratio F_1/v_1 is called the input impedance. If instead a force F_2 is applied to excite the output, then a velocity v_2 results. The ratio F_2/v_2 is called the output impedance. When the force F_1 is applied to the input and the output velocity v_2 results, then the ratio F_1/v_2 is the reverse transfer impedance. When the force F_2 is applied to excite the output and the velocity v_1 results, then the ratio F_2/v_1 is called the forward transfer impedance. These definitions can be

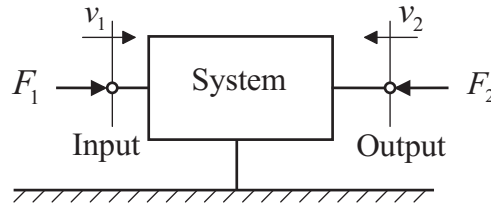


Figure 28. Generalized two-connection system [36].

applied to get the impedance parameters [36]:

$$Z_{11} = \frac{F_1}{v_1} \Big|_{v_2=0}, \quad (94)$$

where Z_{11} is the input impedance under the condition $v_2 = 0$ meaning that the output is clamped (or blocked), i.e., connected to a rigid point. Similarly one gets the output impedance

$$Z_{22} = \frac{F_2}{v_2} \Big|_{v_1=0}. \quad (95)$$

The reverse transfer impedance Z_{12} is

$$Z_{12} = \frac{F_1}{v_2} \Big|_{v_1=0}, \quad (96)$$

where the input is clamped and F_1 is the force required to keep the input velocity $v_1 = 0$. The forward transfer impedance Z_{21} is

$$Z_{21} = \frac{F_2}{v_1} \Big|_{v_2=0}, \quad (97)$$

where the output is clamped and F_2 is the force required to keep the output velocity $v_2 = 0$.

A two connection passive system can be represented by a black box, which is attached to an inertial reference (see Figure 29). If the elements in this system are linear and bilateral, then the relationship between the forces and velocities at the connection points

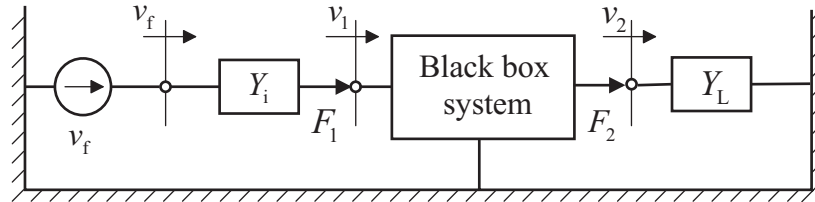


Figure 29. A mechanical system described as a black box, which has two connections and which is attached to an inertial reference. The vibration source is presented by a Norton equivalent system having free velocity v_f and internal mobility Y_i . The load is presented by its mobility Y_L . The forces and velocities at connection points 1 and 2 are noted by F_1, v_1 and F_2, v_2 , respectively [35].

1 and 2 can be expressed as [36]:

$$F_1 = Z_{11}v_1 + Z_{12}v_2, \quad (98)$$

$$F_2 = Z_{21}v_1 + Z_{22}v_2, \quad (99)$$

where the Z_{ii} 's are the impedance parameters. When the forces and the impedance parameters are known, the velocities can be obtained by solving Eqs. (98) and (99).

7.2 Mobility parameters

The mobilities of a generalized system shown in Figure 28 are [36]:

The input mobility Y_{11} is

$$Y_{11} = \left. \frac{v_1}{F_1} \right|_{F_2=0}, \quad (100)$$

where the output is free without no restraining force, i.e., $F_2 = 0$.

The output mobility Y_{22} is

$$Y_{22} = \left. \frac{v_2}{F_2} \right|_{F_1=0}, \quad (101)$$

where the input is free without no restraining force, i.e., $F_1 = 0$.

The reverse transfer mobility Y_{12} is

$$Y_{12} = \left. \frac{v_1}{F_2} \right|_{F_1=0}, \quad (102)$$

where v_1 is the velocity of the free input, $F_1 = 0$, when the force F_2 is applied to excite the output.

The forward transfer mobility Y_{21} is

$$Y_{21} = \left. \frac{v_2}{F_1} \right|_{F_2=0}, \quad (103)$$

where v_2 is the velocity of free output, $F_2 = 0$, when the force F_1 is applied to excite the input.

The relationships between the velocities and forces of the black box system shown in Figure 29 can also be expressed using the mobility parameters Y_{ii} as [36]:

$$v_1 = Y_{11}F_1 + Y_{12}F_2, \quad (104)$$

and

$$v_2 = Y_{21}F_1 + Y_{22}F_2. \quad (105)$$

When the velocities at the connection points and the mobility parameters are known, then the forces are obtained by solving the Eqs (104) and (105).

In the mechanical black box system presented in Figure 29 the vibration source is described by Norton equivalent with free velocity v_f and internal mobility Y_i and the load is given by its load mobility Y_L . The internal mobility of the vibration source and the mobility of the load can be included with the black box mobilities by measuring or calculating the mobility parameters with the load mobility Y_L and internal mobility Y_i in place. In doing so the Eqs. (104) and (105) become [36]

$$v_f = Y'_{11}F_1 + Y_{12}F_2, \quad (106)$$

and

$$0 = Y_{21}F_1 + Y'_{22}F_2. \quad (107)$$

Now the forces and velocities are considered at points 1' and 2. The velocity at point 1' v_1 becomes v_f and the velocity $v_2 = 0$ because no external force is applied. The mobility Y'_{11} is Y_{11} obtained from Eq. (100), and Y'_{22} is Y_{22} obtained from Eq. (101) with Y_L in place [36]. The transfer mobilities are not effected by the external connections. From Eqs. (106) and (107) one obtains the forces [36]

$$F_1 = \frac{v_f Y'_{22}}{Y'_{11} Y'_{22} - Y_{12} Y_{21}} \quad (108)$$

and

$$F_2 = \frac{-v_f Y_{21}}{Y'_{11} Y'_{22} - Y_{12} Y_{21}}. \quad (109)$$

The force $F_L = F_2$ is applied to the load giving rise to load velocity $v_L = F_2 Y_L$. The force at the input connection point 1 is F_1 , since the internal mobility Y_i of the vibration source transmits this force and the velocity at the point 1 is $v_1 = v_f - F_1 Y_1$.

8 Four-pole parameters of mechanical systems

8.1 Theory

The mechanical system (see Figure 30) can be described with the so called mechanical four-pole parameters α_{ij} appearing in the equations between the input force F_1 and velocity v_1 and the respective output force F_2 and output velocity v_2 as [34]

$$F_1 = \alpha_{11} F_2 + \alpha_{12} v_2, \quad (110)$$

$$v_1 = \alpha_{21} F_2 + \alpha_{22} v_2. \quad (111)$$

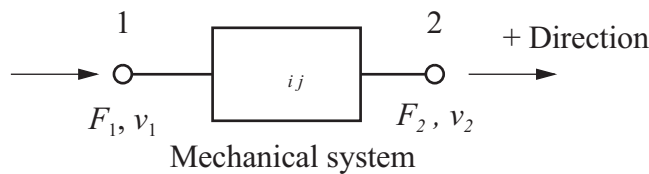


Figure 30. Four-pole parameter notation, adapted from [34], [35].

The four-pole parameters are defined for a particular system and they do not depend on what proceeds or what follows the system. This property allows the calculation of properties of a complicated system comprised of many mechanical elements. The system can be a combination of lumped, linear, mechanical elements like masses, springs, and resistances. The system can be made up also of linear, distributed parameter systems comprising, e.g., beams and plates [34].

The four-pole parameters can be defined from equations [34], [35]:

$$\alpha_{11} = \left. \frac{F_1}{F_2} \right|_{v_2 = 0}, \quad \alpha_{12} = \left. \frac{F_1}{v_2} \right|_{F_2 = 0}, \quad (112)$$

$$\alpha_{21} = \left. \frac{v_1}{F_2} \right|_{v_2 = 0}, \quad \alpha_{22} = \left. \frac{v_1}{v_2} \right|_{F_2 = 0}. \quad (113)$$

In these equations the subscript $v_2 = 0$ means that the output terminal pair is clamped, and the subscript $F_2 = 0$ means that the output terminal pair is free (unrestrained).

According to the reciprocity theorem in a network the transfer impedance or mobility between any two terminal pairs is independent of which terminal pair is taken as the input or output; thus one obtains [35]

$$\left. \frac{F_1}{v_2} \right|_{F_2=0} = \left. \frac{F_2}{v_1} \right|_{F_1=0} \quad (114)$$

or

$$\left. \frac{v_1}{F_2} \right|_{v_2=0} = \left. \frac{v_2}{F_1} \right|_{v_1=0}. \quad (115)$$

Applying the reciprocity theorem the four-pole Eqs. (110) and (111) can be inverted to yield the equations [35]

$$F_2 = \alpha_{22}F_1 + \alpha_{12}v_1 \quad (116)$$

and

$$v_2 = \alpha_{21}F_1 + \alpha_{11}v_1, \quad (117)$$

where use has been made of the relation [35]

$$\Delta = (\alpha_{11}\alpha_{22} - \alpha_{12}\alpha_{21}) = 1. \quad (118)$$

For a symmetrical system it does not matter which terminal is taken to be input or output, thus [35]

$$\alpha_{11} = \alpha_{22}. \quad (119)$$

8.2 Four-pole parameters of a series connected system

The four-pole parameters of the two elements connected in series (see Figure 31) can be obtained considering that the output of the first element is the input of the second element. This can easily be made using matrix notation as follows [34], [35]: using Eqs. (110) and (111) one obtains for element number 1

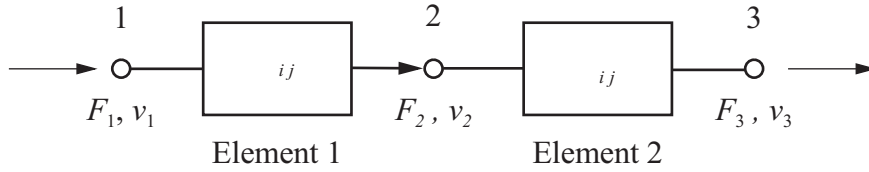


Figure 31. Series connected mechanical elements.

$$\begin{bmatrix} F_1 \\ v_1 \end{bmatrix} = \begin{bmatrix} \alpha'_{11} & \alpha'_{12} \\ \alpha'_{21} & \alpha'_{22} \end{bmatrix} \begin{bmatrix} F_2 \\ v_2 \end{bmatrix} \quad (120)$$

and for element number 2

$$\begin{bmatrix} F_2 \\ v_2 \end{bmatrix} = \begin{bmatrix} \alpha''_{11} & \alpha''_{12} \\ \alpha''_{21} & \alpha''_{22} \end{bmatrix} \begin{bmatrix} F_3 \\ v_3 \end{bmatrix}. \quad (121)$$

Then inserting the Eq. (121) into (120) one obtains

$$\begin{bmatrix} F_1 \\ v_1 \end{bmatrix} = \begin{bmatrix} \alpha'_{11} & \alpha'_{12} \\ \alpha'_{21} & \alpha'_{22} \end{bmatrix} \begin{bmatrix} \alpha''_{11} & \alpha''_{12} \\ \alpha''_{21} & \alpha''_{22} \end{bmatrix} \begin{bmatrix} F_3 \\ v_3 \end{bmatrix}. \quad (122)$$

Then after matrix multiplication one obtains

$$\begin{bmatrix} F_1 \\ v_1 \end{bmatrix} = \begin{bmatrix} \beta_{11} & \beta_{12} \\ \beta_{21} & \beta_{22} \end{bmatrix} \begin{bmatrix} F_3 \\ v_3 \end{bmatrix}. \quad (123)$$

The final four-pole parameters expressed with the aid of the original parameters of the two connected elements are [35]

$$\begin{bmatrix} \beta_{11} & \beta_{12} \\ \beta_{21} & \beta_{22} \end{bmatrix} = \begin{bmatrix} \alpha'_{11}\alpha''_{11} + \alpha'_{12}\alpha''_{21} & \alpha'_{11}\alpha''_{12} + \alpha'_{12}\alpha''_{22} \\ \alpha'_{21}\alpha''_{11} + \alpha'_{22}\alpha''_{21} & \alpha'_{21}\alpha''_{12} + \alpha'_{22}\alpha''_{22} \end{bmatrix}. \quad (124)$$

For a system of n elements one obtains [35]

$$\begin{bmatrix} F_1 \\ v_1 \end{bmatrix} = \left\{ \begin{bmatrix} \alpha'_{11} & \alpha'_{12} \\ \alpha'_{21} & \alpha'_{22} \end{bmatrix} \begin{bmatrix} \alpha''_{11} & \alpha''_{12} \\ \alpha''_{21} & \alpha''_{22} \end{bmatrix} \dots \begin{bmatrix} \alpha^n_{11} & \alpha^n_{12} \\ \alpha^n_{21} & \alpha^n_{22} \end{bmatrix} \right\} \begin{bmatrix} F_{n+1} \\ v_{n+1} \end{bmatrix}. \quad (125)$$

8.3 Four-pole parameters of a parallel connected system

Consider that the parallel connected four-pole elements move so that their input velocities at the common input junction are equal to v_1 and their output velocities, respectively, are equal to v_2 . The force at the input junction is equal to the sum of the input forces of the individual four-pole elements. The output force is also the sum of the forces of the individual fore-pole elements, which are connected parallel as shown in Figure 32 A. The equivalent four-pole parameters of the combined system can be obtained from equations [36]

$$\alpha_{11} = \frac{A}{B}, \quad \alpha_{12} = \frac{AC}{B} - B, \quad \alpha_{21} = \frac{1}{B}, \quad \alpha_{22} = \frac{C}{B}, \quad (126)$$

where

$$A = \sum_{i=1}^n \frac{\alpha_{11}^{(i)}}{\alpha_{21}^{(i)}}, \quad B = \sum_{i=1}^n \frac{1}{\alpha_{21}^{(i)}}, \quad C = \sum_{i=1}^n \frac{\alpha_{22}^{(i)}}{\alpha_{21}^{(i)}}.$$

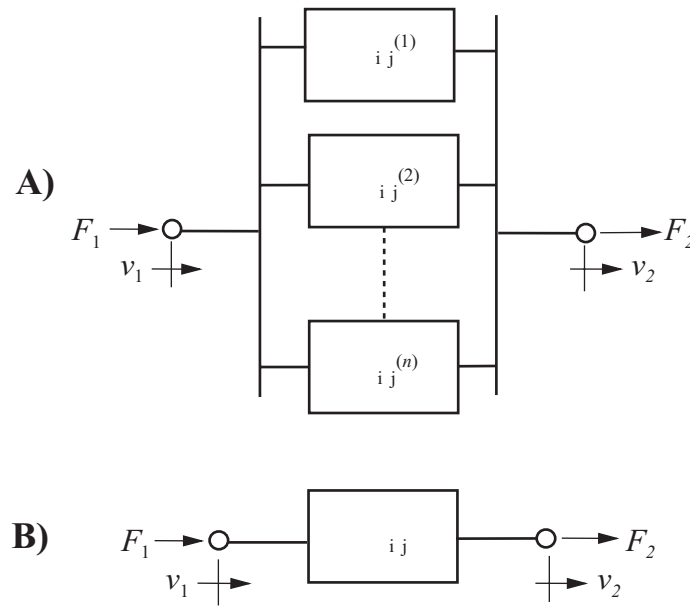


Figure 32. Parallel connected elements in the four-pole method [36].

8.4 Four-pole parameters of lumped systems

8.4.1 Mass

A mass can be considered as a rigid body, so the velocities in the input and output in the four-pole model (see Figure 30 for positive directions) for a mass are equal $v_1 = v_2$. From Newton's law and assuming sinusoidal time dependence ($e^{i\omega t}$) one obtains [34]

$$F_1 - F_2 = m dv_1/dt = m dv_2/dt = i\omega m v_1 = i\omega m v_2.$$

Using these relationships one can write the four-pole Eqs. (110) and (111) for a mass as

$$F_1 = F_2 + i\omega m v_2,$$

$$v_1 = 0 \cdot F_2 + v_2.$$

From these equations one can obtain the four-pole parameters of a mass as [34]

$$\alpha_{11} = 1, \quad \alpha_{12} = i\omega m, \quad \alpha_{21} = 0, \quad \text{and} \quad \alpha_{22} = 1. \quad (127)$$

8.4.2 Spring

The massless spring transmits the force applied to its input to the output so $F_1 = F_2$ (see Figure 30 for positive directions). The force at the end of the spring is obtained as a product of the stiffness k of the spring times the displacement. The relative displacement can be expressed with velocities when the motion is time harmonic as $F_1 = k \left[\frac{v_1}{i\omega} - \frac{v_2}{i\omega} \right]$. So the four-pole Eqs. (110) and (111) can be written in the form

$$F_1 = F_2 + 0 \cdot v_2,$$

$$v_1 = \frac{i\omega}{k} F_2 + v_2.$$

So the four-pole parameters of the ideal massless spring are [34]

$$\alpha_{11} = 1, \quad \alpha_{12} = 0, \quad \alpha_{21} = \frac{i\omega}{k}, \quad \text{and} \quad \alpha_{22} = 1. \quad (128)$$

8.4.3 Resistance

The mechanical resistance transmits the applied force from the input to the output so $F_1 = F_2$ (see Figure 30 for positive directions). For a mechanical resistance caused by a viscous damping the input force F_1 is equal to the mechanical resistance (or damping constant) c times the relative velocity of input point 1 with respect to output point 2. So $F_1 = F_2$, and $F_1 = c(v_1 - v_2)$. These can be rewritten in the form

$$F_1 = F_2 + 0 \cdot v_2, \quad \text{and}$$

$$v_1 = \frac{1}{c} F_2 + v_2.$$

The four-pole parameters of a mechanical resistance are thus [34]

$$\alpha_{11} = 1, \quad \alpha_{12} = 0, \quad \alpha_{21} = 1/c, \quad \text{and} \quad \alpha_{22} = 1. \quad (129)$$

8.4.4 Parallel spring and resistance

In a system of parallel-connected spring and resistance (see Figure 33) the equations for forces and velocities are [35]

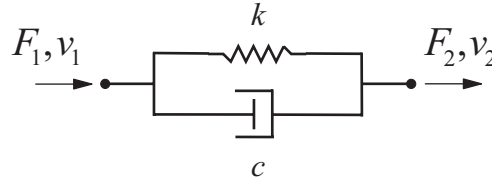


Figure 33. Parallel connected spring and resistance.

$$F_1 = F_2 \quad (130)$$

and

$$v_1 = \kappa^* F_2 + v_2, \quad (131)$$

where

$$\kappa^* = [(k/j\omega) + c]^{-1}. \quad (132)$$

Thus the four-pole parameters are

$$\alpha_{11} = \alpha_{22} = 1, \quad \alpha_{12} = 0, \quad \alpha_{21} = \kappa^*, \quad (133)$$

and

$$\begin{bmatrix} F_1 \\ v_1 \end{bmatrix} = \begin{bmatrix} 1 & 0 \\ \kappa^* & 1 \end{bmatrix} \begin{bmatrix} F_2 \\ v_2 \end{bmatrix} = \begin{bmatrix} 1 & 0 \\ \frac{j\omega}{k[1 + (j\omega c/k)]} & 1 \end{bmatrix} \begin{bmatrix} F_2 \\ v_2 \end{bmatrix}. \quad (134)$$

8.4.5 Dynamic absorber

One can apply the method of series connected lumped elements to get the matrix equation for a dynamic absorber shown in Figure 34

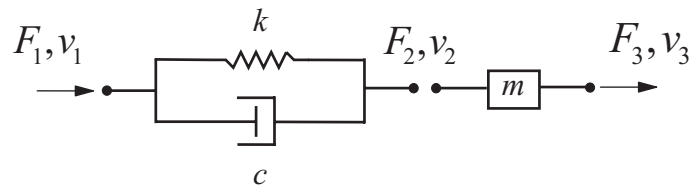


Figure 34. Dynamic absorber.

$$\begin{bmatrix} F_1 \\ v_1 \end{bmatrix} = \begin{bmatrix} 1 & 0 \\ \kappa^* & 1 \end{bmatrix} \begin{bmatrix} 1 & j\omega m \\ 0 & 1 \end{bmatrix} \begin{bmatrix} F_3 \\ v_3 \end{bmatrix} = \begin{bmatrix} 1 & j\omega m \\ \kappa^* & 1 + j\omega m \kappa^* \end{bmatrix} \begin{bmatrix} F_3 \\ v_3 \end{bmatrix}. \quad (135)$$

Normally the dynamic absorber is unterminated. In that case the transfer impedance $Z_T = F_3/v_3 = 0$ and the driving-point impedance Z_{in} is

$$Z_{in} = \frac{F_1}{v_1} = \frac{j\omega m}{1 + j\omega m \kappa^*}, \quad (136)$$

where κ^* is obtained from Eq. (132).

8.4.6 Dynamic absorber in a mechanical system

A dynamic absorber is attached to a mechanical system in Figure 35. For the mechanical system one can write the equation [35]

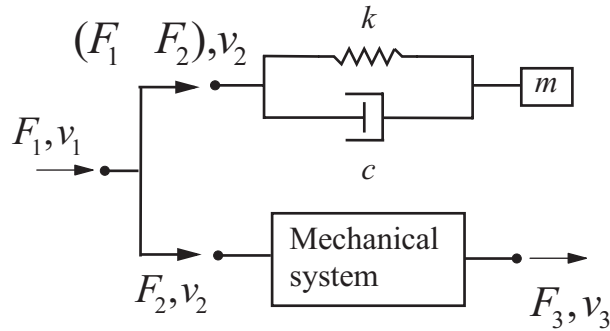


Figure 35. Mechanical system with a dynamic absorber attached [35].

$$\begin{bmatrix} F_2 \\ v_2 \end{bmatrix} = \begin{bmatrix} \alpha_{11} & \alpha_{12} \\ \alpha_{21} & \alpha_{22} \end{bmatrix} \begin{bmatrix} F_3 \\ v_3 \end{bmatrix}. \quad (137)$$

The force balance equation gives

$$F_1 = F_2 + Z_{in} v_2, \quad (138)$$

where Z_{in} is the driving-point impedance of the dynamic absorber given in Eq. (136). Because $v_1 = v_2$, one can write in matrix form [35]

$$\begin{bmatrix} F_1 \\ v_1 \end{bmatrix} = \begin{bmatrix} 1 & Z_{in} \\ 0 & 1 \end{bmatrix} \begin{bmatrix} F_2 \\ v_2 \end{bmatrix}. \quad (139)$$

Inserting the Eq. (137) into Eq. (139) one obtains

$$\begin{bmatrix} F_1 \\ v_1 \end{bmatrix} = \begin{bmatrix} 1 & Z_{in} \\ 0 & 1 \end{bmatrix} \begin{bmatrix} \alpha_{11} & \alpha_{12} \\ \alpha_{21} & \alpha_{22} \end{bmatrix} \begin{bmatrix} F_3 \\ v_3 \end{bmatrix}, \quad (140)$$

and after matrix multiplication

$$\begin{bmatrix} F_1 \\ v_1 \end{bmatrix} = \begin{bmatrix} \alpha_{11} + Z_{in} \alpha_{21} & \alpha_{12} + Z_{in} \alpha_{22} \\ \alpha_{21} & \alpha_{22} \end{bmatrix} \begin{bmatrix} F_3 \\ v_3 \end{bmatrix}. \quad (141)$$

9 Characterization of structure-borne sound source

9.1 Introduction

At the design stage the engineer is often asked to evaluate the resulting vibration and sound level the machine will produce. For airborne sound the source-transmission path-receiver model is well established and it gives good results. A similar approach has not been able to develop for structure-borne sound. There is a fundamental problem how to characterize machines as structure-borne sound sources. When a source is connected to a receiving structure the coupling between these depends on both the source and receiver structural characteristics and the excitation of the source. So the combined system can not be described only with the source characteristics.

9.2 Complex power transmission

The complex transmitted power Q in the one contact point to the receiving structure is obtained from [23]

$$Q = P + iS = \frac{1}{2} \hat{F}^* \hat{v}_r = \frac{1}{2} \hat{F} \hat{v}_r^*, \quad (142)$$

where \hat{F} is the complex amplitude of the force applied on the receiving structure and \hat{v}_r is the complex amplitude of the resulting velocity at the same contact point. The real part P of the complex power Q , where force and velocity are in phase, is the active power flowing from the source into the receiving structure where it propagates further. The imaginary part, the reactive power S , where force and velocity are $\pi/2$ out of phase, goes back and forth through the contact point. Using the point mobility Y_r of the receiving structure at the contact point the complex power can be written in the form

$$Q = \frac{1}{2} |\hat{F}|^2 Y_r = \tilde{F}^2 Y_r, \quad (143)$$

where \tilde{F} is the rms-value of the complex force, or equivalently using velocity

$$Q = \frac{1}{2} \frac{|\hat{v}_r|^2}{|Y_r|^2} Y_r = \frac{\tilde{v}_r^2}{|Y_r|^2} Y_r, \quad (144)$$

where \tilde{v}_r is the rms-value of the complex velocity at the contact point. From Eq. (143) one can see that the complex power Q and the driving-point mobility Y_r of the receiving structure are in same phase. Petersson and Gibbs [40] introduce two quantities relevant to the power transmission:

$$|\hat{v}_r| = \sqrt{2|Q||Y_r|} \quad (145)$$

and

$$P = \text{Re}[Q]. \quad (146)$$

Thus in the description of the power transmission from a source to the receiving structure, the complex power is required [40].

Either a four-pole model or an electrical linear network analogy (see Figure 36) can be used in the determination of the force F_r exerted on the receiving structure and the resulting velocity v_r of the structure [10]. Using the Norton's equivalent system for a velocity source with free velocity v_{sf} exerting the force F_r on the receiver load mobility Y_r then from the Eqs. (92) and (93) one obtains the force

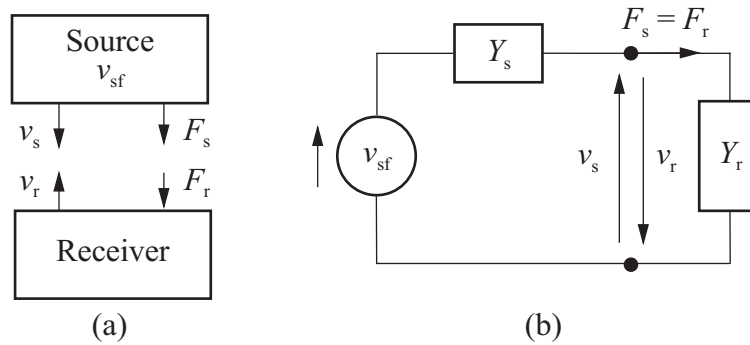


Figure 36. Representation of a source-receiver system in the one contact point case. (a) Four-pole model, (b) linear network analogy model [10].

$$\hat{F}_r = \hat{v}_{sf} / (Y_s + Y_r) \quad (147)$$

and velocity

$$\hat{v}_r = \frac{\hat{v}_{sf}}{Y_s + Y_r} Y_r. \quad (148)$$

Inserting Eqs. (147) and (148) into Eq. (142) one obtains the complex power transmitted [40]

$$Q = \frac{1}{2} \frac{|\hat{v}_{sf}|^2}{|Y_s + Y_r|^2} Y_r = \frac{\tilde{v}_{sf}^2}{|Y_s + Y_r|^2} Y_r. \quad (149)$$

In Eqs. (147)-(149) \hat{v}_{sf} is the complex amplitude of the velocity (\tilde{v}_{sf} is rms-velocity) of the freely vibrating source with no couplings at the contact point. This velocity quantifies the response of the source to all of its internal vibration producing mechanism. It can be measured when the machine is running under normal operating conditions and suspended in free space, e.g., in practise mounted on resilient vibration isolators. It can be considered to represent the activity of the source.

It is seen from Eq. (149) that the power transmitted to the receiving structure depends on the free velocity of the source \hat{v}_{sf} and the mobilities of both the source and the receiving structure. So the power transmission is not only dependent on source-only parameters.

9.2.1 Constant velocity and constant force source

A constant velocity or a constant force source are the two theoretical idealizations which are very seldom encountered. In practice machine and structural design is based on static requirements which lead to structural elements of similar proportions, e.g., thicknesses [40]. Consider a situation where a source is attached at a single point and the motion is considered in only one direction of motion. If the source mobility Y_s is very small compared to the receiver mobility Y_r ($|Y_s| \ll |Y_r|$) then the Eq. (149)

$$Q = \frac{1}{2} \frac{|\hat{v}_{sf}|^2}{|Y_s + Y_r|^2} Y_r = \frac{\tilde{v}_{sf}^2}{|Y_s + Y_r|^2} Y_r$$

reduces to [40]

$$Q = \frac{1}{2} \frac{|\hat{v}_{sf}|^2}{|Y_r|^2} Y_r$$

showing that in this case the complex power transmitted is independent of the mobility of the source. In theory this kind of situation is encountered when a solid massive machine is mounted on a thin foundation plate. Then the velocity at the contact point is the free velocity v_{sf} measured when there are no contacts between the machine and its environment and when the machine is running under normal load. This extreme situation describes the so-called constant velocity source [40].

If instead the source mobility Y_s is very large compared to the receiver mobility Y_r then Eq. (149) reduces to [40]

$$Q = \frac{1}{2} \frac{|\hat{v}_{sf}|^2}{|Y_s|^2} Y_r$$

and then the force at the contact point becomes invariant (constant). This theoretical situation is encountered when a machine with large mobility is mounted on a thick floor [40].

9.2.2 Transmission loss of elastic elements

Between the source and receiver there are often elastic elements, called transmission elements, e.g., chocks, vibration isolators, bolts, pipes, tubes or cables. If there is an elastic element between a simple source and a receiver, then the velocities at its top and bottom ends, v_1 and v_2 respectively, can be written as [40]

$$\hat{v}_1 = \hat{F}_1 Y_{11} + \hat{F}_2 Y_{12}, \quad (150)$$

and

$$\hat{v}_2 = \hat{F}_1 Y_{21} + \hat{F}_2 Y_{22}, \quad (151)$$

where Y_{ii} are the driving-point mobilities and Y_{ij} the transfer mobilities.

It can be shown that the transmitted complex power from source to the receiver is obtained from [40]

$$Q = Q_0 \frac{|Y_s + Y_r|^2 |Y_{21}|^2}{|(Y_s + Y_{11})(Y_r + Y_{22}) - Y_{12}Y_{21}|^2}, \quad (152)$$

where Q_0 is from Eq. (149) calculated complex power without the transmission element in place, and the transmission efficiency t can be defined as ([10] in [40])

$$t = \frac{|Y_s + Y_r|^2 |Y_{21}|^2}{|(Y_s + Y_{11})(Y_r + Y_{22}) - Y_{12}Y_{21}|^2}. \quad (153)$$

One sees from Eq. (153) that in addition to element mobilities both the source and receiver mobilities will effect on the transmission efficiency. This differs from the force or displacement transmissibility [41] which considers only one field variable at a time [40].

An approximate expression for the transmission efficiency when the element mobilities are larger that the source and receiver mobilities is [40]

$$t' = |Y_s + Y_r|^2 \frac{|Y_{21}|^2}{|Y_{11}Y_{22} - Y_{12}Y_{21}|^2}. \quad (154)$$

In the approximate Eq. (154) for t' the second factor is the square of the ratio (transfer impedance) of force at a blocked end to the velocity at the excited end [40]. In the general case its mobility matrix describes the transmission element

$$Y_T = \begin{bmatrix} Y_{11} & Y_{12} \\ Y_{21} & Y_{22} \end{bmatrix}. \quad (155)$$

When elements are linear, passive and bilateral then the reciprocity principle applies and $Y_{12} = Y_{21}$. If the elements are in addition symmetrical then $Y_{11} = Y_{22}$.

9.2.3 Source descriptor and coupling function

9.2.3.1 One-point-connected systems

For the description of the complex power transmission at one contact point from the vibration source to the receiving structure Mondot and Petersson [10] introduced the ratio of the magnitude of the receiver and source mobilities, $\alpha = |Y_r|/|Y_s|$, and the phase difference between these mobilities, $\Delta\phi = \phi_r - \phi_s$. They proposed that the source characterization can be made with two functions: the source descriptor S describes the ability of the source to produce power and the coupling function Cf gives the proportion of this power which is manifested, defining these functions, respectively, as

$$S = \frac{\tilde{v}_{sf}^2}{Y_s^*}, \quad (156)$$

$$Cf = Y_s^* Y_r / |Y_s + Y_r|^2, \text{ or } Cf = \alpha e^{i\Delta\phi} / (\alpha^2 + 2\alpha \cos \Delta\phi + 1), \quad (157)$$

where \tilde{v}_{sf} is the rms-velocity of the free source at the contact point, Y_s^* is the complex conjugate of the source mobility, and Y_r is the receiver mobility. The complex power in Eq. (149) can be obtained with the aid of the source descriptor and the coupling function from

$$Q = SCf. \quad (158)$$

The source descriptor S has the units of power and it depends only on source data, the velocity v_{sf} of the free source and the source mobility at the contact point Y_s . The coupling function Cf is a function of the source and receiver mobilities at the interface and it describes the dynamic properties of these coupled structures at the contact point. For any phase difference between the source and receiver mobilities the level of the coupling function attains its maximum when the magnitudes of these mobilities are equal. When the magnitude ratio is kept constant, then the largest coupling is obtained for the largest phase difference [10]. The magnitude of the coupling function is low when the mobilities are largely different in magnitude. Under these conditions the mobilities are called unmatched and the transmission is essentially independent of the phase difference between the source and receiver mobilities [10]. When the mobilities are nearly of equal magnitude, the magnitude of the coupling function can be high depending on the phase difference. Under these conditions the mobilities can be called matched and the power transmission is dependent both on the source descriptor and the mobility matching at the interface [10].

The active power P , the real part of the complex power Q , is the quantity, which is controlled when the structure-borne sound power transmission or propagation needs to be reduced. The active power P can be written using the source descriptor S and the coupling function Cf in the form

$$P = |S| |Cf| (\cos \phi_s \cos \Delta\phi - \sin \phi_s \sin \Delta\phi). \quad (159)$$

When the source, source descriptor, is known the power transmission is obtained using the coupling function. The most favourable contact point can be selected estimating the minimum giving coupling function. One has to design sources and receivers so that lightly damped vibration modes can be avoided, thus the phase difference of the source and receiver mobilities can be kept small. When lightly damped resonant structures are used then the comparable magnitudes of the mobilities of the source and receiving structure cause considerable transmission of vibration and power [10].

The source descriptor has some distinct properties: It is a function of the source involving only source variables. It has the units of power, which enables the comparison of different components of motion. In one-point uni-directional system both the source descriptor and the coupling function involve only variables which are measurable when the source and the receiver are not coupled together and therefore the prediction of the transmitted power is possible [14].

9.2.3.2 Multi-point-connected systems

The characterization of machines as vibrational sources is fundamental in the control of structure-borne sound. The dynamic coupling between the source and receiver does not allow the use of transmitted power in the source characterization. Some proposals have been made to standardize the structure-borne sound emission [9] for the case when the source is stable these include the constant force or velocity sources [23]. Theoretically in the general case these ideas do not work. Fulford and Gibbs [14], [15], [16] have studied further the ideas of Mondot and Petersson [10] applying the source descriptor and coupling function in multi-point-connected systems.

In a general motion six degrees of freedom are possible, three translational and three rotational, and the source and the receiver can be coupled at many points. In the analysis of this system coupling between all points and all components of motion has to be taken into account. Using the source mobility matrix, $[Y_s]$, the receiver mobility matrix, $[Y_r]$, and the force ratio vector, $\{F_j^m / F_i^n\}$, the transmitted power can be obtained from [14]

$$P_i^n = \frac{(v_{sf_i}^n)^2}{2 \left| [Y_s] \{F_j^m / F_i^n\} + [Y_r] \{F_j^m / F_i^n\} \right|^2} \operatorname{Re} \{ [Y_r] \{F_j^m / F_i^n\} \}. \quad (160)$$

The Eq. (160) shows the complexity of the determination of power transmission in multi-point-connected systems [14]: For N connection points the receiver and source matrices are $6N \times 6N$ matrices of complex and frequency dependent elements. It is difficult to compare different mobility terms and compare the significance of the source and receiver mobility. Also it is difficult to see what are the dominant transmission paths of structure-borne sound. To get better understanding of the power transmitted the force ratios should be known.

Fulford and Gibbs use the concept of effective point mobility to address the problems mentioned using the definition for point n in direction i presented in [43]

$$Y_{ii}^{nn\Sigma} = Y_{ii}^{nn} + \sum_{m=1, m \neq n}^N Y_{ii}^{nm} \frac{F_i^m}{F_i^n} + \sum_{j=1, j \neq i}^6 Y_{ij}^{nn} \frac{F_j^n}{F_i^n} + \sum_{m=1, m \neq n}^N \sum_{j=1, j \neq i}^6 Y_{ij}^{nm} \frac{F_j^m}{F_i^n}, \quad (161)$$

where Y_{ij}^{nm} are the transfer mobilities when force is acting at the point m and direction j to the point n and direction i and F_j^m / F_i^n are the force ratios, respectively. The different terms in Eq. (161) highlight the important transmission paths. The first term is the direct path, and the second (sum) term is due to the couplings between other points to point n in the direction of motion i . The third (sum) term is due to the couplings between other motion directions j and direction i in the point n under consideration, and the fourth (sum) term is due to couplings from other points m and other motion directions than the motion direction i under consideration.

In multi-point-connected systems the effective point mobility is analogous to the point mobility. The source descriptor and the coupling function for a point n and in motion direction i for a multi-point-connected system are thus analogously [14]

$$S_i^n = \left| v_{sf,i}^n \right|^2 / 2 Y_{s,ii}^{nn\Sigma*}, \quad (162)$$

$$Cf_i^n = Y_{s,ii}^{nn\Sigma*} Y_{r,ii}^{nn\Sigma} / \left| Y_{s,ii}^{nn\Sigma} + Y_{r,ii}^{nn\Sigma} \right|^2. \quad (163)$$

The transmitted complex power Q_i^n in the point n and direction i is obtained from product

$$Q_i^n = S_i^n Cf_i^n. \quad (164)$$

The real part of complex power gives the active power P_i^n , and the total active power is obtained by the sum of all P_i^n . In the effective point mobility of a multi-point-connected system there are the force ratios, and they are dependent on both the source and receiver structures. Thus one has to predict or estimate these force ratios in some manner [14]. The force ratios in a receiver system came under consideration through the concept of effective point mobility. In the theoretical consideration of translational forces Mondot, Petersson and Gibbs used assumption that they have unity magnitude and zero phase [14]. If only translational motion is considered, the effective point mobility has been estimated by [14]

$$Y_{ii}^{nn\Sigma} = Y_{ii}^{nn} + \sum_{m=1, m \neq n}^N Y_{ii}^{nm}, \quad (165)$$

where only contribution of other points in the same direction is taken into account. If in a linear system the contribution from N contact points can be assumed to cancel through superposition, each mobility and force ratio has different phase, and the effective point mobility reduces to the point mobility [14]

$$Y_n^{nn\Sigma} = Y_{ii}^{nn}. \quad (166)$$

This assumption is equivalent to the assumption that the contact points are uncoupled. When taking into account both the excitation of the source and its structural characteristics a simple assumption is that the excitation is the free velocity of the contact points and the point mobility of the source in these points. Thus the force at the contact points is [14]

$$F_i^n = v_{sf_i}^n / Y_{sii}^{nn}. \quad (167)$$

A more accurate estimation needs the coupling terms between contact points, i.e., the transfer mobilities, but this leads to complicated expressions for the forces and effective mobility.

9.2.4 Characteristic power

In a single contact point case it is assumed that a source is linear and vibrates as a result of the action of internal forces which are independent of the attachment to any receiving structure [80]. The free velocity \tilde{v}_{sf} of the source is assumed to characterize the activity of the source and the mobility Y_s is assumed to characterize its passive properties at the contact point [80]. The complex power that is transmitted through the contact point is given by Eq. (149) repeated here for clarification [80]

$$Q = |\tilde{v}_{sf}|^2 \cdot Y_r / |Y_r + Y_s|^2. \quad (168)$$

where \tilde{v}_{sf} is the rms free velocity (\tilde{v}_{sf} is complex amplitude), Y_r and Y_s are the receiver and source mobility respectively.

Using the complex ratio of receiver to source mobility $\alpha = Y_r / Y_s$ Eq. (168) can be written in a dimensionless form [80]

$$C_c = Q / |S_c| = |\alpha| / (|1 + \alpha|^2 e^{j\theta_r}), \quad (169)$$

where $S_c = |\tilde{v}_{sf}|^2 / Y_s^*$, θ_r is the phase of the receiver mobility, and C_c is the so-called coupling factor.

The magnitude and real part of the dimensionless power transmitted from a source of a given phase when connected to a receiver of opposite phase is drawn in Figure 37. When the source mobility is high in relation to the receiver mobility ($|\alpha| \ll 1$), the blocked mounting condition is approximated and the power transfer is inefficient. On the other hand, when the source mobility is low in relation to the receiver mobility ($|\alpha| \gg 1$), the free mounting condition is approximated and again the power transfer is inefficient. These extreme cases of low power transfer are shown by asymptotic lines in Figure 37. The power transfer obtains its maximum for any phase angle when $|\alpha| = 1$.

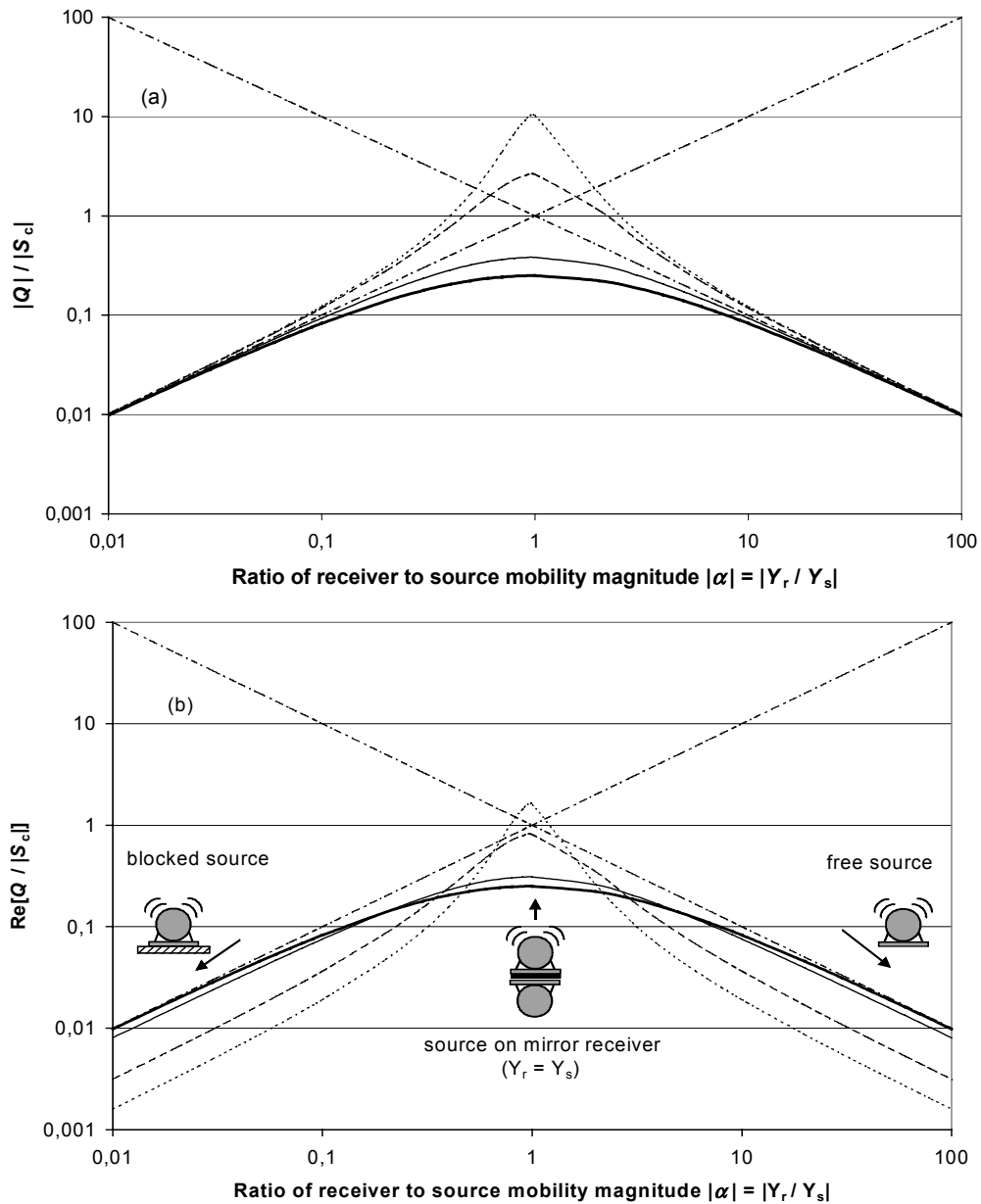


Figure 37. (a) Magnitude, and (b) real part of the power via a single contact point from a source of various mobility phases to a receiver of opposite phase ($\theta_r = -\theta_s$). Diagonal lines indicate blocked and free source asymptotes. Phase θ : **—** 0 ; **—** $0,2\pi$; **- - -** $0,4\pi$; **.....** $0,45\pi$. Adapted from [7] and [80].

From Eq. (168) the maximum complex power is obtained when the mobilities of source and receiver are complex conjugate ($Y_r = Y_s^*$) [10]

$$Q(Y_r = Y_s^*) = S_a = |\tilde{v}_{sf}|^2 \cdot Y_s^* / [2 \operatorname{Re}(Y_s)]^2. \quad (170)$$

The "maximum available power" (MAP) that is transmitted from this source through its contact point to any receiving structure is obtained from [80]

$$\operatorname{Re}[Q(Y_r = Y_s^*)] = \operatorname{Re}(S_a) = |\tilde{v}_{sf}|^2 / 4 \operatorname{Re}(Y_s). \quad (171)$$

In Figure 37 (b) is drawn the real part of Eq. (169) for $\theta_r = -\theta_s$, that is the MAP, for four different values of source mobility phase.

When source and receiver mobilities are equal in magnitude and phase ($Y_r = Y_s$) then from Eq. (168) is obtained [80]

$$Q(Y_r = Y_s) = S_m = |\tilde{v}_{sf}|^2 \cdot 1/4(Y_s^*). \quad (172)$$

This is called the "mirror" power, because it is the power transmitted when the source is connected to receiver which is a mirror image of itself [80]. The magnitude of the mirror power is independent of source mobility phase, whereas the magnitude of MAP depends on the source mobility phase. For most sources, the magnitude of the mirror power is less than the MAP power. In a special case of a source of zero mobility phase both powers are equal [80].

The intersection point of the low mobility and the high mobility source asymptotes in Figure 37 is of interest. In this point the force is equal to the blocked force ($F_{bl} = \hat{v}_{sf} / Y_s$) and the velocity is the free velocity, and power is obtained from [80]

$$Q(F = F_{bl}, \hat{v} = \hat{v}_{sf}) = S_c = |\tilde{v}_{sf}|^2 \cdot 1/Y_s^*. \quad (173)$$

This is four times the "mirror" power obtained from Eq. (172). Mondot and Petersson [10] call the result of Eq. (173) the source descriptor. Moorhouse introduced for this result a new term the "characteristic power" to be able to enlarge the discussion to include also the multiple point contacts, because it differs from the characterization by Mondot and Petersson. This work was extended to multiple point and component contact also in [80].

10 Mobility functions and free velocities

10.1.1 Machine mobilities

The mount footing is typically a flat plate for a large range of machines [44]. The dynamics of this kind of mount can be modelled as a plate-spring-mass system (see Figure 38). The mass presents the machine body and the spring the local stiffness of the footing. The boundary

conditions, material and dimensions of the plate determine the stiffness. For this model the point mobility is obtained from [15]

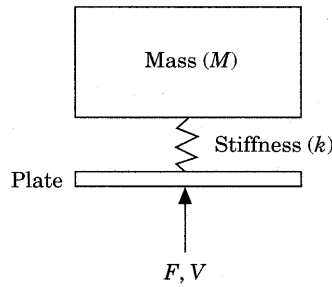


Figure 38. Model of a machine mount point [15].

$$Y = (k - \omega^2 m) / i\omega m k, \quad (174)$$

where m is the mass of the machine, k the local stiffness of the mount footing, and ω is the angular frequency. At low frequencies the mass term dominates the expression and in the mobility curve (see Figure 39) a mass controlled region (magnitude decrease of 6 dB per octave with a phase of $-\pi/2$) is seen. Thereafter at higher frequencies is seen a stiffness controlled region (magnitude increase of 6 dB per octave with a phase of $\pi/2$). Between these two regions is seen notch caused by an anti-resonance frequency determined by the mass and local stiffness

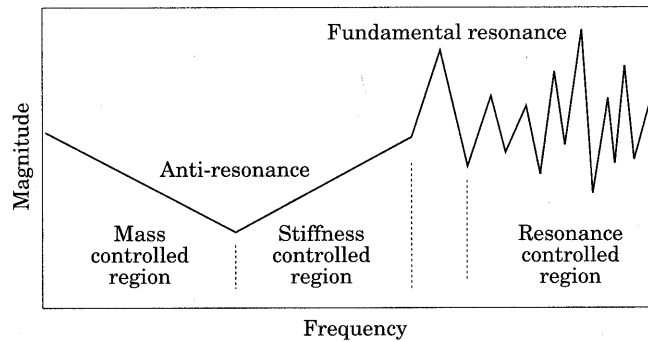


Figure 39. Generalized point mobility of machine mount [15].

$$\omega_0 = \sqrt{k/m}. \quad (175)$$

After the stiffness controlled region the plate will begin to bend and its fundamental frequency starts the resonance controlled region, where a more detailed model is needed.

10.1.1.1 Mobility in mass controlled region

The machine can be modelled as a rigid body in the mass controlled region. If the co-ordinate axes coincide with the principal inertia axes of the body of the machine, the mobility is obtained from [15]

$$Y = (1/i\omega)(1/m + y_0 y / I_{xx} + x_0 x / I_{yy}), \quad (176)$$

where x_0 and y_0 describe the position of the force with respect to the centre of gravity, x and y are the co-ordinates of the response point, and the moments of inertia are I_{xx} and I_{yy} (see [15]).

10.1.1.2 Mobility in stiffness controlled region

In the stiffness controlled region the size, material and boundary conditions of the mount plate control the mobility and the main body of the machine can be ignored in the analysis [15]. Fulford and Gibbs consider in the analysis plate- and flange-like mount conditions (see Figure 40). They also consider cantilever flanges and local plate deformation (see Figure 41).

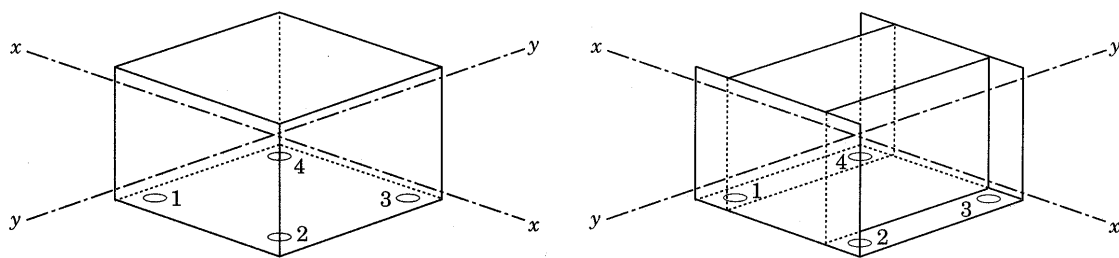


Figure 40. Machine with a plate-like base (left) and with a flange-like base [15].

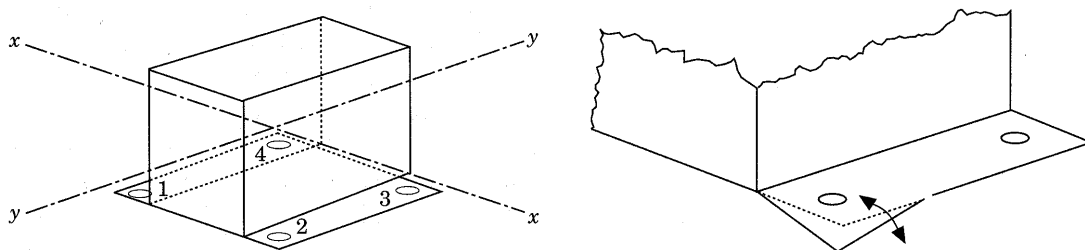


Figure 41. Machine with cantilever flanges (left) and local plate deformation [15].

10.1.1.3 Mobility in resonance controlled region

The transfer Y^{tr} and point mobility Y^{pt} of the machine base are dependent on the modal interaction in the resonance region of the mobility curve. Mode shapes and mode frequencies depend on the material, dimensions and boundary conditions; and the modal interaction depends on the frequency, excitation position, reception position and material damping. This is why the analytical determination of the relationship $Y^{\text{tr}} / Y^{\text{pt}}$ is difficult [15].

Skudrzyk subdivided the resonance region into four frequency regions: a) low frequencies ($\alpha > 5$), b) transition frequencies ($1 < \alpha < 5$), c) high frequencies ($\alpha \approx 1$), and d) very high frequencies ($\alpha \leq 1$). The ranges were determined by the ratio α of average modal spacing ε_ν (rad/s) to the half-power bandwidth $\eta\omega_\nu$ of a mode ν given in [45] and denoted by α in [15]

$$\alpha = \varepsilon_\nu / \eta\omega_\nu, \quad (177)$$

where η is the material loss factor, and ω_ν is the angular frequency of the mode ν . The frequencies in the regions c) and d) are not of concern as to the mobilities of machines [15]. The modal spacing of a thin mount plate transversely excited is obtained from [15]

$$\varepsilon_\nu = 3,6c_L h / A, \tag{178}$$

where c_L is the quasi-longitudinal wave speed, h plate thickness, and A plate area. From Eqs. (177) and (178) is obtained

$$\alpha = 3,6c_L h / \eta A \omega_\nu. \tag{179}$$

Using values $\eta = 0,001$ and upper frequency limit of 10 kHz, the plate area required to have $\alpha = 1$ for a 3 mm thick plate is 1 m² and for thicker plates the area will be larger than 1 m² [15]. This example shows that these two regions of Skudrzyk are not applicable in engineering practice. For the region b) the plate are with same assumptions will be about 0,2 m² which is of practical concern. In the low frequency region where $\alpha > 5$ the mobility will have well separated peaks. Even in this region it is not possible to predict the exact mobility spectra excluding the simplest structures. It is considered that only the mean value and the envelope which bounds the upper and lower peaks can be predicted with acceptable accuracy [15].

10.1.2 Floor mobilities

The estimation of the effective mobilities of the receiving structure is needed if power transmission needs to be evaluated. Many times in engineering applications the receiving structure is a floor. The floor cannot be considered as a free body and so a mass controlled region will not be seen in the curve of the point mobility. Typically the mobility curve of a floor behaves as shown in Figure 42.

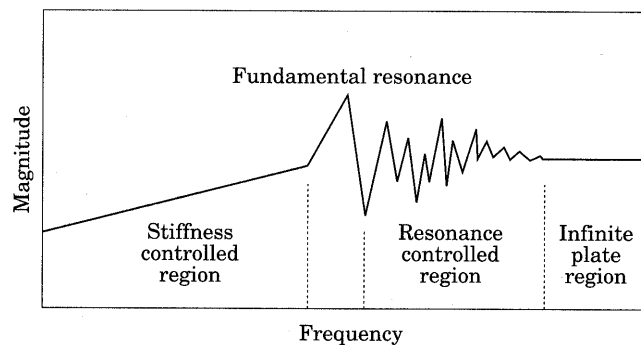


Figure 42. Generalized point mobility of floor mount [15].

10.1.3 Free velocities of machine

The free velocity of a machine is caused by all the internal exciting mechanisms. The excitation mechanisms are so varied that it is impossible to develop a general theoretical model for the free velocity. Instead usually measured values are used.

In the mass controlled region of mobilities the machine moves as a rigid body. In this region all the free velocities will be approximately of equal magnitude [15]. In the stiffness controlled region the magnitudes and the phases of the free velocities depend on the details of the machine. In the resonance controlled region the wave behaviour dominates and the magnitude or phase of the free velocities cannot be predicted. For symmetrical structures approximately equal magnitudes or trends can be waited [15].

11 Measurement techniques

11.1 Mobility measurement

During the early 1960's techniques for measuring mechanical impedance became widely available after the development of new measuring equipment [48]. At that time the "Round Robin" test conducted by the U.S. Naval Research Laboratory was performed to assess how consistently impedance properties could be measured by different people and laboratories [48]. During the 1970's the techniques were developed further and soon they were used in the form of mobility measurements. Especially the development of computer-controlled measurement techniques and the use of sophisticated analysis programs, e.g., modal analysis, made these techniques applicable in the engineering work.

There were considerable developments in the mobility measurement techniques and at the same time the number of organizations making these measurements increased. So it was felt that there is a need to assess the accuracy and consistency of mobility measurements and analyses. Thus during the period 1978-1980 another survey of mobility measurement techniques and of associated modal analysis methods was conducted [48], [49]. This consisted of two parallel and identical surveys, which were performed in the UK, and in France for measuring structural mobility properties [48]. In the survey special test structures covering the frequency range from 2 Hz up to 50 kHz were circulated between the participating laboratories. The survey showed that no individual factor could be found to explain the scatter in the measurement results. Instead, four main points were identified to influence on the quality of measurements [48]:

- The method of suspension of the structure; the requirement being the free-free condition for testing and excitation perpendicular to the suspension is preferred
- The method of attaching the shaker and/or the measuring transducers; lightness of the transducers and the attachment devices and the rigidity or flexibility of the drive rod connecting the vibration exciter and the test structure
- The excitation techniques used to generate vibration in the structure; harmonic, random or transient excitation depending on the measurement application
- The total time taken by various methods to produce a good mobility measurement."

In the assessment of the survey it was found that it is neither possible nor appropriate to name the best method for measuring mobilities. The methods are complex and it depends on the particular application which method suits best to the measurement task [49]. These findings are still valid even the mobility measurement techniques have become as a standard tool for vibration engineers.

Today methods of experimental determination of mechanical mobility are standardized and well documented in various standards [21], [42].

12 Structure-borne sound power transmission from machines

12.1 Power calibration of receiving structure

12.1.1 Introduction

At present there is no standardized or otherwise agreed measurement method for the determination of the source strength or the structural power transmission from sources to receiving structures [51]. However, much theoretical and experimental work has been done on these subjects (see. e.g., [40], [52], [53], [54], [55], [56], [80]). Some of these methods, e.g., [52], [53], [54], are based on "terminal power" of the isolated, free source and the coupling characteristics that take into account the source and receiver mobilities. The transmitted power at each contact point and motion co-ordinate is obtained as a time-averaged product of the force and velocity components at the contact point. The estimation of contact forces is very difficult. This estimation is avoided if some kind of calibration method is available. In addition in engineering applications the structural power transmission often needs to be measured "in situ" preferably before the source is installed or in a worse case after the installation has been made.

12.1.2 Power transmission from source machine to receiving structure

In a multi-point-connected system of N contact points and 6 degrees of freedom there are $n = 6N$ coupling co-ordinates or terminals. If the force is time harmonic with the time dependence $e^{i\omega t}$, where ω is the angular frequency, then the time-averaged power transmitted to the receiver in the i th terminal is $P_i = \frac{1}{2} \text{Re}(\hat{F}_i \hat{v}_i^*)$, where \hat{F}_i and \hat{v}_i are the complex amplitudes of the interface force and coupled velocity at the terminal i . The velocity at the i th terminal is caused by all the contact forces, \hat{F}_j . Remembering that mobility sums the velocity response one obtains in terms of the receiver transfer mobilities $Y_R(\omega) = Y_{R,ij}$, which relate the velocity at the terminal i to the exciting force at the terminal j , expression $v_i = \sum_{j=1}^n Y_{R,ij} \hat{F}_j$. The total power transmitted to the receiving structure is obtained by summing the powers of each terminal i , so $P_i = \sum P_i$

$$P = \frac{1}{2} \text{Re} \sum_{i=1}^n \hat{F}_i \sum_{j=1}^n Y_{R,ij}^* F_j^* = \frac{1}{2} \text{Re} \left\{ \left\{ \hat{F} \right\}^T \left[Y_R^* \right] \left\{ \hat{F}^* \right\} \right\}, \quad (180)$$

where the last expression is given in matrix form [51].

12.1.2.1 Power transmission estimate over contact zone

The transmitted power can be estimated using the concept of the contact zone. If the cross coupling terms between terminals are assumed to be negligible, then an approximate expression is obtained as [51]

$$P \approx \sum_{i=1}^n \overline{F_i^2} \operatorname{Re}(Y_{R,ii}) = \sum_{i=1}^n \overline{v_i^2} \operatorname{Re}(Y_{R,ii}) / |Y_{R,ii}|^2, \quad (181)$$

where time averaged mean squared values (rms-values squared) of the contact force ($\overline{F_i^2} = F_{i,\text{rms}}^2 = \frac{1}{2} |\hat{F}_i|^2$) and coupled velocity ($\overline{v_i^2} = v_{i,\text{rms}}^2 = \frac{1}{2} |\hat{v}_i|^2$) has been used.

If the receiver input mobilities which were measured before the source was installed are available, then the Eq. (181) can be used when estimating the transmitted power using the *in-situ* measured coupled velocities when the source is installed and operating normally. The Eq. (181) has been found to give reasonably good accuracy in the estimation when frequencies are over the modes of the rigid body motion of the source or receiver [51].

12.1.3 Power calibration of receiving structure

In the Department of Acoustic Technology of Technical University of Denmark has been developed a method for the estimation or determination of power transmission based on a *power calibration* of the receiving structure [51]. This calibration is made before the source is installed. This technique has been successfully used both for the power transmission measurements and for the source strength characterization [51].

12.1.3.1 Calibration of receiving structure

The power calibration of the receiving structure developed by Mogens Ohlrich [51] is based on the relationship between power input at a point and the associated energy response of an arbitrarily chosen control region in the far-field of the receiving structure (see Figure 43). The far-field means a suitable region outside the contact zone, e.g. adjacent panels.

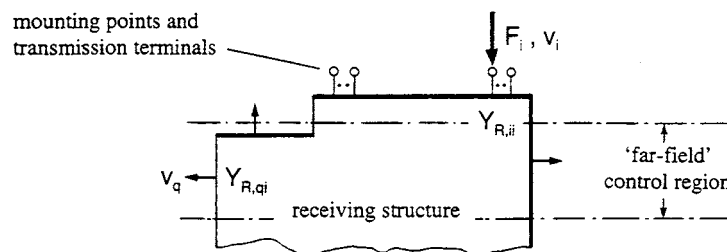


Figure 43. Far-field power calibration of receiving structure by applying a known external force F_i at the i th terminal point [51].

When an external point force F_i is applied at the i th receiver terminal having diving-point mobility $Y_{R,ii}$, the power inputted is $P_i = \overline{F_i^2} \text{Re}(Y_{R,ii})$. This force causes at an arbitrary other position q in the far-field region of the receiver vibration with mean squared normal velocity [51]

$$\overline{v_q^2} = |Y_{R,qi}|^2 \overline{F_i^2}, \quad (182)$$

where $Y_{R,qi}$ is the transfer mobility when force is exciting at terminal i and velocity response is measured in terminal q . Averaging spatially these velocity responses over the far-field control region one obtains the partial energy response E_q [51]

$$E_q = \int_{M_q} \overline{v_q^2} dm_q, \quad (183)$$

where M_q is the mass of the control region and dm_q is the local mass element of the structural part considered. If instead substructures of uniform thickness and average mass m_r are used then the integration is replaced by summation

$$E_q = \sum_r m_r \langle \overline{v_r^2} \rangle \equiv M_q \langle \overline{v_q^2} \rangle, \quad (184)$$

where r is the number of substructures and $\langle \overline{v_r^2} \rangle$ is the time averaged mean squared velocity spatially averaged over the r th substructure, $M_q = \sum m_r$, and $\langle \overline{v_q^2} \rangle$ is the mass-weighted or "energy velocity" of the far-field control region [51]. If spatially averaged transfer mobility is used then from Eq. (182) one obtains [51]

$$\overline{F_i^2} = \frac{\sum m_r \langle \overline{v_r^2} \rangle}{\sum m_r \langle |Y_{R,ri}|^2 \rangle} = \frac{M_q \langle \overline{v_q^2} \rangle}{M_q \langle |Y_{R,qi}|^2 \rangle}. \quad (185)$$

The estimation of substructure masses m_r is uncritical; because they have the same weight when the spatially averaged velocity $\langle \overline{v_q^2} \rangle$ and the transfer mobility $\langle |Y_{R,qi}|^2 \rangle$ are determined [51]. Using the Eq. (185) one obtains the power inputted to the receiving structure [51]

$$P_i = \overline{F_i^2} \text{Re}(Y_{R,ii}) = \langle \overline{v_q^2} \rangle \frac{\text{Re}(Y_{R,ii})}{\langle |Y_{R,qi}|^2 \rangle} = \langle \overline{v_q^2} \rangle \text{Re}(\alpha_{qi}), \quad (186)$$

where

$$\text{Re}(\alpha_{qi}) = \text{Re}(Y_{R,ii}) / \langle |Y_{R,qi}|^2 \rangle \quad (187)$$

is the frequency dependent function of proportionality, which is robust and insensitive to variations in drive point properties and forcing directions [51]. This insensitivity is obvious because this function is equal to $\omega\eta M$ if the whole far-field region includes the entire structure with the total mass M and total loss factor η [51].

12.1.3.2 Reference power estimate

Estimation of the velocity responses and transfer mobilities can be made using space averaging unless the structure is made of structural parts with non-uniform mass distribution whereupon the velocity response and transfer mobility must be averaged using Eqs. (184) and (185). It has been shown that for a homogenous structure such a result is correct both for the power inputted by a point force and for a distribution of excitation forces ([24, p. 333] in [51]). In practise the averaging can be made over free to four representative terminals giving transmitted power P as an average of these uncorrelated estimates

$$P = \left\langle \overline{v_q^2} \right\rangle \left\langle \frac{\text{Re}(Y_{R,ii})}{\left\langle |Y_{R,qi}|^2 \right\rangle} \right\rangle_i = \left\langle \overline{v_q^2} \right\rangle \left\langle \text{Re}(\alpha_{qi}) \right\rangle_i. \quad (188)$$

The steps in this measurement technique are [51]:

- (a) Select suitable free or four terminals of the receiving structure. Then measure their driving-point mobility using a broadband force excitation. In addition measure the energy response of the selected far-field control region M_q and determine the spatially averaged square transfer mobility. Average the results of these measurements to get the proportionality function $\left\langle \text{Re}(\alpha_{qi}) \right\rangle_i$.
- (b) Install the source machine under consideration. Then the machine is operated under the load conditions required. Thereafter measure the energy response caused by the operating machine in the far-field control region M_p and determine the spatially averaged mass weighted velocity response $\left\langle \overline{v_q^2} \right\rangle$ using Eq. (184).
- (c) The power transmitted from the source to the receiver is obtained by multiplying the result of the power calibration (a) with the result of (b). This estimate is called the reference power estimate.

12.1.3.3 Calibration with source machine installed

In practise it may happen that the source is already installed and the measured mobilities of the receiving structure are not available. However, after the installation it is often possible to measure the total driving-point mobility Y_{ii} and the total transfer mobility Y_{qi} of the coupled source-receiver system (see Figure 44). Using these total mobilities and providing that the driving-point mobility of the source $Y_{S,ii}$ or receiver $Y_{R,ii}$ is available, at least in one coupling co-ordinate (terminal), then one can estimate the power transmission. In addition it is assumed that the cross coupling between

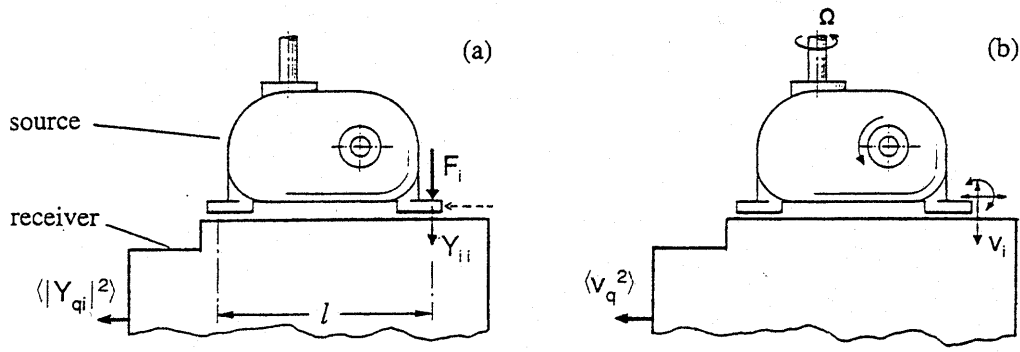


Figure 44. Far-field calibration of receiving structure by using terminal i as drive point [51].

terminals is negligible. This means that the source and receiver are assumed to be connected in parallel at the terminal i thus the total driving-point Y_{ii} and transfer mobility Y_{qi} are obtained from [51]

$$Y_{ii} \approx \frac{Y_{S,ii} Y_{R,ii}}{Y_{S,ii} + Y_{R,ii}} \quad (189)$$

and

$$Y_{qi} = \frac{Y_{S,ii} Y_{R,qi}}{Y_{S,ii} + Y_{R,ii}}, \quad (190)$$

where $Y_{S,ii}$ and $Y_{R,ii}$ are the driving-point mobility of the source and receiver when they are uncoupled. Solving Eqs. (189) and (190) for $Y_{R,qi}$ and $Y_{R,ii}$ (or $Y_{S,ii}$) and substituting these into Eq. (188) one obtains [51]

$$P_S = \left\langle \overline{v_q^2} \right\rangle \left\langle \frac{|Y_{ii}|^2 \operatorname{Re}(1/Y_{ii} - 1/Y_{S,ii})}{\langle |Y_{qi}|^2 \rangle} \right\rangle_i, \quad \text{when } Y_{S,ii} \text{ is known} \quad (191)$$

or

$$P_R = \left\langle \overline{v_q^2} \right\rangle \left\langle \frac{|Y_{ii}|^2 \operatorname{Re}(1/Y_{R,ii})}{\langle |Y_{qi}|^2 \rangle} \right\rangle_i, \quad \text{when } Y_{R,ii} \text{ is known} \quad (192)$$

where P_S gives the estimate when the driving-point mobility $Y_{S,ii}$ of the source is known and P_R when the driving-point mobility $Y_{R,ii}$ of the receiver is known.

12.1.4 Application examples

12.1.4.1 Box receiver and engine foundation of ship

The transmission power estimates when Eq. (191) is used has been tested for different mounting and receiver arrangements. In these tests a small-scale source (see Figure 45) mounted on a box receiver or a testbed receiver has been used [51]. The results of these estimations were compared with the results obtained using the reference power transmission method according to Eq. (188).

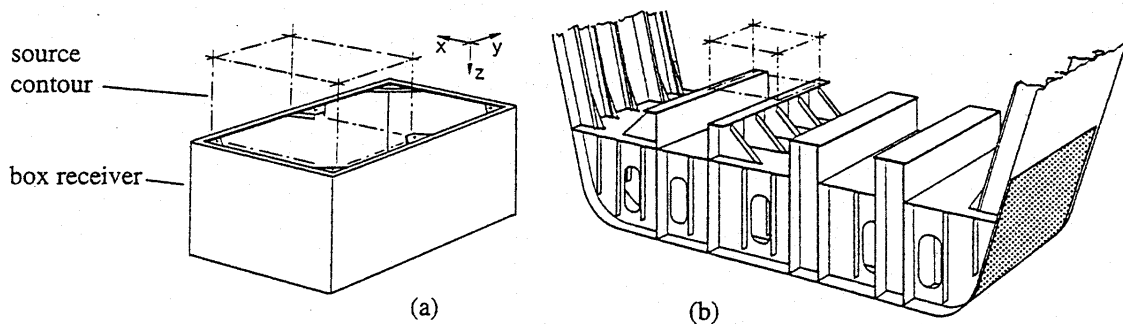


Figure 45. Source-receiver arrangement with: (a) Box receiver; (b) testbed receiver (ship model) [51].

The receiving structures (see Figure 45) were: (a) an open box-type receiver of size 630 x 390 x 280 mm with four 3 mm steel plates welded together and a bolted-on 1,5 mm thick steel plate in the bottom. All plates were covered with a unconstrained layer of damping material giving a frequency independent overall loss factor 0,03; (b) a scale model of a ship's engine foundation, which is more rigid, relatively large welded steel-plate structure with foundation plates 8 mm thick and other parts typically 2,5 mm thick and overall loss factor 0,025 [51].

The far-field region of the five-panel box receiver comprised of the two side panels and the bottom panel. In the engine foundation model the horizontal plates closely adjacent to the built-up foundation structure were used as the far-field region. The measured proportionality functions are nearly identical for the different mounting points despite of the large differences in their input mobilities (see Figure 46).

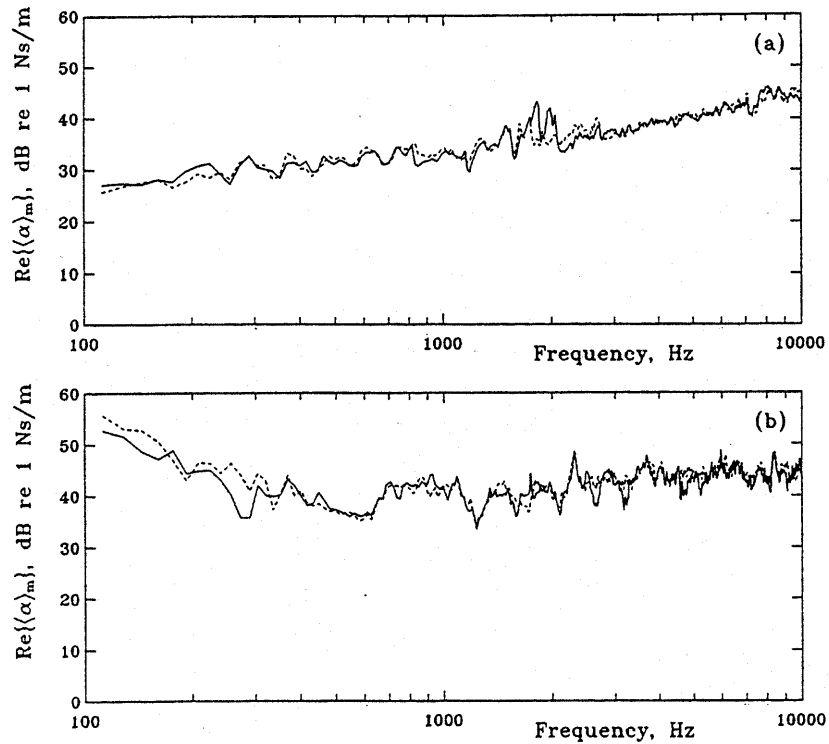


Figure 46. Proportionality functions $\langle \text{Re}(\alpha_{q_i}) \rangle$ for different drive points. (a) Box receiver excited at: ——— center bracket, - - - - - corner bracket. (b) Testbed receiver excited at: ——— end point, - - - - - centre point [51].

The source strength of a vibrational source can be characterized by its free terminal powers when the source is freely suspended [51]. In Figure 47 is seen the power components of the source used in these experiments. The source was oriented in the y-direction so the y-component dominates the measured power components as expected.

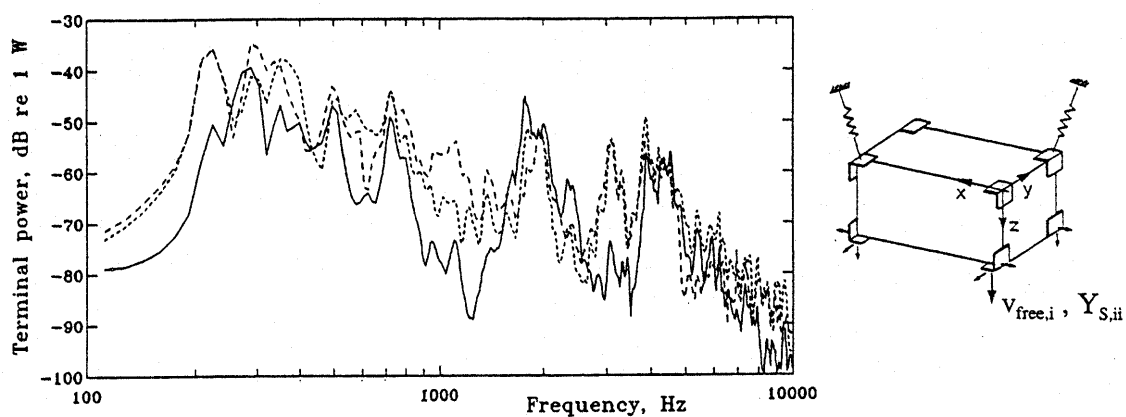


Figure 47. Modulus of free terminal power of source, averaged in the translational directions: x, - - - - - y, ——— z [51].

In Figure 48 are seen the differences between the source and receiver mobilities in the x and z direction.

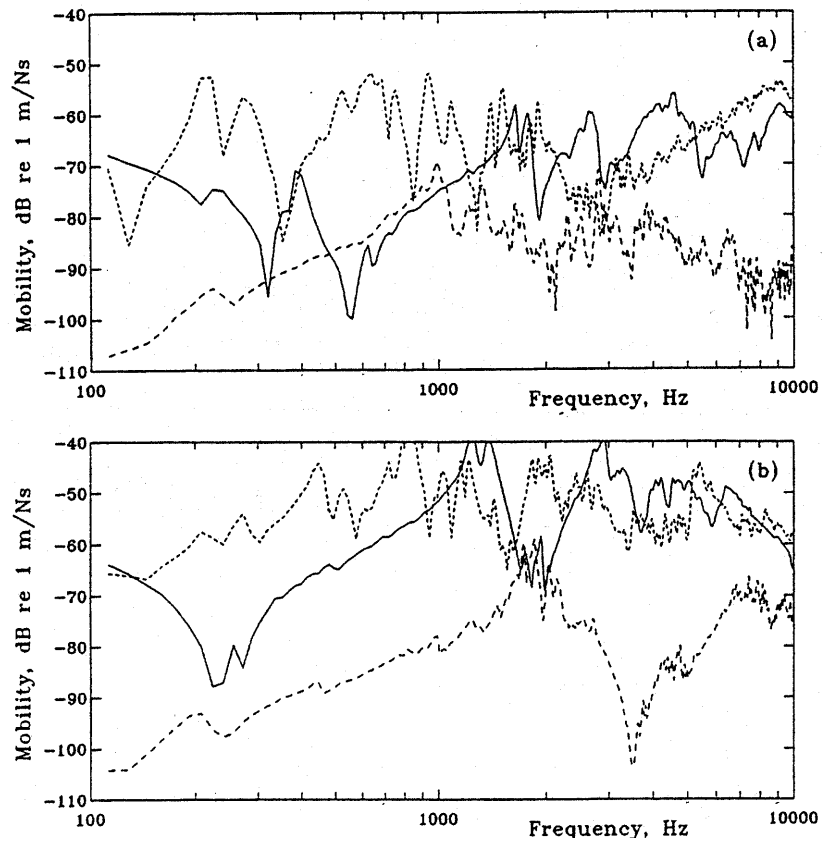


Figure 48. Driving-point mobilities in the translational direction: (a) x horizontal; (b) z vertical. Results are for: — source, box receiver, ----- testbed receiver [51].

Transmitted power estimates for the source mounted rigidly to either the box or the testbed receiver is shown in Figure 49. The full line gives the reference power estimate

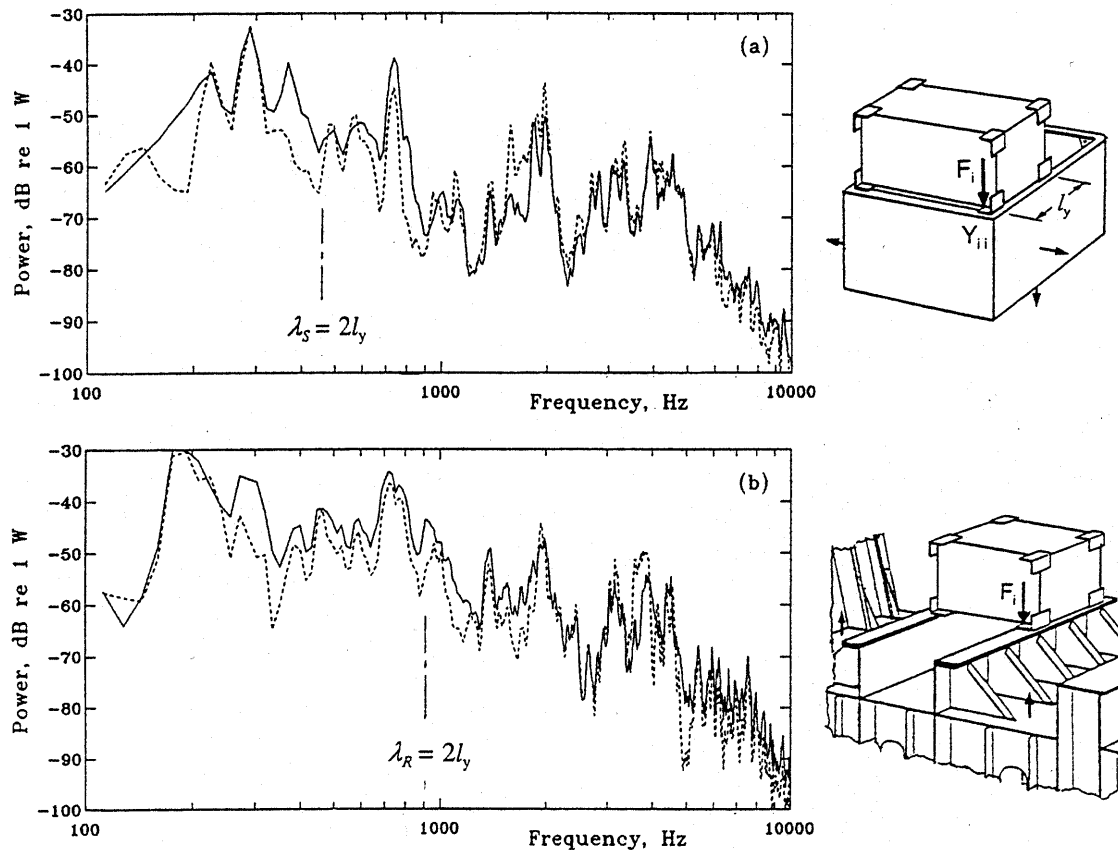


Figure 49. Power transmitted from source to: (a) box receiver; (b) testbed receiver. Method of estimation: *in-situ* estimate from a single external drive point and Eq. (191), —— reference power estimate from Eq. (188) [51].

obtained using Eq. (188) and the dash line gives the *in-situ* estimate obtained using Eq. (191) when the driving-point mobility $Y_{S,ii}$ of the source is known in only one terminal, which is the vertical z co-ordinate at one contact point. This demonstrates what is achievable with a minimum experimental effort [51]. It is seen that the degrading effect of neglecting the cross couplings occurs in the low frequency range below the frequency corresponding to $\lambda \approx 2l$. The wavelength λ is the longest flexural wavelength in the structural parts controlling the interface contact of the source or receiver and l is shortest distance between adjacent contact points, see Figure 44 (a) Figure 49 (a).

12.1.4.2 Helicopter fuselage

A 3/4-scale model of a helicopter fuselage was used in the study of structural power transmission from gearbox to fuselage [51]. The gearbox is mounted to the fuselage using four vertical lift-rods with ball-and-socket joints at both ends and in the horizontal direction it is mounted with two torque-rods which are clamped at both ends. The far-field region where the velocity response was measured comprised of three panels, forward roof panel and left- and right-hand side panel areas of the fuselage. The estimation of structural power transmission was made with Eq. (192). This requires that the driving-point mobilities of the receiver (fuselage) are known in the input terminals used, instead the driving-point mobilities of the source are not required. The three excitation points were at the upper part of a lift-rod. The estimation results are compared with power calibration in Figure 50. In one-third octave

bands the deviations are within ± 4 dB when frequency is over 250 Hz. At the lower frequencies the cross

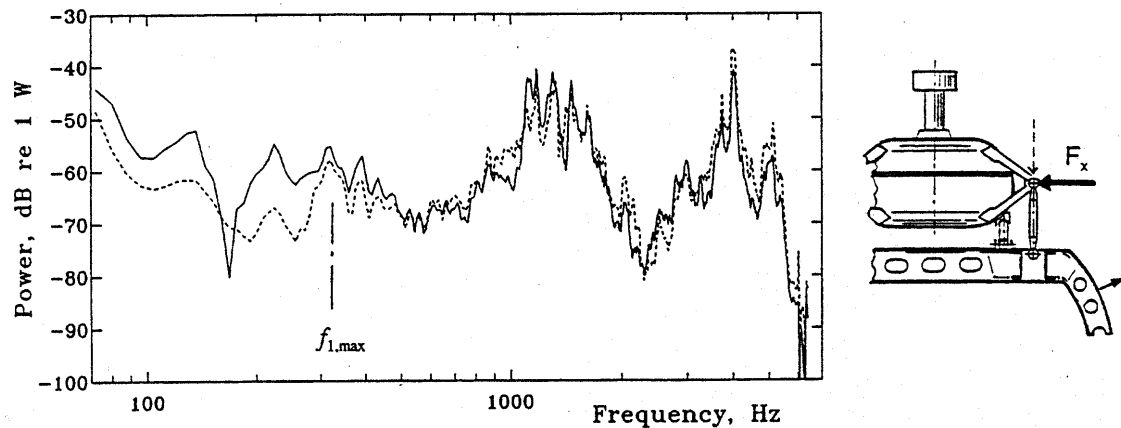


Figure 50. Power transmitted from gearbox to helicopter fuselage. Method of estimation: in-situ estimate averaged from three external drive terminals using Eq. (192), —— reference power estimate from Eq. (188) [51].

couplings effect on the accuracy. In addition it should be remembered that there are the two horizontal camped torque-rods which transmit structural power.

12.1.5 Applicability of in-situ estimation method

The structural power calibration of the receiving structure before the source machine is installed is an unbiased and general reference method. It can be used as a general method when approximate measurement methods or theoretical power transmission predictions are validated [51].

The approximate in-situ method described can be used when the driving-point mobilities of either source machine or receiving structure are unknown. This method gives a reasonable accuracy when the frequency is over the bounding frequency. The accuracy in one-third octave bands is of order ± 4 dB that was found with a helicopter fuselage example. When frequency is lower than the bounding frequency the accuracy is limited by cross couplings to be of the order ± 10 dB. In built-up structures made of plate-like parts the bounding frequency is approximately determined by the frequency for which the shortest distance between mounting points is equal to half the largest flexural wavelength of the source or receiving structures which control power transmission. If structures are more complex then the bounding frequency is the higher of the fundamental node frequencies which is obtained from the input mobilities [51].

12.2 Surface power or equivalent source power

The equivalent source power method ([54], [58], [59]), also called the surface power method, can be used when evaluating the vibration characteristics of machines or when estimating the power produced by their internal forces. The method has been found reliable and only little effected by the mounting conditions of the machines.

Determination of surface source power requires three series of measurements ([54], [57]): (1) the driving-point mobility $Y_{jj}(\omega) = v_j / F_j$ at the point j where external point force excitation F_j is applied, (2) the spatially averaged squared transfer mobility $\langle |Y_{pj}(\omega)|^2 \rangle = \langle v_{pj}^2 \rangle / F_j^2$, which relates the velocity responses at the suitably selected response points p to a suitably selected external excitation point j on the casing, and (3) the spatially averaged mean-squared velocity $\langle v_p^2 \rangle$ at the point p of the surface of the machine casing when the machine is running at specified rotational speed and load.

From (2) and (3) one can estimate the equivalent mean squared point force $F_j^2 \equiv F_{eq,j}^2$ which is required to produce the same mean squared vibration $\langle v_{pj}^2 \rangle = \langle v_p^2 \rangle$ which gives

$$F_{eq,j}^2 = \langle v_p^2 \rangle / \langle |Y_{pj}(\omega)|^2 \rangle. \quad (193)$$

The equivalent force generally depends on the selected excitation point; however, the structure-borne power it produces is rather insensitive [58]. Using the value of the equivalent force from Eq. (193) one obtains the time averaged complex power $J_{eq,j} = P_{eq,j} + iQ_{eq,j}$ that this force produces as [54]

$$J_{eq,j} = F_{eq,j}^2 Y_{jj}^*(\omega) = F_{eq,j}^2 |Y_{jj}(\omega)| e^{-i\phi_j(\omega)} = \langle v_p^2 \rangle \frac{|Y_{jj}(\omega)| e^{-i\phi_j(\omega)}}{\langle |Y_{pj}(\omega)|^2 \rangle}. \quad (194)$$

The real part $P_{eq,j}$ is the time averaged real power. The imaginary part $Q_{eq,j}$ is the time averaged reactive power. It is proportional to the time averaged difference of kinetic energy E_k and potential energy E_p of the total system: $Q_{eq,j} = 2\omega \overline{(E_k - E_p)}$, where ω is the angular frequency. The complex power takes into account the non-resonant forced vibrations of compact sources and local vibrations at the excitation points [58].

The important internal forces and structural modes are taken into account by making a number of estimations of $F_{eq,j}$ and $J_{eq,j}$. From these uncorrelated estimates one gets an average complex source power of the source [54]

$$J_{eq} = \langle J_{eq,j} \rangle = \langle v_p^2 \rangle \left\langle \frac{Y_{jj}^*(\omega)}{\langle |Y_{pj}(\omega)|^2 \rangle} \right\rangle = \langle v_p^2 \rangle \langle \alpha_{pj}(\omega) \rangle. \quad (195)$$

12.2.1 Excitation and response points

The external excitation points to get the best results are selected to be the rigid parts of the casing, i.e., in stiffened shell or panel areas over ribs [54]. The locations and directions of the exciting forces used should include the directions of dominating internal excitation forces

ensuring that most of the structural modes are excited. Three or four excitation points have been found to give accurate results [57].

The averaged transfer mobility and mean squared velocity of the machine casing are measured in the direction of normal to the surface at a number of points to get a representative estimate of its kinetic energy [57].

12.2.2 Machinery mounting conditions

The equivalent source power method gives reliable results, whether the source is resiliently mounted (i.e., freely suspended with ideal boundary conditions) or rigidly mounted to the receiving structure. This method also works when the modal density of the structure-borne sound source is low [57].

The equivalent source power method was tested when the 3/4-scale model of a helicopter gearbox was freely suspended and installed in the helicopter fuselage. In these tests four external excitation points. Points A, B, and C were "hard" and point D relatively soft (Figure 51). In Figure 51 (b) is presented the driving-point mobility at

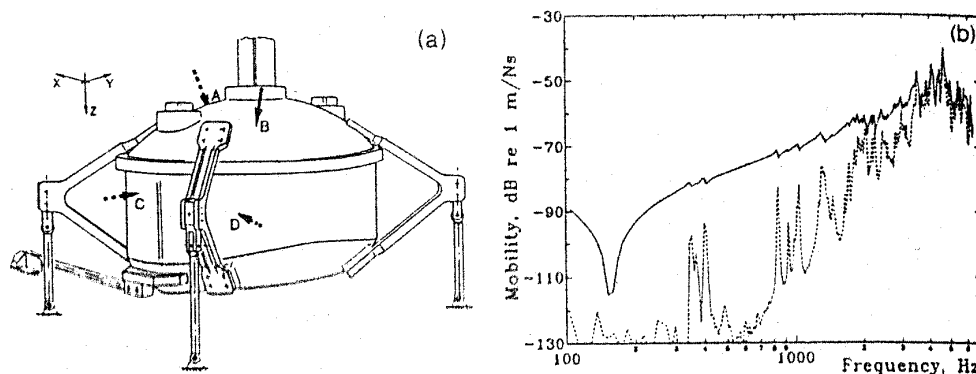


Figure 51. (a) Positions of excitation points A, B, C, and D normal to gearbox surface. (b) Driving-point mobility of excitation point B: — modulus, ---- real part [57].

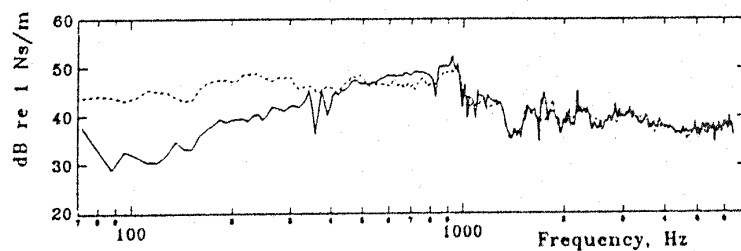


Figure 52. Proportionality function $\text{Re}\langle \alpha_{pj}(\omega) \rangle$ of gearbox, averaged from estimates based on excitation points A, B, C, and D on casing. Gearbox mounting conditions: — freely suspended, ---- installed in helicopter [57].

point B. In Figure 52 is presented the proportionality function $\text{Re}\langle \alpha_{pj}(\omega) \rangle$ of helicopter gearbox. It was averaged from the estimates obtained when the excitation was at points A, B, C and D on the casing. The gearbox was investigated under two mounting conditions: when it was freely suspended and when it was mounted in the helicopter fuselage.

13 Power transmission through vibration isolator

13.1 Dynamic stiffness matrix and general concepts

In ISO 10846 standard stiffness-type quantities are used for the experimental characterization of vibration isolators under static preload [60]. The characterization uses three blocks: the vibration source, a number n of isolators and the receiving structures (Figure 53). An assumption is made that there is a point contact at each connection between source and isolator and between isolator and receiver. At each contact point a force vector \mathbf{F} which contains three orthogonal forces and three orthogonal moments and a displacement vector \mathbf{u} which contains three orthogonal translational and three orthogonal rotational components are assigned.

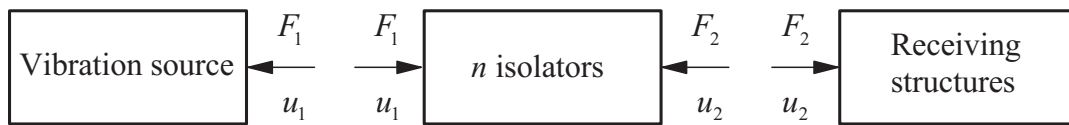


Figure 53. Schematic presentation of source/isolator/receiver system. At the connection point one component of each force and velocity vectors F_1, u_1, F_2 and u_2 is shown [60].

Let us consider a simple case of unidirectional vibration transmission through one vibration isolator. The positive directions of forces and velocities used to define the impedance and mobility parameters are shown in Figure 54. Using these definitions of

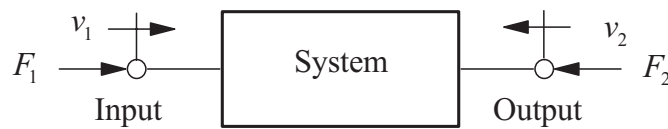


Figure 54. Positive directions of forces F and velocities v at the input and output of a system [36].

positive directions the isolator equilibrium may be expressed with the following stiffness equations:

$$F_1 = k_{1,1}u_1 + k_{1,2}u_2, \tag{196}$$

$$F_2 = k_{2,1}u_1 + k_{2,2}u_2, \tag{197}$$

where $k_{1,1}$ and $k_{2,2}$ are driving-point stiffnesses when the isolator is blocked at the opposite side (i.e. when displacement $u_2 = 0$ or $u_1 = 0$, respectively); $k_{1,2}$ and $k_{2,1}$ are blocked transfer stiffnesses, i.e. they denote the ratio between the force on the blocked side and the

displacement on the driven side [60]. For passive isolators $k_{1,2} = k_{2,1}$, because passive linear isolators are reciprocal. At high frequencies the equality any more holds owing to additional inertial forces. At low frequencies, where only elastic and damping forces are of significance, all $k_{i,j}$ terms are equal. These equations hold for single frequencies and F_i and u_i are phasors and $k_{i,j}$ are complex quantities. In matrix form the Eqs. (196) and (197) are

$$\mathbf{F} = \mathbf{K} \cdot \mathbf{u}, \quad (198)$$

where the dynamic stiffness matrix is

$$\mathbf{K} = \begin{bmatrix} k_{1,1} & k_{1,2} \\ k_{2,1} & k_{2,2} \end{bmatrix}. \quad (199)$$

The vibration isolator excites the receiving structure with force F_2 , which is obtained with the driving-point stiffness k_r of the receiving structure from Eq. [63], [60]

$$k_r = -\frac{F_2}{u_2}. \quad (200)$$

The minus sign is due to the sign conventions presented in Figure 53 and Figure 54. From Eqs. (197) and (200) one obtains the exciting force F_2 [63], [60]

$$F_2 = \frac{k_{2,1}}{1 + \frac{k_{2,2}}{k_r}} u_1. \quad (201)$$

From Eq. (201) is seen that for a given source displacement u_1 , the force F_2 depends both on the isolator driving-point dynamic stiffness $k_{2,2}$ and on the receiver driving-point dynamic stiffness k_r . If $|k_{2,2}| < 0,1 \cdot |k_r|$, then the force F_2 approximates the blocking force to within 10 % and [60]

$$F_2 \approx F_{2,\text{blocking}} = k_{2,1} u_1. \quad (202)$$

A vibration isolator is effective only if on both sides of the isolator the dynamic stiffness is large. Eq. (202) represents the situation at the receiving side. This forms the basis of the measurement methods of ISO 10846. Measurement of the blocked dynamic transfer stiffness for an isolator under static preload is easier than measurement of the complete stiffness matrix. In addition it describes the isolator dynamic characteristic under its intended use.

If at each contact point the forces and displacements can be characterized with six orthogonal components (three translations, three rotations) then the isolator may be described as a 12-port [63]. In the Cartesian co-ordinate system (Figure 55) the generalized displacement vector \mathbf{u}_1 at the input of the isolator is [60]

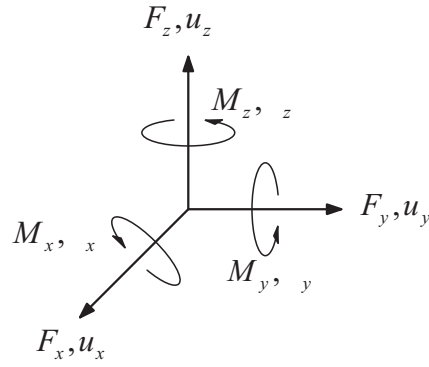


Figure 55. Cartesian co-ordinate system with axes x , y , and z and used notations: F is force, M is moment, u is translational displacement and γ is rotational displacement [60].

$$\mathbf{u}_1 = \{u_{1x}, u_{1y}, u_{1z}, \gamma_{1x}, \gamma_{1y}, \gamma_{1z}\}^T, \quad (203)$$

where $(u_{1x}, u_{1y}$ ja $u_{1z})$ are the translational displacements and $(\gamma_{1x}, \gamma_{1y}$ ja $\gamma_{1z})$ are the rotational displacements. At the output the generalized displacement vector \mathbf{u}_2 is

$$\mathbf{u}_2 = \{u_{2x}, u_{2y}, u_{2z}, \gamma_{2x}, \gamma_{2y}, \gamma_{2z}\}^T. \quad (204)$$

The generalized force vector at the input of the isolator is [60]

$$\mathbf{F}_1 = \{F_{1x}, F_{1y}, F_{1z}, M_{1x}, M_{1y}, M_{1z}\}^T, \quad (205)$$

with three translational forces F_{ij} and three moments M_{ij} as its components. At the output the generalized force vector \mathbf{F}_2 is written equivalently

$$\mathbf{F}_2 = \mathbf{F}_{2, \text{blocking}} = \{F_{2x}, F_{2y}, F_{2z}, M_{2x}, M_{2y}, M_{2z}\}^T, \quad (206)$$

where the components are the three blocking forces and the three blocking moments [60]. Using the generalized forces and displacements the Eq. (198) can be written in the form

$$\mathbf{F} = \begin{Bmatrix} \mathbf{F}_1 \\ \mathbf{F}_2 \end{Bmatrix} = \mathbf{K} \cdot \mathbf{u} = \begin{bmatrix} \mathbf{K}_{11} & \mathbf{K}_{12} \\ \mathbf{K}_{21} & \mathbf{K}_{22} \end{bmatrix} \begin{Bmatrix} \mathbf{u}_1 \\ \mathbf{u}_2 \end{Bmatrix}. \quad (207)$$

This equation can be expanded as

$$\begin{Bmatrix} F_{1x} \\ F_{1y} \\ F_{1z} \\ M_{1x} \\ M_{1y} \\ M_{1z} \\ F_{2x} \\ F_{2y} \\ F_{2z} \\ M_{2x} \\ M_{2y} \\ M_{2z} \end{Bmatrix} = \begin{bmatrix} k_{1,1} & k_{1,2} & \cdots & k_{1,6} & k_{1,7} & k_{1,8} & \cdots & k_{1,12} \\ \vdots & \vdots & \ddots & \vdots & \vdots & \vdots & \ddots & \vdots \\ k_{6,1} & k_{6,2} & \cdots & k_{6,6} & k_{6,7} & k_{6,8} & \cdots & k_{6,12} \\ k_{7,1} & k_{7,2} & \cdots & k_{7,6} & k_{7,7} & k_{7,8} & \cdots & k_{7,12} \\ \vdots & \vdots & \ddots & \vdots & \vdots & \vdots & \ddots & \vdots \\ k_{12,1} & k_{12,2} & \cdots & k_{12,6} & k_{12,7} & \cdots & \cdots & k_{12,12} \end{bmatrix} = \begin{Bmatrix} u_{1x} \\ u_{1y} \\ u_{1z} \\ \gamma_{1x} \\ \gamma_{1y} \\ \gamma_{1z} \\ u_{2x} \\ u_{2y} \\ u_{2z} \\ \gamma_{2x} \\ \gamma_{2y} \\ \gamma_{2z} \end{Bmatrix}, \quad (208)$$

where can be seen the meaning of the elements of 12×12 stiffness matrix. With the submatrix \mathbf{K}_{21} and displacement \mathbf{u}_1 the generalized blocking force \mathbf{F}_2 is [75]

$$\begin{Bmatrix} F_{2x} \\ F_{2y} \\ F_{2z} \\ M_{2x} \\ M_{2y} \\ M_{2z} \end{Bmatrix} = \begin{bmatrix} k_{F_{2x},u_{1x}} & k_{F_{2x},u_{1y}} & k_{F_{2x},u_{1z}} & k_{F_{2x},\gamma_{1x}} & k_{F_{2x},\gamma_{1y}} & k_{F_{2x},\gamma_{1z}} \\ k_{F_{2y},u_{1x}} & k_{F_{2y},u_{1y}} & k_{F_{2y},u_{1z}} & k_{F_{2y},\gamma_{1x}} & k_{F_{2y},\gamma_{1y}} & k_{F_{2y},\gamma_{1z}} \\ k_{F_{2z},u_{1x}} & k_{F_{2z},u_{1y}} & k_{F_{2z},u_{1z}} & k_{F_{2z},\gamma_{1x}} & k_{F_{2z},\gamma_{1y}} & k_{F_{2z},\gamma_{1z}} \\ k_{M_{2x},u_{1x}} & k_{M_{2x},u_{1y}} & k_{M_{2x},u_{1z}} & k_{M_{2x},\gamma_{1x}} & k_{M_{2x},\gamma_{1y}} & k_{M_{2x},\gamma_{1z}} \\ k_{M_{2y},u_{1x}} & k_{M_{2y},u_{1y}} & k_{M_{2y},u_{1z}} & k_{M_{2y},\gamma_{1x}} & k_{M_{2y},\gamma_{1y}} & k_{M_{2y},\gamma_{1z}} \\ k_{M_{2z},u_{1x}} & k_{M_{2z},u_{1y}} & k_{M_{2z},u_{1z}} & k_{M_{2z},\gamma_{1x}} & k_{M_{2z},\gamma_{1y}} & k_{M_{2z},\gamma_{1z}} \end{bmatrix} \begin{Bmatrix} u_{1x} \\ u_{1y} \\ u_{1z} \\ \gamma_{1x} \\ \gamma_{1y} \\ \gamma_{1z} \end{Bmatrix}. \quad (209)$$

The elements of submatrix \mathbf{K}_{21} have the following meaning:

$$k_{7,1} = k_{F_{2x},u_{1x}} = \frac{F_{2x,\text{blocking}}}{u_{1x}} \quad \text{and} \quad k_{10,4} = k_{M_{2x},\gamma_{1x}} = \frac{M_{2x,\text{blocking}}}{\gamma_{1x}}, \quad \text{etc.}$$

Owing to symmetry many of elements will be equal to zero and some non-zero elements may be equal in magnitude see examples in [60] and [63]. In practise often one, two or three diagonal elements is sufficient to describe the dynamic stiffness properties of isolator in the translational directions. In practical cases it must be considered which translational directions are important. Sometimes owing to the geometry and properties of the isolator it may have large transverse stiffness and may also have large rotational stiffness. When isolators of this kind are applied in thin-walled structures and for rather high frequency isolation then the rotational stiffness components may be important and must be included in the measurements and analysis [60].

13.2 Determination of power transmitted via vibration isolator

13.2.1 Direct method

In the direct method the time averaged vibrational power which is transmitted through a vibration isolator is determined by measuring the force and velocity directly ([19], [64], [65], and [74]) (see Figure 56). In the direct measurement method at each contact point one must measure the force and vibration velocity in each excitation direction. In practise this is not always possible because the force transducer cannot be installed in series with the isolator. For example following reasons can prevent installation of force transducer: there is not room enough, the machine cannot be lifted because its shaft alignment cannot be changed, the measurement must be made *in-situ*, force transducer is not mechanically durable, attachment is not possible or its mass distorts the measurement results.

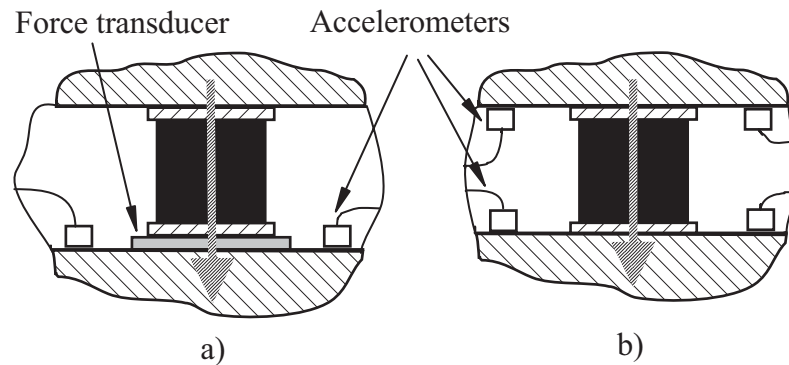


Figure 56. Determination of structure-borne sound power transmission through an isolator. a) Direct method, and b) indirect method. Vibrational energy flows in the direction of the hatched arrow [64].

13.2.2 Indirect method

Structure-borne sound power transmission through an isolator can be determined indirectly using cross-spectral methods [61], [62], [63], and [64]. In this method the force is not measured directly. It is determined indirectly using the transfer stiffness of the isolator and the displacement of the upper surface of the isolator (see Figure 56). For these reasons the method is often applicable if the measurements are to be made *in-situ* provided that there is enough space for the mounting of transducers.

Let us consider a vibration isolator under unidirectional excitation at the input point 1 and that the output point 2 is blocked, e.g., its displacement is zero. The force exerted by the isolator on the receiving structure is obtained from Eqs. (197) and (200) as

$$F_2 = k_{2,1}u_1 + k_{2,2}u_2 = \frac{k_{2,1}}{1 + \frac{k_{2,2}}{k_r}}u_1 \approx k_{2,1}\left(1 - \frac{k_{2,2}}{k_r}\right)u_1, \quad (210)$$

where $k_{2,1}$ is the blocked transfer stiffness over the isolator, i.e. it denotes the ratio between the force on the blocked side and the displacement on the driven side, $k_{2,2}$ is the driving-point stiffness when the isolator is blocked at the opposite side, u_1 is the vibration displacement at the input point 1 and u_2 is the vibration displacement at the output point 2. The approximation is valid within 10 % when $|k_{2,2}| < 0,1 \cdot |k_r|$ [60].

The time average of structure-borne sound power transmitted $\langle P \rangle_t$ to the structure in one contact point is obtained as time average of the product between the exciting force and the resulting velocity. This can be calculated from equation (e.g. [63], [31])

$$\langle P \rangle_t = E[F_2(t) \cdot v_2(t)] = R_{F_2 v_2}(0) = \text{Re} \int_0^\infty G_{F_2 v_2}(f) df, \quad (211)$$

where $E[]$ denotes the expected value of the expression inside the brackets, $R_{F_2 v_2}(0)$ is the cross-correlation function between the force $F_2(t)$ and velocity $v_2(t)$ signals as a function of the delay time $\tau = 0$, and $G_{F_2 v_2}(f)$ is the one sided cross spectral density function between the force $F_2(f)$ and velocity $v_2(f)$ signals. When the force and velocity are determined using the measured acceleration signals then Eq. (211) can be written as

$$\langle P \rangle_t = \int_0^\infty \frac{\text{Im}}{\omega^3} \left[\hat{k}_{2,1}^* \left(1 - \frac{\hat{k}_{2,2}^*}{\hat{k}_r^*} \right) G_{a_1 a_2}(f) \right] df \approx \int_0^\infty \frac{\text{Im}}{\omega^3} \left[\hat{k}_{2,1}^* G_{a_1 a_2}(f) \right] df, \quad (212)$$

where $G_{a_1 a_2}(f)$ is the one sided cross spectral density between the measured acceleration signals $a_1(f)$ at the input and $a_2(f)$ at the output of the vibration isolator, $\hat{k}_{2,1}$ is the blocked transfer stiffness of the isolator, $\hat{k}_{2,2}$ is the blocked driving-point stiffness of the isolator, \hat{k}_r is the driving-point stiffness of the receiving structure, $(\hat{\cdot})$ denotes Fourier transform, and symbol $(\cdot)^*$ denotes complex conjugate. Usually the driving-point stiffness of the receiving structure is much larger than the driving-point stiffness of a soft vibration isolator and then the approximations of Eq. (210) and (212) can be used. From Eq. (212) one can see that for the determination of the structure-borne sound power transmission through a vibration isolator the dynamic blocked transfer stiffness of the isolator is needed. The dynamic blocked transfer stiffness can be determined using test rigs constructed for this purpose (e.g. [63], [64], [67], [68], [71], [72]). In addition the acceleration signal a_1 on the excited side and the acceleration signal a_2 on the output side of the isolator are measured using standardized method [73]. With these quantities the approximate time average of the transmitted power can be determined. In case that there are many isolators one can assume that the power transmitted through one isolator is independent on the power transmitted through other isolators. Then the approximate time average of the total power through N isolators is obtained as a sum

$$\langle P \rangle_{t, \text{tot}} = \sum_{i=1}^N \langle P_i \rangle_t, \quad (213)$$

where $\langle P_i \rangle_t$ is the time average of the power transmitted through isolator i .

13.2.3 Generalization of the indirect method

The characterization of the dynamic properties of vibration isolators can be generalized to include all directions of translational and rotational vibrations using generalized force and displacement at contact points (e.g. [63], [64]). If forces and moments can be characterized by six orthogonal components including three translations and three rotations, then the isolator may be described as a 12-port [63]. Using the generalized force defined in Eq. (205) and (206) and the generalized displacement redefined in Eq. (203) and (204) the Fourier transformed equilibrium equations can be written

$$\hat{\mathbf{F}}_1 = \hat{\mathbf{K}}_{11} \hat{\mathbf{u}}_1 + \hat{\mathbf{K}}_{12} \hat{\mathbf{u}}_2, \quad (214)$$

and

$$\hat{\mathbf{F}}_2 = \hat{\mathbf{K}}_{21} \hat{\mathbf{u}}_1 + \hat{\mathbf{K}}_{22} \hat{\mathbf{u}}_2, \quad (215)$$

where $\hat{\mathbf{K}}_{11}$ and $\hat{\mathbf{K}}_{22}$ are the Fourier transformed blocked dynamic driving-point 6 x 6 stiffness matrices and $\hat{\mathbf{K}}_{12}$ and $\hat{\mathbf{K}}_{21}$ are the Fourier transformed blocked dynamic transfer 6 x 6 stiffness matrices [64]. From reciprocity it follows that $\hat{\mathbf{K}}_{12} = \hat{\mathbf{K}}_{21}^T$, $\hat{\mathbf{K}}_{11} = \hat{\mathbf{K}}_{11}^T$ and $\hat{\mathbf{K}}_{22} = \hat{\mathbf{K}}_{22}^T$, with T denoting a transpose [64]. In vibration isolation the objective is to get a large source-receiving structure path stiffness mismatch. Usually driving-point stiffness of the receiving structure is much larger than the isolator stiffness, then [63]

$$\hat{\mathbf{F}}_2 \approx \hat{\mathbf{K}}_{21} \hat{\mathbf{u}}_1. \quad (216)$$

This approximation reduces the number of needed stiffness elements for a single isolator to $36 = 6 \times 6$. Further reductions can be obtained due to isolator shape symmetries (see [60], [63], [75]). The metal plates at the ends of an isolator can be considered to be integrated to the receiving structure, because the stiffness mismatch is at the rubber-plate interface [64]. In cases where the approximation of Eq. (216) can not be used Eq. (215) still applies resulting to element number $72 = 6 \times 6 + 6 \times 6$ for the accurate force estimation at the receiving structure [64].

With cross-spectral techniques the power transmission through vibration isolator to receiving structure in different degrees of freedom can be determined indirectly [64], [66]. The total power transmitted is obtained as a sum of powers in different degrees of freedom. In the measurement technique one needs to measure the vibration velocities of resiliently mounted machinery. This can be made using standardized methods [73]. Also the needed dynamic transfer stiffnesses of isolators can be measured using standardized methods described in [60], [74], [75].

Amunarriz has studied the power transmission over a cylindrical rubber isolator [66]. The diameter of the isolator was 100 mm, height 54 mm and hardness 40° IRH (International Rubber Hardness). In the frequency range 20 Hz - 1 kHz 97 % was transmitted by translational degrees of freedom, 2,1 % by cross couplings and 0,9 % by rotational degrees. At low frequencies in the frequency range 20 Hz - 500 Hz the share of translational degrees was 96 % and that of rotational degrees 4 %. At high frequencies in the frequency range

500 Hz - 1 kHz the share of translational degrees decreases to 91 % and there is an increase in the contribution of rotational degrees reaching 5 % and cross couplings reaching 4 % [66]. These approximate results can give guidance when considering the effect of rotational and cross coupling components in the power transmission through vibration isolators in engineering applications.

14 Research and test facilities of vibration isolators

14.1.1 Research and facilities at KTH, Sweden

In Sweden at KTH, The Royal Institute of Technology, active research and testing has been done for years in The Marcus Wallenberg Laboratory for Sound and Vibration Research (MWL) led by professor Anders Nilsson [64], [65], [66].

Let us take an example of the research work done in this laboratory. Leif Kari has measured in six degrees of freedom up to 1 000 Hz the blocked dynamic transfer stiffness of a cylindrical rubber vibration isolator under four different static preloads [64]. He has also developed models and made theoretical calculations of transfer stiffness of rubber mounts. He applied correlation technique and stepped sine excitation to improve the signal to noise ratio. Indirect test method is used in the KTH test rig (Figure 57). Kari has studied a vulcanized natural rubber isolator. Its length was 50 mm, radius 50 mm, and hardness 40° IRH (International Rubber Hardness). The allowed continuous static load was limited to 3 000 N. He measured the axial static force due to axial deformation in the domain 0 - 12 mm in steps of approximately 1 mm. The measured axial dynamic stiffness in the frequency range 50 - 1 000 Hz under different preloads is presented in Figure 59 and Figure 60. The stiffness magnitude curve in Figure 59 is plateau like in the low frequencies up to about 400 Hz. Thereafter the curve rises to a peak at 500 Hz, drops to a trough, rises to a second peak and so on. Taking into account the magnitude curve with the phase curve, the three peaks occur likely at anti resonance and the first and the third troughs are likely connected to resonances [64].

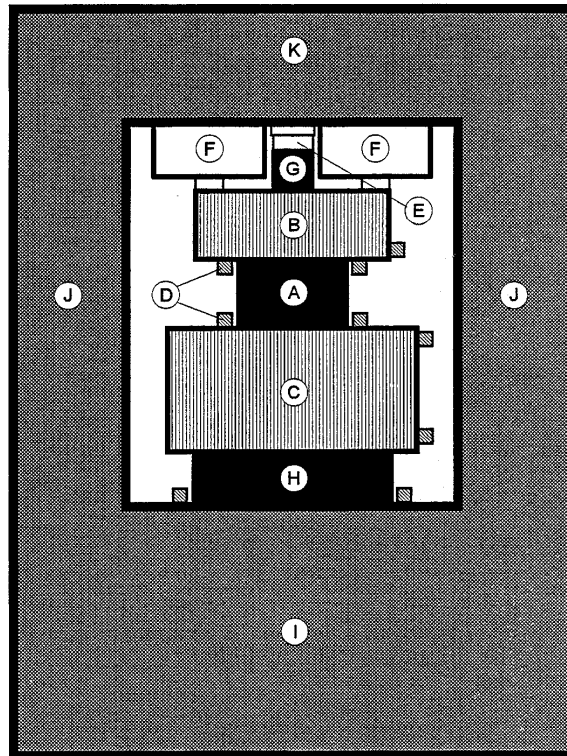


Figure 57. Schematic presentation of the test rig of vibration isolators at KTH [65]. It is based on indirect method. The parts are: A isolator under test, B force distribution plate, C blocking mass, D piezoelectric accelerometers, E strain gage, F electrodynamic vibration generators, G upper auxiliary isolator, H lower auxiliary isolator, I heavy and rigid frame, J strong columns, and K crosshead.

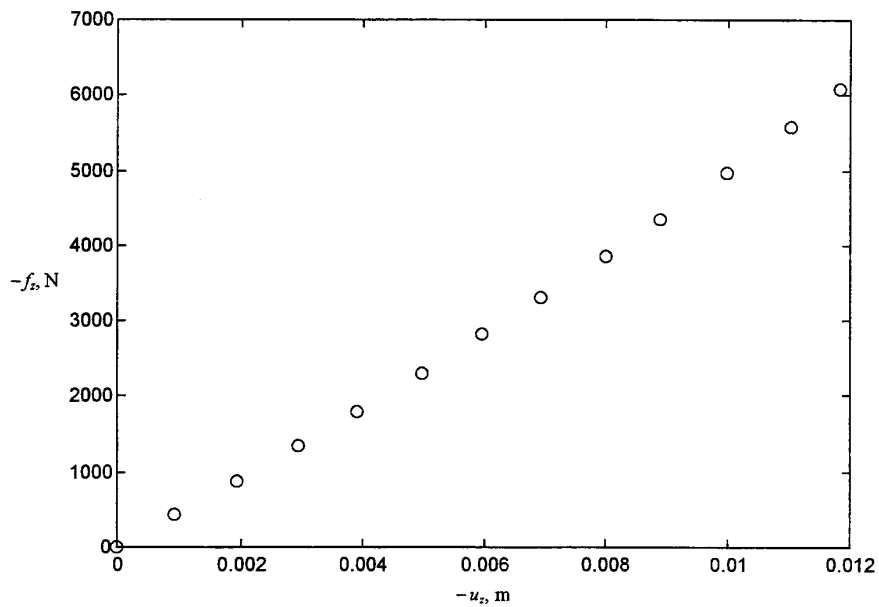


Figure 58. Measured axial compression force versus corresponding displacement. Test object is the rubber vibration isolator [64].

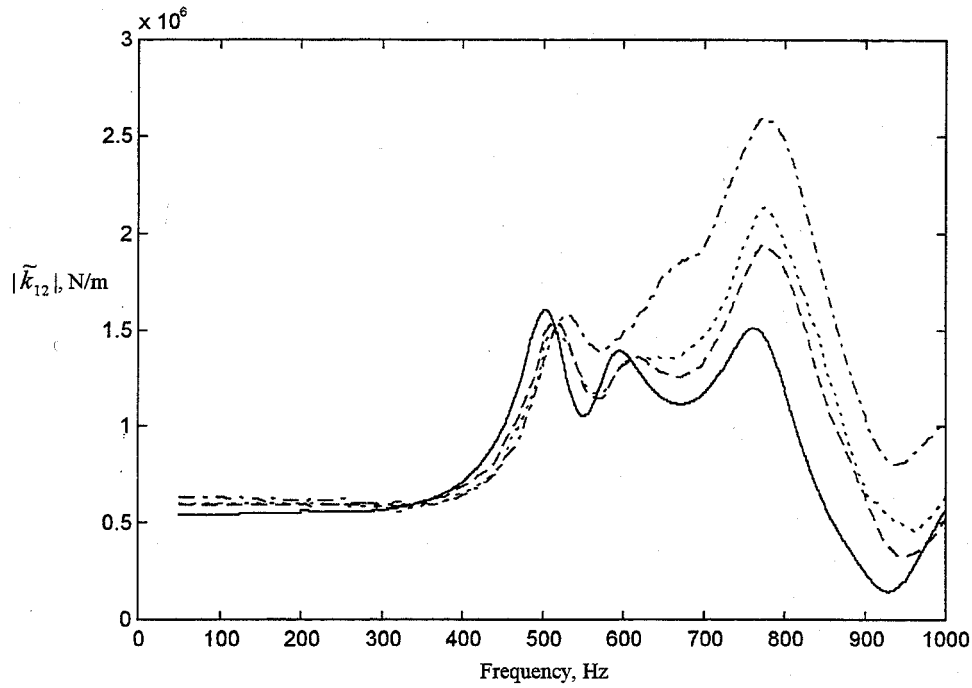


Figure 59. Measured magnitude of transfer stiffness. Test object is the rubber vibration isolator. 0 N (solid thin), 1 600 N (dashed), 2 100 N (dotted) and 3 350 N preload (dash-dotted) [64].

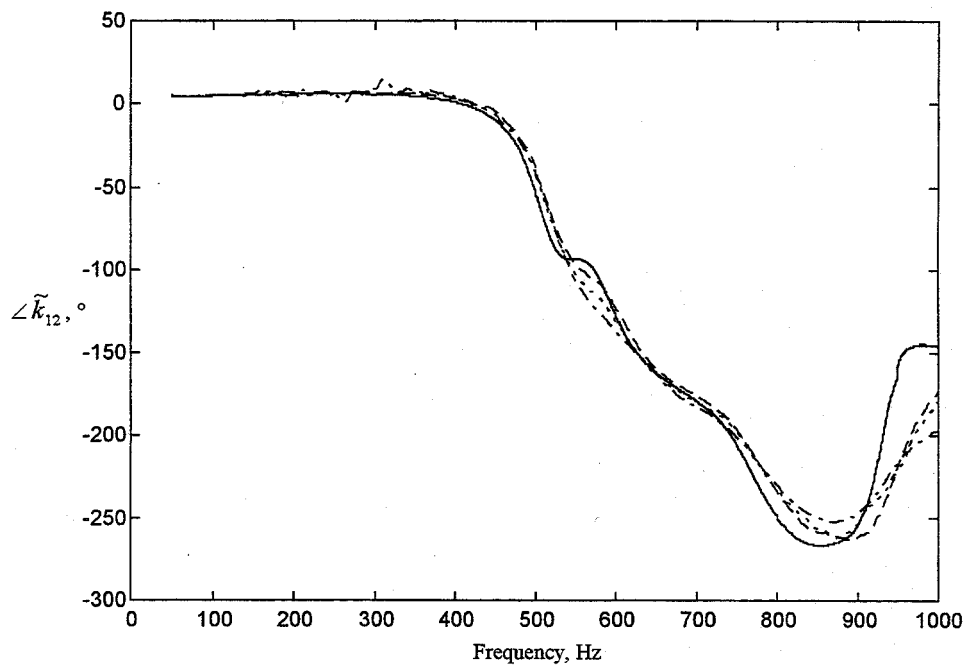


Figure 60. Measured unwrapped phase of transfer stiffness. Test object is the rubber vibration isolator. 0 N (solid thin), 1 600 N (dashed), 2 100 N (dotted) and 3 350 N (dash-dotted) [64].

14.1.2 Research and facilities at AMRL, Australia

In Australia testing of vibration isolators is made in The Aeronautical and Maritime Research Laboratory (AMRL). This laboratory belongs to Defence Science and Technology Organization (DSTO). There Dickens and Norwood propose a two-mass method to determine the four-pole parameters of a uni-directional asymmetrical vibration isolator [67]. They have developed and tested a test rig shown in Figure 61.

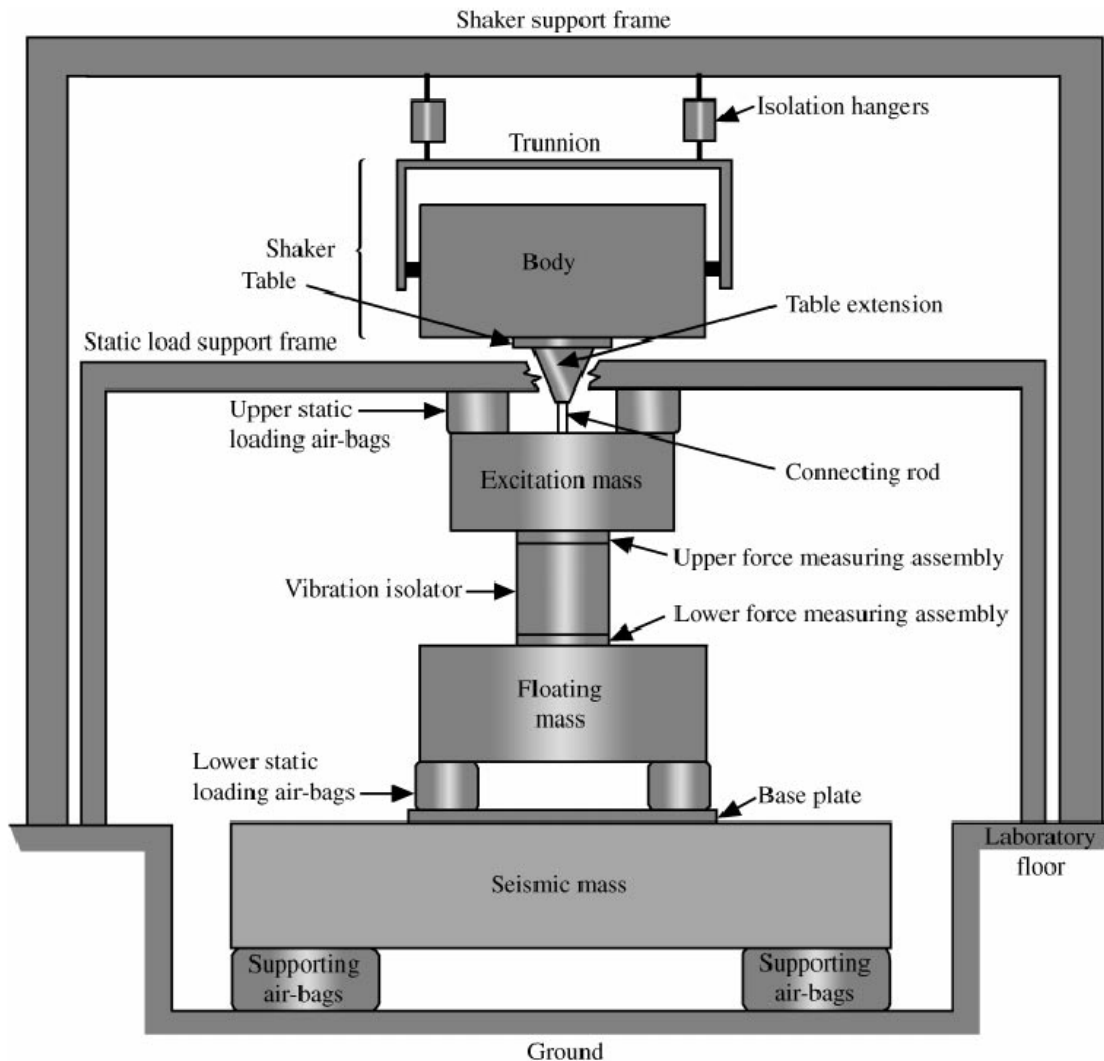


Figure 61. Schematic diagram of vibration isolator test rig [67].

The test rig employs the floating mass method and direct force measurement and it may also employ the two-mass method. Vibration isolators operated in lateral and transverse orientations may also be tested with this test facility. Vibration isolator is mounted between two large masses. An electro-dynamic shaker via the excitation mass applies the dynamic load. The floating mass provides a reaction force to the output force of the vibration isolator. Air bags are used to produce easily adjustable static load. They also give good vibration isolation between the mass and the supporting structure. The seismic mass of 22 tons with dimensions $3\text{ m} \times 3\text{ m} \times 1\text{ m}$ is made of reinforced concrete. It is supported on four air bags. The mounted natural frequency of this test facility is approximately 1,2 Hz. The upper frame supports the shaker. The lower frame provides the reaction forces for the upper static loading

air bags. The two frames are used to reduce the coupling between the preloading structure and the shaker. The vibration due to flanking transmission is 90 dB smaller than the vibration level due to direct transmission. The vibration velocities at input and output of the vibration isolator are measured with accelerometers attached to the excitation and floating masses. The dynamic force applied by the excitation mass to the vibration isolator is measured directly with a force measuring assembly consisting of eight force transducers. The test facility is constructed to measure dynamic stiffness in the range of $1 \times 10^5 - 2 \times 10^7$ N/m with preloads varying from 1,5 to 30 kN and over a frequency range from 10 Hz to 2 000 Hz [68].

With the test facility it is possible to determine the four-pole parameters of an uni-directional or bi-directional, and asymmetrical or symmetrical vibration isolator under static load. Generally vibration isolators incorporating some form of active control are examples of uni-directional vibration isolators [68].

The method proposed by Dickens and Norwood to dynamically characterize vibration isolators with four-pole parameters has three advantages [67]. Firstly, the characterization is independent of the method. Traditionally the transmissibility of a vibration isolator is determined by attaching a mass on the isolator, which in turn is supported on a rigid foundation. Then a shaker excites the mass and the output of the vibration isolator is considered to be blocked. The transmissibility is determined as the ratio of the output force of the vibration isolator to the input force exerted to the mass. So it depends on the supported mass, and is not independent on the test arrangement. Secondly, at high frequencies evident mass effects of the vibration isolator are taken into account. In traditional methods the distribution of mass and stiffness of the vibration isolator are not included. So the massless spring model fails to predict the existence of the longitudinal standing waves which reduce the performance of real vibration isolators. Thirdly, the four-pole parameters of a complicated mechanical system can be computed from the four-pole parameters of its components.

The traditional methods for the determination of four-pole parameters of a vibration isolator under static preload use blocked test configuration. Because asymmetrical vibration isolators require additional information which is obtained by reversing the vibration isolator in the test rig meaning that its input and output sides are interchanged. This procedure is inapplicable for uni-directional vibration isolators as for active vibration isolators [67].

14.1.3 Research and facilities at TNO TPD, The Netherlands

The TNO Institute of Applied Physics - Technisch Physische Dienst (TNO TPD) has been carrying out an active and extensive research on resilient elements since 1975. In this context various test facilities have been developed for measuring the sound transfer and the dynamic stiffness of resilient components in the six degrees of freedom under normal operational conditions, such as static preload and internal pressure [71], [72]. In the test rigs the real component properties can be measured for multi-directional excitation under operational static load. In a test rig (Figure 62 and Figure 63)

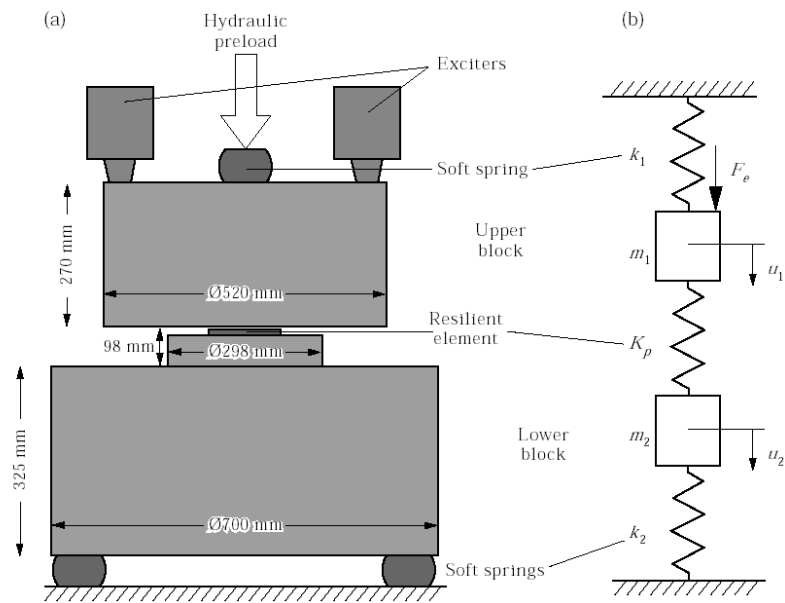


Figure 62. (a) Schematic diagram of the measurement apparatus (not to scale), showing main dimensions. (b) Equivalent mass-spring system [69].

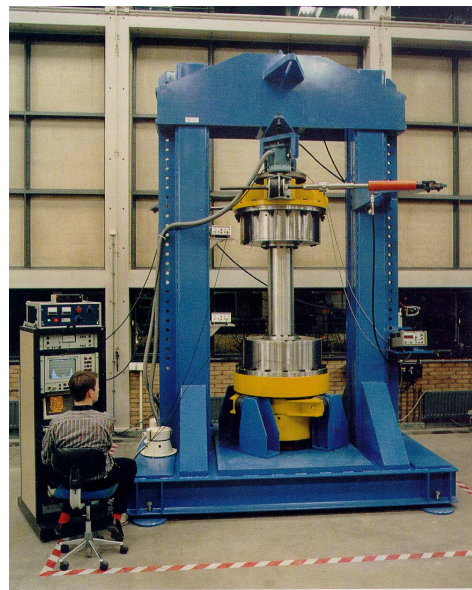


Figure 63. Test facility with a flexible shaft under test in the axial excitation mode (torsional preload with two hydraulic cylinders) [71].

the vibration isolator under test is assembled between two masses. The upper mass simulates the machine side and acts as an excitation mass. The lower mass is used to determine the so-called blocked forces, which a flexible element exerts on high impedance seating. The seating is the local attachment point on the receiving substructure to which the "lower" end of the isolator is attached [19]. The frequency range of interest determines the sizes and dimensions of these masses. In the measurement range over the natural frequency of the system the sound transfer functions and the dynamic stiffnesses can be determined. Changing the direction of excitation this determination can be made in all other degrees of freedom. Flexible soft couplings up to 1 m diameter and 75 kNm torsional preload can be tested in the largest test rig. The torsional preload is obtained with pneumatic or hydraulic auxiliaries.

Resilient mountings can be measured in a hydraulic pressure test bench. The mounting is assembled between two masses, which vibrate as free, rigid bodies in the frequency range considered. The mounting and the masses are decoupled from the frame with auxiliary soft mountings. These mountings provide support and static preload. The electrodynamic shaker connected to the excitation mass produces the excitation. The measurements are made using accelerometers. Selection of masses and auxiliary mountings provides a useful measurement frequency range from 20 Hz to 2 000 Hz [71], [72]. The dimensions of the masses can be changed to obtain the upper measurement limit of 4 kHz [70]. In the largest test rig the preload can be 100 tons. The measurements are made according to standard ISO 10846, parts 1-5 [72].

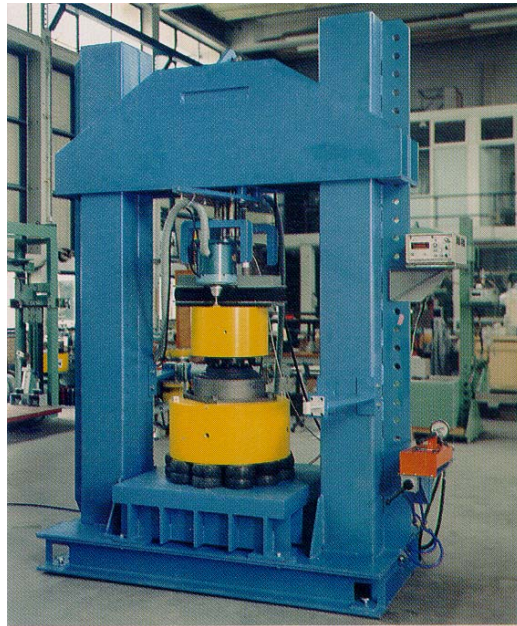


Figure 64. Test facility with rubber mounting under test in the vertical excitation mode [71]. Bellows and flexible hoses can be tested in similar test rigs as is used for mountings and couplings (see Figure 65). The measurements are made under real pressure conditions inside the elements.

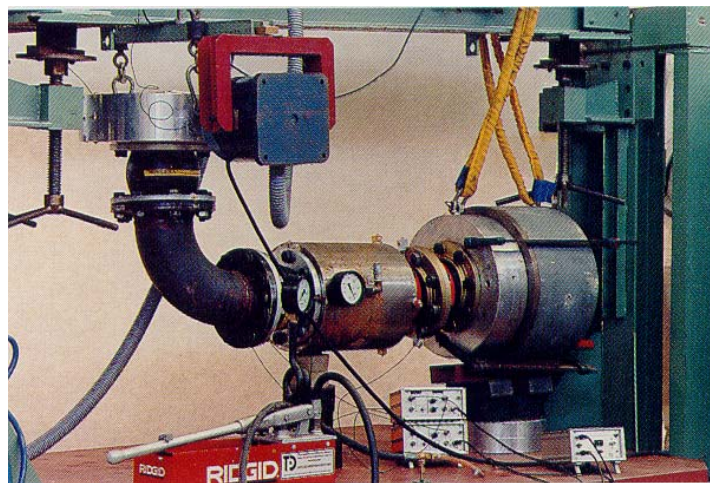


Figure 65. Test facility for flexible hoses and bellows. An auxiliary system (mass and house) has been connected to eliminate the effects of fluid-borne sound transmission to the blocking mass [71].

14.1.4 Research and facilities at HUT and VTT, Finland

A test facility (Figure 66) for the measurement of dynamic properties of vibration isolators under preload according to the direct method of ISO 10846 was constructed by Laboratory for Mechanics of Materials and VTT Industrial Systems [76], [79]. This laboratory belongs to the Department of Mechanical Engineering at Helsinki University of Technology. It is located at Espoo city. The research of dynamic properties of vibration isolators done in co-operation with participants from both organizations is one subprogram of the technology program Control of Vibration and Sound VÄRE (1999-2002). This programme is funded by National Technology Agency (Tekes) of Finland.

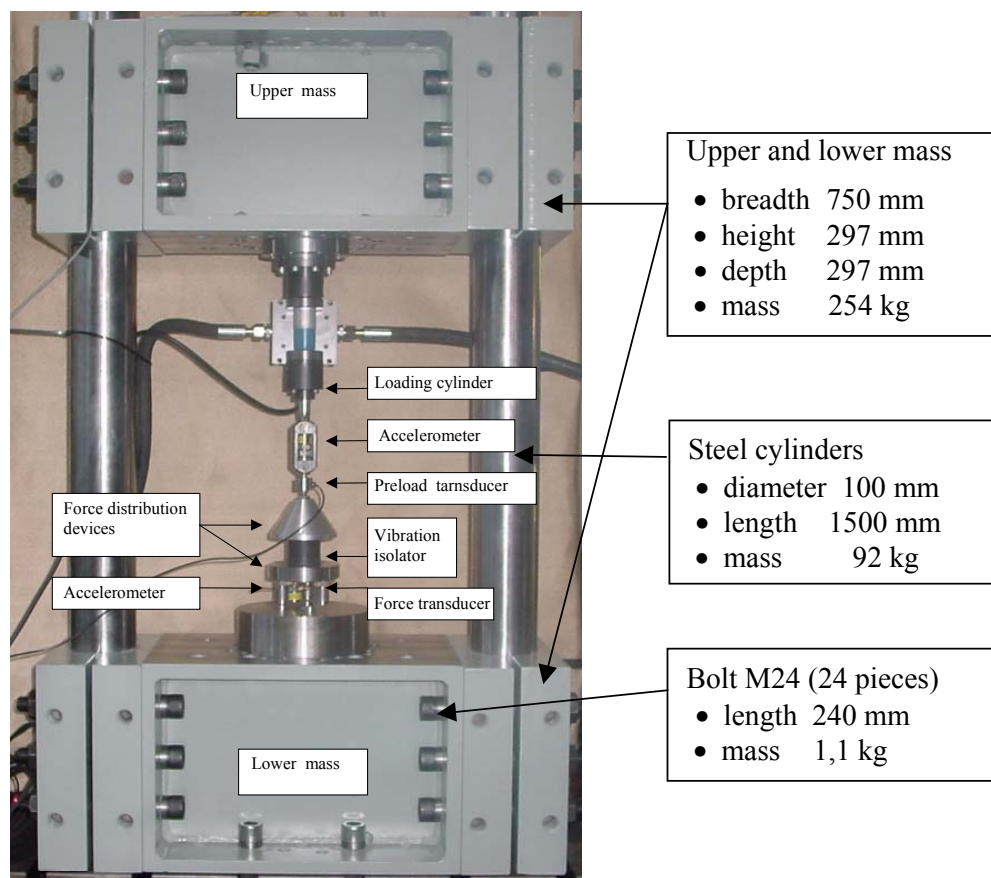


Figure 66. Test rig for the measurement of dynamic properties of vibration isolators according to the direct method of ISO 10846 at Helsinki University of Technology, Department of Mechanical Engineering in the Laboratory for Mechanics of Materials in Espoo city.

Two steel cylinders form the frame of the test rig. Between them is attached two adjustable masses. The total mass of the frame structure is 720 kg. Some modifications were made to the original test rig [76], and now the test rig is planned to achieve the following operating parameters [79]:

- The requirements of ISO 10846 are fulfilled in the application area
- Displacement amplitude of the excitation from 0,1 to 2 mm
- Static preload up to 4 kN
- Frequency range up to 240 Hz, but depends on preload and amplitude
- Vibration isolators with diameters up to 200 mm can be attached. The length of a vibration isolator is not fixed, because the location of the upper mass can be adjusted.

Some research has been done on wire rope vibration isolators using the indirect method of ISO 10846, part 3 [77], [78]. This wire rope research belongs also to VÄRE technology programme. The test facilities of VTT Industrial Systems in the research area Intelligent Products and Services include the Ling Dynamic Systems 455 series vibrator with mass 81,6 kg. It may produce a maximum sinusoidal force of 489 N when external cooling fan is used. When only natural cooling is used then only a force of 177 N is available. The available frequency range is from 10 Hz to 7 500 Hz. The maximum displacement amplitude of the shaker table is 9,5 mm and the maximum velocity 2,5 m/s. Maximum acceleration of bare table is 117 g. Effective mass of the moving system is 0,43 kg. A rated force, random rms flat spectrum 20 - 2 000 Hz, of 283 N can be achieved with payload equal to or greater than armature moving mass of 0,43 kg.

VTT Industrial Systems has also mechanical test facilities at Espoo including electrodynamical vibrators. Their main characteristics are maximum force 35,6 kN, frequency range 5 ... 2 000 Hz, maximum acceleration 1 100 m/s², maximum velocity 1,8 m/s, and maximum amplitude 50 mm.

15 Conclusions

Typically a machine is mounted on a flexible foundation. These installations are to be designed for minimum vibration and sound radiation. In these analysis vibrational power transmission analysis, both analytical and experimental, is beneficial when the transmission paths from machine are assessed. The power transmitted from a machine to its foundation is not only dependent on the source strength of the machine, but it is also dependent both on the source and receiver dynamical characteristics. That is why a designer needs to know the receiver and source mobilities with the free velocity of the machine to be installed. If the machine is mounted via a set of vibration isolators, then their dynamic transfer stiffness is needed. This can be obtained using standardized measurements. Depending on the application a unidirectional model may be sufficient, otherwise the dynamic characteristics of isolators needs to be known in other relevant translational and rotational degrees of freedom.

Experimentally the power transmission can be estimated in-situ. This method is based on the structural power calibration of the receiving structure, which is made before the source is installed. An approximate transmission estimate can be obtained with the source already installed, provided that either the source or receive mobility is available at the contact points.

There is still a need for continued research work towards internationally accepted methods for the characterization of structure-borne sound sources and for predicting the transmission of structure-borne sound power into source foundations and receiving structures. However, progress has been made in recent years in this respect. Engineers being unable to predict vibration and sound levels of real structures all but at very low frequencies using numerical packages like FEM or BEM are seeking other solutions like energy-related methods. In these methods the structure-borne sound power can be used in the prediction of resulting vibration and sound levels.

References

- [1] ISO/TR 11688-1. Acoustics - Recommended practice for the design of low-noise machinery and equipment - Part 1: Planning. Geneva: International Organization for Standardization, 1995. 36 pp.
- [2] ISO/TR 11688-2. Acoustics - Recommended practice for the design of low-noise machinery and equipment - Part 2: Introduction to the physics of low-noise design. Geneva: International Organization for Standardization, 1998. 46 pp.
- [3] ISO/TR 11690-3. Acoustics - Recommended practice for the design of low-noise workplaces containing machinery - Part 3: Sound propagation and noise prediction in workrooms. Geneva: International Organization for Standardization, 1997. 36 pp.
- [4] Koopmann, G. H. & Fahline, J. B. Designing quiet structures. A sound power minimization approach. San Diego. Academic Press, 1997. 244 pp.
- [5] Pierce. A. D. Acoustics. An introduction to its physical principles and applications. 2nd. ed. New York: The Acoustical Society of America, 1991. 678 pp.
- [6] Carlsson, U. Mechanical mobility: A tool for the analysis of vibrations in mechanical structures (Doctoral thesis). Stockholm: Technical acoustics, Department of Vehicle Engineering, Royal Institute of Technology. Marcus Wallenberg Institute for Sound and Vibration Research, 1993. 333 pp. (TRITA-FKT Report 9331)
- [7] Fahy, F. Manfred Heckl memorial lecture: The role of experimentation in vibroacoustics. In: Proc. of the third European Conference on Noise Control, EURO-NOISE 98. Munich, Germany. Oldenburg, Germany: German Acoustical Society (DEGA), 1998. Pp. 3-14.
- [8] Lyon, R. H. & DeJong, R. G. Theory and application of statistical energy analysis. 2nd. ed. Boston, Massachusetts, USA: Butterworth-Heinemann. 1995. 277 pp.
- [9] Wolde, T. ten & Gadefelt, G. R. Development of standard measurement methods for structureborne sound emission. Noise Control Engineering Journal, 1987. Vol. 28, no. 1, pp. 5-14.
- [10] Mondot, J. M. & Pettersson, B. Characterization of structure-borne sound sources: The source descriptor and the coupling function. Journal of Sound and Vibration, 1987. Vol. 114, no. 3, pp. 507-518.
- [11] Koh, Y. K. & White, R. G. Analysis and control of vibrational power transmission to machinery supporting structures subjected to a multi-excitation system, Part I: Driving point mobility matrix of beams and rectangular plates. Journal of Sound and Vibration, 1996. Vol. 196, no. 4, pp. 469-493.
- [12] Koh, Y. K. & White, R. G. Analysis and control of vibrational power transmission to machinery supporting structures subjected to a multi-excitation system, Part II: Vibrational power analysis and control schemes. Journal of Sound and Vibration, 1996. Vol. 196, no. 4, pp. 495-508.
- [13] Koh, Y. K. & White, R. G. Analysis and control of vibrational power transmission to machinery supporting structures subjected to a multi-excitation system, Part III: Vibrational power cancellation and control experiments. Journal of Sound and Vibration, 1996. Vol. 196, no. 4, pp. 509-522.
- [14] Fulford, R. A. & Gibbs, B. M. Structure-borne sound power and source characterisation in multi-point-connected systems, Part 1: Case studies for assumed force distributions. Journal of Sound and Vibration, 1997. Vol. 204, no. 4, pp. 659-677.
- [15] Fulford, R. A. & Gibbs, B. M. Structure-borne sound power and source characterization in multi-point-connected systems, Part 2: About mobility functions and three velocities. Journal of Sound and Vibration, 1999. Vol. 220, no. 2, pp. 203-224.

- [16] Fulford, R. A. & Gibbs, B. M. Structure-borne sound power and source characterization in multi-point-connected systems, Part 3: Force ratio estimates. *Journal of Sound and Vibration*, 1999. Vol. 225, no. 2, pp. 239-282.
- [17] Grice, R. M. & Pinnington, R. J. A method for the vibration analysis of built-up structures, Part I: Introduction and analytical analysis of the plate-stiffened beam. *Journal of Sound and Vibration*, 2000. Vol. 230, no. 4, pp. 825-849.
- [18] Grice, R. M. & Pinnington, R. J. A method for the vibration analysis of built-up structures, Part II: Analysis of the plate-stiffened beam using a combination of finite element analysis and analytical impedances. *Journal of Sound and Vibration*, 2000. Vol. 230, no. 4, pp. 851-875.
- [19] White, R. G. Power transmission measurement and control in structures. In: Pavic, G. (ed.) *Novem 2000 proceedings*. Lyon, France, 31 August-2 September, 2000. Lyon: Laboratoire Vibrations Acoustique, INSA de Lyon, 2000. 11 pp.
- [20] Fahy, F. *Foundations of Engineering Acoustics*. San Diego. Academic Press, 2001. 443 pp.
- [21] ISO 7626-1. 1986. *Vibration and shock - Experimental determination of mechanical mobility - Part 1: Basic definitions and transducers*. Geneva: International Organization for Standardization. 23 pp.
- [22] ISO 2041. 1990. *Vibration and shock - Vocabulary*. Geneva: International Organization for Standardization. 59 pp.
- [23] Cremer, L., Heckl, M. & Ungar, E. E. (transl.). *Structure-borne sound*. 2nd. ed. Berlin: Springer-Verlag, 1988. 573 pp.
- [24] Cremer, L., Heckl, M. & Ungar, E. E. (transl.). *Structure-borne sound*. Berlin: Springer-Verlag, 1973. 528 pp.
- [25] Ten Wolde, T., Verheij, J. W. & Steenhoek, H. F. Reciprocity method for the measurement of mechano-acoustical transfer functions. *Journal of Sound and Vibration*, 1975. Vol. 42, no. 1, pp. 49-55.
- [26] Fahy, F. *Sound and Structural Vibration. Radiation, Transmission and Response*. London: Academic Press, 1985. 309 pp.
- [27] Goyder, H. G. D. & White, R. G. Vibrational power flow from machines into built-up structures, Part I: Introduction and approximate analyses of beam and plate-like foundations. *Journal of Sound and Vibration*, 1980. Vol. 68, no. 1, pp. 59-75.
- [28] Goyder, H. G. D. & White, R. G. Vibrational power flow from machines into built-up structures, Part II: Wave propagation and power flow in beam-stiffened plates. *Journal of Sound and Vibration*, 1980. Vol. 68, no. 1, pp. 77-96.
- [29] Goyder, H. G. D. & White, R. G. Vibrational power flow from machines into built-up structures, Part III: Power flow through isolation systems. *Journal of Sound and Vibration*, 1980. Vol. 68, no. 1, pp. 97-117.
- [30] O'Hara, G. J. Mechanical impedance and mobility concepts. *The Journal of the Acoustical Society of America*, 1967. Vol. 41, no. 5, pp. 1180-1184.
- [31] Nilsson, A. C. *Vibroacoustics, Part I*. Stockholm: KTH, Department of Vehicle Engineering, MWL The Marcus Wallenberg Laboratory for Sound and Vibration Research, 2000, 208 pp. (Royal Institute of Technology - TRITA-FKT 2000:14.)
- [32] Nilsson, A. C. *Vibroacoustics, Part II*. Stockholm: KTH, Department of Vehicle Engineering, MWL The Marcus Wallenberg Laboratory for Sound and Vibration Research, 2000, 263 pp. (Royal Institute of Technology - TRITA-FKT 2000:15.)
- [33] Rubin, S. Mechanical immittance- and transmission-matrix concepts. *The Journal of the Acoustical Society of America*, 1967. Vol. 41, no. 5, pp. 1171-1179.
- [34] Molloy, C. T. Use of four-pole parameters in vibration calculations. *The Journal of the Acoustical Society of America*, 1957. Vol. 29, no. 7, pp. 842-853.

- [35] Snowdon, J. C. Mechanical four-pole parameters and their application. *Journal of Sound and Vibration*, 1971. Vol. 15, no. 3, pp. 307-323.
- [36] Hixson, E. L. Mechanical impedance. In: Harris, C. M. (ed.). *Shock and vibration handbook*. 3rd ed. New York: McGraw-Hill, 1988. Chapter 10.
- [37] Petersson, B. & Plunt, J. On effective mobilities in the prediction of structure-borne sound transmission between a source structure and a receiving structure, Part I: Theoretical background and basic experimental studies. *Journal of Sound and Vibration*, 1982. Vol. 82, no. 4, pp. 517 - 529.
- [38] Petersson, B. & Plunt, J. On effective mobilities in the prediction of structure-borne sound transmission between a source structure and a receiving structure, Part II: Procedures for the estimation of mobilities. *Journal of Sound and Vibration*, 1982. Vol. 82, no. 4, pp. 531 - 540.
- [39] Petersson, B. & Plunt, J. *Stomljudstransmission från maskiner till undederlag*. Göteborg: Avdelning för Byggnadsakustik, Chalmers Tekniska Högskola, 1979. 51 pp. + app. 17 pp. (Rapport 79-13)
- [40] Petersson, B. A. T. & Gibbs, B. M. Towards a structure-borne sound source characterization. *Applied Acoustics*, 2000. Vol. 61, no. 3, pp. 325-343.
- [41] Beranek, L. L. (ed.). *Noise and Vibration Control*. Rev. ed. Cambridge, MA, USA: Institute of Noise Control Engineering, 1988. 672 pp.
- [42] ISO 7626-2. 1990. *Vibration and shock - Experimental determination of mechanical mobility - Part 2: Measurements using single-point translation excitation with an attached vibration exciter*. Geneva: International Organization for Standardization. 21 pp.
- [43] Petersson, B. A. T. & Gibbs, B. M. Use of the source descriptor concept in studies of multi-point and multi-directional vibrational sources. *Journal of Sound and Vibration*, 1993. Vol. 168, no. 1, pp. 157-176.
- [44] Petersson, B. A. T. & Plunt, J. *Structure-borne sound transmission from machinery to foundations*. Gothenburg, Sweden: Department of Building Acoustics, Chalmers University of Technology, 1980. 120 pp. (Report 80-19)
- [45] Skudrzyk, E. J. The mean-value method of predicting the dynamic response of complex vibrators. *The Journal of the Acoustical Society of America*, 1980. Vol. 67, no. 4, pp. 1105-1135.
- [46] Skudrzyk, E. J. Understanding the dynamic behaviour of complex vibrators. *Acustica*, 1987. Vol. 64, no. 3, pp. 123-147.
- [47] Gibbs, B. M., Petersson, B. A. T. & Qiu, S. The characterization of structure-borne emission of building services machinery using the source descriptor concept. *Noise Control Engineering Journal*, 1991. Vol. 37, no. 2, pp. 53-61.
- [48] Ewins, D. J. State-of-the-art assessment of mobility measurements – A summary of European results. *The Shock and Vibration Bulletin*, 1981. Bulletin 51, Part 1, pp. 15-35.
- [49] Ewins, D. J. State-of-the-art assessment of mobility measurement techniques (SAMM) - – Summary of results. *Journal of the Society of Environmental Engineers*, 1981. Vol. 20, no. 1, pp. 3-13.
- [50] ISO 7626-5. 1994. *Vibration and shock - Experimental determination of mechanical mobility - Part 5: Measurements using impact excitation with an exciter which is not attached to the structure*. Geneva: International Organization for Standardization. 22 pp.
- [51] Ohlrich, M. In-situ estimation of structural power transmission from machinery source installations. In: Jacobsen, F. (ed.) *Proceedings of the Sixth International Congress on Sound and Vibration*. Copenhagen, Denmark, 5-8 July, 1999. Lungby: Department of Acoustic Technology, Technical University of Denmark, 1999. Vol. 5, pp. 2149-2160.

- [52] Ohlrich, M. A simple structural power method for determining the vibratory strength of machinery sources. In: Proceedings of Euro-Noise 98. München, Germany, 4-7 October, 1998. Vol. 1, pp. 383-388.
- [53] Ohlrich, M. Terminal source power for predicting structure-borne sound transmission from a main gearbox to a helicopter fuselage. In: Bernhard, R. J. & Bolton, J. S. (ed.). Proceedings of Inter-Noise 95. Newport Beach, California, USA, 10-12 July, 1995. Vol. 1, pp. 555-558.
- [54] Ohlrich, M. & Larsen, C. Surface and terminal source power for characterization of vibration sources at audible frequencies. In: Kuwano, S. (ed.). Proceedings of Inter-Noise 94. Yokohama, Japan, 29-31 August, 1994. Vol. 1, pp. 633-636.
- [55] Moorhouse, A. T. & Gibbs, B. M. Prediction of the structure-borne noise emission of machines: Development of a methodology. *Journal of Sound and Vibration*, 1993. Vol. 167, no. 2, pp. 223-237.
- [56] Moorhouse, A. T. & Gibbs, B. M. Structure-borne sound power emission from resiliently mounted fans: Case studies and diagnosis. *Journal of Sound and Vibration*, 1995. Vol. 186, no. 5, pp. 781-803.
- [57] Ohlrich, M. The use of surface power for characterisation of structure-borne sound sources of low modal density. In: Hill, F. A. & Lawrence, R. (ed.). Proceedings of Inter-Noise 96. Liverpool, United Kingdom, July 30 - August 02, 1996. Book 3, pp. 1313-1318.
- [58] Ohlrich, M. & Crone, A. An equivalent force description of gearbox sources applied in prediction of structural vibration in wind turbines. In: Proceedings of Inter-Noise 88. Pp. 479-484.
- [59] Laugesen, S. & Ohlrich, M. The vibrational source strength descriptor using power input from equivalent forces: a simulation study. *Acta Acoustica*, 1994. Vol., no. 2, pp. 449-459.
- [60] ISO 10846-1. Acoustics and vibration - Laboratory measurement of vibro-acoustic transfer properties of resilient elements - Part 1: Principles and guidelines. Geneva: the International Organization for Standardization, 1997. 20 pp.
- [61] Pinnington, R. J. & White, R. G. Power flow through machine isolators to resonant and non-resonant beams. *Journal of Sound and Vibration*, 1981. Vol. 75, no. 24, pp. 179-197.
- [62] Pinnington, R. J. Vibrational power transmission to a seating of a vibration isolated motor. *Journal of Sound and Vibration*, 1987. Vol. 118, no. 1, pp. 123-139.
- [63] Verheij, J. W. Multi-path sound transfer from resiliently mounted shipboard machinery (Doctoral thesis). Delft, The Netherlands: Technisch Physische Dienst TNO-TH (Institute of Applied Physics TNO-TH), 1982. 267 pp.
- [64] Kari, L. Structure-borne sound properties of vibration isolatos (Doctoral thesis). Stockholm: Royal Institute of Technology, Department of Vehicle Engineering. The Marcus Wallenberg Laboratory for Sound and Vibration Research, 1998. 26 pp. + appendices A-D. (TRITA-FKT Report 9802)
- [65] Kari, L. Dynamic transfer stiffness measurements of vibration isolators in the audible frequency range. *Noise Control Engineering Journal*, 2001. Vol. 49, no. 2, pp. 88-102.
- [66] Amunarriz, G. Indirect measurements of structure-borne sound energy flow through vibration isolators (Master Thesis). Stockholm: Royal Institute of Technology, Department of Vehicle Engineering. The Marcus Wallenberg Laboratory for Sound and Vibration Research, 1999. 57 pp. + appendices. 18 pp. (TRITA-FKT Report 9902)
- [67] Dickens, J. D. & Norwood, C. J. Universal method to measure dynamic performance of vibration isolators under static load. *Journal of Sound and Vibration*, 2001. Vol. 244, no. 4, pp. 685-696.

- [68] Dickens, J. D. & Norwood, C. J. Design of a test facility for vibration isolator characterisation. *Acoustics Australia*, 1997. Vol. 25, no. 1, pp. 23- 28.
- [69] Thompson, D. J., van Vliet, W. J. & Verheij, J. W. Developments of the indirect method for measuring the high frequency dynamic stiffness of resilient elements. *Journal of Sound and Vibration*, 1998. Vol. 213, no. 1, pp. 169-188.
- [70] Thompson, D. J. & Verheij, J. W. The dynamic behaviour of rail fasteners at high frequencies. *Applied Acoustics*, 1997. Vol. 52, no. 1, pp. 1-17.
- [71] Flexible components. Netherlands organization for applied scientific research TNO. TNO Institute of Applied Physics. Leaflet 8-89. 4 pp.
- [72] Ship Acoustics. Testing quality and the acoustic properties of flexible elements. TNO TPD. Leaflet 112001/200. 2 pp.
- [73] ISO 9611. Acoustics - Characterization of sources of structure-borne sound with respect to sound radiation from connected structures - Measurement of velocity at the contact points of machinery when resiliently mounted. Geneva: the International Organization for Standardization, 1996. 19 s.
- [74] ISO 10846-2. Acoustics and vibration - Laboratory measurement of vibro-acoustic transfer properties of resilient elements - Part 2: Dynamic stiffness of elastic supports for translatory motion - Direct method. Geneva: The International Organization for Standardization, 1997. 18 s.
- [75] ISO/FDIS 10846-3. Acoustics and vibration- Laboratory measurement of vibro-acoustic transfer properties of resilient elements - Part 3: Dynamic stiffness of resilient supports for translatory motion (Indirect method). Geneva: The International Organization for Standardization, 2002. 38 s.
- [76] Rantala, J. Development of Testing Arrangement for Vibration Isolators Based on ISO 10846 Standard. Espoo: Helsinki University of Technology. Department of Mechanical Engineering. Laboratory for Mechanics of Materials 2000. 19 pp. + app. 10 pp. (in Finnish)
- [77] Linjama, J. & Juntunen, M. Estimation of dynamic properties of resilient mounts. In: Friswell, M. I., Mottershead, J. E. & Lees, A. W. (ed.). *Proceedings of the Second International Conference. Identification in Engineering systems*. Swansea, UK, March 29-31, 1999. Pp. 74 - 83.
- [78] Juntunen, M. & Linjama, J. A test method for estimation of dynamic properties of isolators. In: Güemes, J. A. (ed.). *Proceedings of European COST F3 Conference on SYSTEM IDENTIFICATION & STRUCTURAL HEALTH MONITORING*. Vol. 2. Madrid, Spain, June, 2000. Madrid: Universidad Politécnica de Madrid, Spain. Pp. 815 - 829.
- [79] Keinänen, J. Testing and modelling dynamic properties for vibration isolators. Espoo: Helsinki University of Technology, Department of Mechanical Engineering, Laboratory for Mechanics of Materials, 2002. 95 pp. + app. (Master of Science thesis)
- [80] Moorhouse, A. T. On the characteristic power of structure-borne sound sources. *Journal of Sound and Vibration*, 2001. Vol. 248, no. 3, pp. 441-459.